

**EFFECTS OF CIGARETTE SMOKING ON RESPIRATORY
AND CARDIOVASCULAR SYSTEMS OF ALBINO RAT:
HISTOLOGICAL, PHYSIOLOGICAL, AND BIOCHEMICAL
STUDIES.**

By

Wajdy Joma'a Mohammad Al-Awaida

Supervisor

Dr. Ziad A. Shraideh, Prof.

Co-Supervisor

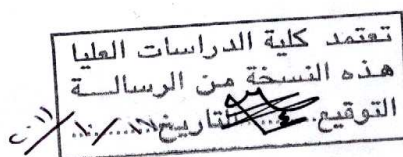
Dr. Ghaleb M. Abuereish, Prof.

Co-Supervisor

Dr. Darwish Badran

**This Dissertation was Submitted in Partial Fulfillment of the
Requirements for the Doctor of Philosophy Degree in Biological
Sciences.**

**Faculty of Graduate Studies
The University of Jordan**



October, 2011

COMMITTEE DECISION

This Thesis/Dissertation (Effects of Cigarette Smoking on Respiratory and Cardiovascular Systems of Albino rat: Histological, physiological, and biochemical studies) was Successfully Defended and Approved on 10/10/2011.

Examination Committee

Dr. Ziad A. Shraideh (Supervisor)
Prof. of Cell Biology

Dr. Ghaleb M. Abuereish (Coadvisor)
Prof. of Biochemistry/Molecular Biology

Dr. Darwish M. Badran (Coadvisor)
Assoc. Prof. of Anatomy & Histology

Dr. Ahmad M. Disi (Member)
Prof. of Comparative Vertebrate Anatomy/Taxonomy
& Ecology

Dr. Ibrahim M. Ibrahim (Member)
Prof. of Biochemistry

Dr. Jumah M. Shakhaneh (Member)
Prof. of Animal Physiology
(Mutah University)

Signature

Ziad A. Shraideh

G.M. Abuereish

Darwish M. Badran

Ahmad M. Disi

Ibrahim M. Ibrahim

J. Shakhaneh

تعتمد كلية الدراسات العليا
هذه النسخة من الرسالة
التوقيع: *[Signature]* التاريخ: 10/10/2011

Part of this work is published in” Shraideh, Z., Awaidah, W., Najar, H., and Musleh, M. (2011). A modified smoking machine for monitoring the effect of tobacco smoke on albino rats. The Jordan Journal of Biological Sciences, 4: 109-112. (appendix D).

DEDICATION

***To my parents, my wife, my children,
my brothers, and my sisters***

ACKNOWLEDGEMENTS

I sincerely thank my supervisors Prof. Ziad Shraideh, Prof. Ghaleb M. Abuereish, and Dr. Darwish Badran for their guidance, constructive suggestions, and continuous support. My sincere thanks are to the members of the committee for their helpful comments. My thanks are extended to Prof. Shtaywy Abdalla for his valuable notes and fruitful ideas for this study. Nevertheless, my thanks are extended to my colleagues, friends, and the employees in the departments of Biological Sciences, University of Jordan.

LIST OF CONTENTS

	Page
Committee Decision	ii
Dedication	iv
Acknowledgements	v
List of contents	vi
List of tables	xiii
List of figures	xiv
List of abbreviations	xviii
List of appendices	xxii
Abstract	xxiv
 1. INTRODUCTION	 1
1.1. Specific aims	4
 2. LITERATURE REVIEW	 6
2.1. Normal basic histology of studied tissues	6
2.1.1. Trachea	6
2.1.2. Alveoli of the lung	7

2.1.3. Myocardium cells	7
2.1.4. Aorta	8
2.2. Smooth muscles	9
2.2.1. Structure of smooth muscle cell	9
2.2.2. Morphology and types of smooth muscles	10
2.2.3. Excitation-contraction coupling of smooth muscle	11
2.2.4. Regulation of smooth muscle contraction	12
2.2.5. Mechanisms of intracellular Ca^{+2} increase	13
2.2.6. Mechanisms of cytosolic Ca^{+2} removal	13
2.2.7. Smooth muscle relaxation	14
2.3. Cardiac muscle	16
2.3.1. Cardiac excitation-contraction coupling	17
2.3.2. Regulation of cardiac excitation-contraction coupling	17
2.4. Morphological changes caused by cigarette smoking	18
2.5. Physiological effects of cigarette smoking	22
2.6. Effect of smoking on antioxidant enzymes activities	25
2.7. Cigarette smoke-induced apoptosis	27
2.8. Smoking machine	29
3. MATERIALS AND METHODS	30
3.1. Chemicals	30

3.2. Experimental design	31
3.3. The digital smoking machine	31
3.4. The effects of cigarette smoke on histology of the cardiovascular and respiratory systems: Light microscopy	31
3.4.1. Protocol of light microscopy	31
3.5. The effects of cigarette smoke on tissue ultrastructure	32
3.5.1. Procedure of transmission electron microscopy	32
3.5.1.1. Preparation of blocks	32
3.5.1.2. Sectioning, Staining and Microscopy	32
3.6. Detection of apoptosis in tissue sections	33
3.6.1. TUNEL assay procedure (TUNEL kit, Promega)	33
3.7. In Vitro physiological studies	34
3.7.1. Isolated, perfused heart system	34
3.7.1.1. Protocol	34
3.7.1.2. Preparation of cigarette smoke extracts (CSE)	35
3.7.1.3. The effect of cigarette smoke extract and L-nicotine on the isolated perfused heart	35
3.7.2. Tissue bath experiments	36
3.7.2.1. Protocol	36
3.7.2.2. Concentration-effects of CSE and pure L-nicotine on the contractility of aortic and tracheal smooth muscles	36
3.8. Biochemical studies	37

3.8.1. Cell extraction	37
3.8.2. Assay of catalase (CAT) activity	37
3.8.3. Assay of glucose-6-phosphate dehydrogenase (G6PD) activity	37
3.8.4. Assay of glutathione Peroxidase (GPx) activity	38
3.9. Spectrophotometric determination of nicotine in CSE	38
3.9.1. Method principle	38
3.9.2. Protocol	38
3.10. Protein content determination	39
3.11. Statistical analysis	39
4. RESULTS	40
4.1. Spectrophotometric determination of L-nicotine	40
4.1.1. Calibration curve	40
4.1.2. L- Nicotine content in CSE	40
4.2. Calibration curve for Lowry's assay using bovine serum albumin (BSA) as standard	41
4.2.1. Calibration curve	41
4.3. <i>In Vitro</i> physiological studies	42
4.3.1. Tissue bath experiments	42
4.3.1.1. Effect of cigarette smoke extract (CSE) on isolated smooth muscle preparations	42
4.3.1.2. Effect of pure L-nicotine on isolated smooth muscle preparations	43

4.3.2. Isolated perfused heart experiments	50
4.3.2.1. Effect of CSE on the isolated perfused heart	50
4.3.2.2. Effect of L-nicotine on the isolated perfused heart	50
4.4. Correlation of antioxidant enzyme activities with tissue inflammation in rats during smoke exposure.	55
4.4.1. Catalase activity in cigarette smoke-exposed rats and in recovery rats	55
4.4.2. Glutathione peroxidase activity in cigarette smoke-exposed rats and in recovery rats.	56
4.4.3. G6PD activity in cigarette smoke-exposed rats and in recovery rats.	57
4.4.4. Rat liver, lung, and kidney inflammation during smoke exposure and recovery.	58
4.5. The ability of cigarette smoke to induce apoptosis in tissue sections	64
4.5.1. Effect on the trachea	64
4.5.2. Effect on the aorta	64
4.5.3. Effect on heart ventricles	64
4.5.4. Effect on the lung	64
4.6. Histological studies	70
4.6.1. Studying the effect of cigarette smoke and its recovery by light microscopy	70
4.6.1.1. Effect on the trachea	70
4.6.1.2. Effect on alveoli of the lung	70
4.6.1.3. Effect on the aorta	70

4.6.1.4. Effect on heart ventricles	71
4.6.2. Studying the effect of cigarette smoke and its recovery by transmission electron microscopy	71
4.6.2.1. Effect on the trachea	71
4.6.2.2. Effect on alveoli of the lung	72
4.6.2.3. Effect on heart ventricles	72
5. DISCUSSION	112
5.1. Physiological studies	112
5.1.1. Rat isolated perfused heart experiments	112
5.1.1.1. Effect of CSE and L-nicotine on isolated perfused heart	112
5.1.2. Tissue bath experiments	113
5.1.2.1. Effect of CSE on aorta	113
5.1.2.2. Effect of pure L-nicotine on aorta	114
5.1.2.3. Effect of CSE on trachea	114
5.1.2.4. Effect of pure L-nicotine on trachea	115
5.2. Biochemical studies	116
5.2.1. Correlation of antioxidant enzyme activities with tissue inflammation during smoke exposure of rats and smoke cessation	116
5.3. Spectrophotometric determination of nicotine concentration in cigarette smoke extract	119
5.4. The smoking machine	120
5.5. The ability of cigarette smoke to induce apoptosis in tissue (or	120

slices?) sections	
5.6. Histological studies	121
5.6.1. Effect of cigarette smoke on the trachea	121
5.6.2. Effect of cigarette smoke on the alveoli of the lung	122
5.6.3. Effect of cigarette smoke on the aorta	124
5.6.4. Effect of cigarette smoke on the heart ventricles	125
5.6.5. Recovery period	125
6. CONCLUSION AND RECOMMENDATIONS	126
7. REFERENCES	127
8. APPENDICES	146
9. ABSTRACT IN ARABIC	155

LIST OF TABLES

Table		Page
Table 1.	L-nicotine content in the different CSE concentrations	40
Table 2.	The maximum response induced by CSE on rat isolated aorta and trachea preparations	42
Table 3.	The maximum response induced by L-nicotine on rat isolated aorta and trachea preparations	43
Table 4.	Catalase specific activity compared to control in the cigarette smoke-exposed rats and after recovery period in liver, kidney and lung tissues of rats	55
Table 5.	Glutathione peroxidase specific activity compared to control in the cigarette smoke-exposed rats and after recovery period in liver, kidney and lung tissues of rats	56
Table 6.	G6PD specific activity compared to control in the cigarette smoke-exposed rats and after recovery period in liver, kidney and lung tissues of rats	57

LIST OF FIGURES

Figure		Page
Figure 1.	Cumulative concentration-effect curve of CSE on carbachol-precontracted tracheal rings	44
Figure 2.	Cumulative concentration-effect curve of CSE on rat phenylephrine-precontracted aorta	45
Figure 3.	Cumulative concentration-effect curve of L-nicotine on carbachol-precontracted tracheal rings	46
Figure 4.	Cumulative concentration-effect curve of L-nicotine on rat phenylephrine-precontracted aorta	47
Figure 5.	Effects of various concentrations of cigarette smoke extract (CSE) on rat isolated phenylephrine-precontracted aorta, and carbachol- precontracted trachea	48
Figure 6.	Effects of various concentrations of L-nicotine on rat isolated phenylephrine-precontracted aorta, and carbachol- precontracted trachea	49
Figure 7.	Concentration-effect curve of CSE on the rate and force of rat isolated perfused heart	51
Figure 8.	Concentration-effect curve of L-nicotine on the rate and force of rat isolated perfused heart	52
Figure 9.	Effects of increasing concentrations of cigarette smoke extract (CSE) on rat isolated perfused heart	53
Figure 10.	Effects of increasing concentrations of L-nicotine on rat isolated heart	54

Figure 11.	Normal morphology of lung alveoli in a control rat	59
Figure 12.	Lung tissue of cigarette smoke-exposed rat	59
Figure 23.	Lung tissue of cigarette smoke-exposed rat after the recovery period	60
Figure 14.	Normal morphology of liver in a control rat	60
Figure 15.	Liver tissue of cigarette smoke-exposed rat	61
Figure 16.	liver tissue of cigarette smoke-exposed rat after the recovery period	61
Figure 17.	Normal morphology of kidney in a control animal	62
Figure 18.	Kidney tissue of cigarette smoke-exposed rat	62
Figure 19.	Kidney tissue of cigarette smoke-exposed rat after the recovery period	63
Figure 20.	Normal tracheal tissue (TUNEL staining)	65
Figure 21.	Tracheal tissue from cigarette smoke-exposed rat (TUNEL staining)	65
Figure 22.	Normal aortic tissue (TUNEL staining)	66
Figure 23.	Aortic tissue from cigarette smoke-exposed rat (TUNEL staining)	66
Figure 24.	Normal heart ventricular tissue (TUNEL staining)	67
Figure 25.	Heart ventricular tissue from cigarette smoke-exposed rat (TUNEL staining)	67
Figure 26.	Normal lung alveoli (TUNEL staining)	68

Figure 27.	Lung alveoli from cigarette smoke-exposed rat (TUNEL staining)	68
Figure 28.	Magnified picture of several typical apoptotic cells (TUNEL staining)	69
Figures 29-30.	Section of normal tracheal tissue	73
Figures 31-33.	Trachea of cigarette smoke-exposed rat	74-75
Figures 34-35.	Section from tracheal mucosa of cigarette smoke-exposed rat after the recovery period	75-76
Figures 36-37.	Control lung alveoli	76-77
Figure 38.	An enlarged image of normal a terminal bronchiole	77
Figures 39-43.	Lung tissues of cigarette smoke-exposed rat	78-80
Figures 44-48.	Lung tissues of cigarette smoke-exposed rat after the recovery period	80-82
Figure 49.	Normal histology of the aorta	83
Figures 50-52.	Aortic tissue from cigarette smoke-exposed rat	83-84
Figures 53-54.	Aortic tissue from cigarette smoke-exposed rat after the recovery period	85
Figures 55-56.	Normal heart ventricular tissue	86
Figures 57-60.	Heart ventricular tissue of cigarette smoke-exposed rat	87-88
Figures 61-63.	Heart ventricular tissue of cigarette smoke-exposed rat after the recovery period	89-90

Figure 64.	Thin section of control tracheal tissue	91
Figure 65.	Closer image at a normal tracheal goblet cell	92
Figures 66-68.	Thin section in the tracheal epithelium of cigarette smoke-exposed rat	93-95
Figure 69.	Thin section in the tracheal epithelium of cigarette smoke-exposed rat after the recovery period	96
Figures 70-71.	Thin section of control alveolar epithelium	97-98
Figures 72-76.	Thin section in the alveolar epithelium of cigarette smoke-exposed rat	99-103
Figure 77.	Thin section in the alveolar epithelium of cigarette smoke-exposed rat after the recovery period	104
Figures 78-79.	Thin section of control heart ventricular tissue	105-106
Figures 80-82.	Thin section of heart ventricular tissue of cigarette smoke-exposed rat	107-109
Figure 83-84.	Thin section of heart ventricular tissue of cigarette smoke-exposed rat after the recovery period	110-111

LIST OF ABBREVIATIONS

ADP: Adenosine diphosphate.

AESA: Aqueous extract of smokeless tobacco.

ANS: Autonomic nervous system.

ATP: Adenosine triphosphate.

cADPR: cyclic adenosine diphosphate ribose.

CaM: Calmodulin.

cAMP: Cyclic adenosine monophosphate.

CAT: Catalase.

CCh: Carbachol

cGMP: Cyclic guanosine monophosphate.

CICR: Ca^{+2} -induced Ca^{+2} releases.

CO: Carbon monoxide.

CS: Cigarette smoke.

CSE: Cigarette smoke extract.

DCs: Dendritic cells.

DAG: Diacylglycerol.

AMs: Alveolar macrophages.

SPA: Surfactant protein A.

EDR: Endothelium-dependent relaxation.

G6PD: Glucose-6-phosphate dehydrogenase.

GPx: Glutathione peroxidase.

IP3: Inositol 1,4,5-trisphosphate.

Lpx: Lipid peroxidation.

MLC kinase: Myosin light chain kinase.

MLCP: Myosin light chain phosphatase.

MSS: Mainstream smoke.

MyBP-C: Myosin binding protein C.

NO: Nitric oxide.

NOS: Nitric oxide synthase.

Pap: Papaverine.

PBS: Phosphate buffered saline.

PE: Phenylephrine.

PKA: cAMP-dependent protein kinase.

PKC: Protein kinase C.

PKG: cGMP-dependent protein kinase

PLB: Phospholamban.

PLC: Phospholipase C.

PMCA: Plasma membrane Ca^{+2} ATPase.

PSS: Physiological saline solution

RER: Rough endoplasmic reticulum.

rMLC: Regulatory myosin light chain.

ROCK: Rho-associated kinase

ROS: Reactive oxygen species.

rTdT: Recombinant terminal deoxynucleotidyl transferase.

RyRs: Ryanodine receptors.

SERCA: Sarcoplasmic reticulum Ca^{+2} –ATPase.

SOD: Superoxide dismutas.

SER: Sarcoplasmic reticulum.

SS: Sidestream smoke.

KHs: Krebs-Henseleit solution.

TEM: Transmission electron microscopy

TM: Tropomyosin.

TnC: Troponin C.

TnI: Troponin I.

TnT: Troponin T.

VDCCs: L-type voltage-dependent calcium channels.

List of Appendices

Appendix		Page
Appendix A	Preparation of solutions	146
1	10% Saline formalin	146
2	Alcoholic eosin Y	146
3	Lithium carbonate	146
4	Egg albumin	146
5	rTdT reaction mix	146
6	Stock sodium cacodylate buffer	147
7	Working buffer	147
8	Washing buffer	147
9	8% Paraformaldehyde	147
10	Karnovsky's fixative	147
11	The embedding medium (Spurr's medium)	147
12	Aqueous uranyl acetate	148
13	Lead citrate	148
14	Physiological saline solution	148
15	Papaverine hydrochloride	148

16	Carbamoylcholine chloride (Carbachol)	148
17	Phenylephrine hydrochloride	148
18	L-nicotine	149
19	Sodium hydroxide	149
20	Potassium permanganate	149
21	Protein content determination	149
21.1	Analytical reagents	149
21.2	Protocol	150
Appendix B	Spectrophotometric determination of L-nicotine	151
Appendix C	Protein determinations	153

EFFECTS OF CIGARETTE SMOKING ON RESPIRATORY AND CARDIOVASCULAR SYSTEMS OF ALBINO RAT: HISTOLOGICAL, PHYSIOLOGICAL, AND BIOCHEMICAL STUDIES

By

Wajdy Joma'a Mohammad Al-Awaida

Supervisor

Dr. Ziad A. Shraideh, Prof

Co-Supervisor

Dr. Ghaleb M. Abuereish, Prof

Co-Supervisor

Dr. Darwish Badran

ABSTRACT

This research was an attempt to reveal the effects of cigarette smoking on rat tissues at the cellular level, through exposing a group of experimental male albino rats to the cigarette smoke for three months on a daily basis, using a special modified smoking machine.

Exposure of albino rats for 3 months to cigarette smoke caused drastic histological changes in the tracheal epithelium including epithelial cells proliferation, disruption of its cilia, presence of inclusion bodies, cytoplasmic vacuolization and mitochondria aggregates in the apical portion of epithelial cells. There was a marked thickening in the alveolar wall of lung alveoli, collapsed alveoli and blood extravasations and obvious damaging in the multilamellar bodies of type II pneumocytes together with cytoplasmic vacuolization and chromatin condensation. In aorta, there was a thickening of internal elastic lamina and elastic lamellae in the tunica media. There was a slight contraction of smooth muscle, and endothelial cells disruption. In heart ventricles was a separation between cardiac muscle fibers and also between myofibrils. Congested blood vessels were observed in the heart ventricle. In heart ventricles, mitochondria were the most affected organelles by cigarette smoke. Inflammatory cell infiltration was present nearly in all examined tissues. Cigarette smoke was able to induce apoptosis only in lung alveoli.

In tissue bath experiments, the cigarette smoke extracts (CSE) and L-nicotine induced biphasic change in the tone of isolated precontracted-tracheal and aortic smooth muscles. In the case of isolated perfused heart, CSE and L-nicotine induced in most concentrations a significant concentration- dependent reduction of the force and the rate of contraction of the perfused heart. One gram of cigarette tobacco produces an equivalent of 57 mg L-nicotine in CSE. In comparison with control animals, cigarette smoke exposure lowers the specific activity of antioxidant enzymes in the liver, kidney

and lung tissues. However, during the recovery period the enzyme activities returned to normal levels.

A modified smoking machine has been constructed and used for monitoring the effects of cigarette smoke on albino rats. Long-term administration of cigarette smoke lowers the activity of antioxidant enzymes in liver, lung, and kidney. These alterations may be one of the factors for induced inflammation in these organs. The effect was nearly reversible. Cigarette smoke causes severe histological effects especially in trachea and lung alveoli. It induces also apoptosis only in lung alveoli. Smoking has more severe inhibitory and damaging effects on lung due to the differential load of metabolites of cigarette smoke in this organ. L-nicotine is expected to be CSE component that causes biphasic tone changes of isolated rat aorta and trachea. L-nicotine is expected to be CSE component that causes a significant concentration-dependent decrease in the force and rate of the contractions of perfused heart

1. INTRODUCTION

Smoking is the act of inhaling and exhaling the fumes from burning plant materials, especially tobacco. It is consumed in the form of cigarettes, cigars, chew, pipes or water-pipe (Hoffmann and Wynder, 1986).

About 1.25 billion humans smoke cigarettes daily and therefore smoking presents a worldwide social problem (Proctor, 2001). The spread of smoking is very fast among world population so that recent estimate suggests that nearly 82,000 to 99,000 young people start the habit of smoking each year (Malson *et al.*, 2001). In the USA, 3000 adolescent start smoking every day, almost a million teenagers annually (Kessler, 1995). A study involving the university students in north of Jordan indicated that prevalence of smoking is 35.0% (of these totals 56.9% were males and 11.4% were females) (Khader and Alsadi, 2008). The majority of these students were daily cigarette smokers.

The smoke generated from burning tobacco is divided into two types: Mainstream smoke and Sidestream smoke. The mainstream is the smoke which is inhaled by the smoker from tobacco product during puffing. The sidestream is the smoke which is emitted by burning cigarette between puffs. The sidestream smoke usually contains higher concentrations of toxic and carcinogenic agents than the mainstream smoke (Stephen, 2010).

Cigarettes contain more than 4,000 identified chemical compounds including 60 known carcinogens (Stephen, 2010). The gaseous components of mainstream smoke (92% of the total smoke) involve 400-500 different gases which include carbon-monoxide, nitrogen oxide, hydrogen cyanide, formaldehyde and ozone. Particulate matter (8% of mainstream smoke) contains tar product such as naphthalene, pyrene

and nitrosamine (Kaiserman and Rickkert, 1992; Yarnell, 1996; Ding *et al.*, 2008 ;Stephen, 2010) and metal such as cadmium, polonium, selenium, mercury, lead and arsenic (Galażyn-Sidorczuk *et al.*, 2008 ; Stephen, 2010). According to a report by Public Health Laboratories, Maryland, USA, 1997, the Jordanian cigarettes contain about twice the amount of nicotine and tar which is found in non-Jordanian cigarettes.

Cigarette smoking is associated with 400,000 deaths annually from cardiovascular diseases in the United State alone (U. S. Public Health Service, 2005). There is a clear relationship between the degree and duration of exposure to cigarette smoking and incidence of cardiovascular events (Fitzgerald, 1997; Leone, 1993; 1994; Ambrose and Barua, 2004). The deleterious effect of cigarette smoking on the cardiovascular system, would lead to coronary artery disease, atherosclerosis and peripheral vascular disease. Also, smoking has been implicated in the development of cerebrovascular diseases and aortic dilatation (Goich, 1995; Leone, 1995; Nakamura, 2008; Desai *et al.*, 2009). On the other hand, the effects of cigarette smoking extends far beyond the individual smoker and include both direct assault of passive smoking on the non-smoker and the staggering economic burden placed on the health care system by smoking related illness (Glantz and Parmley, 1991; Metsios *et al.*, 2007).

The carbon-monoxide and nicotine of tobacco smoking have been mainly implicated in acute cardiovascular disease (Higman and Powell, 1994; Thomas, 1993; Maziak, *et al.*, 2004). The nicotine in cigarette stimulates the sympathetic nervous system with consequent effect on the heart rate and peripheral vasoconstriction with consequent elevation of blood pressure (Higman and Powell, 1994). The physiological effects of carbon monoxide are associated with increase carboxy-hemoglobin level, which reduces the oxygen capacity of blood (Higman and Powell, 1994).

Cigarette smoking increases the risk of developing cancer in different organs of the body and increase their metastasis rates (Terry *et al.*, 2003; Kobrinsky *et al.*, 2003). Cigarette smoking is responsible for 90% of all lung cancer, which is the main type of cancer causing death in the world (Greenlee *et al.*, 2001; Hecht, 2003; Stampfli and Anderson, 2009). Also, smoking is the major source of chronic obstructive pulmonary disease (COPD), the fourth leading cause of death in the United States (Anderson and Smith, 2003). The high risk of smoke decreases with time after giving up smoking, however long-term ex-smokers may approach but not completely recover the health state of nonsmokers (IARC, 1986).

Cigarette smoke contains and generates various reactive oxygen species (ROS) and reactive nitrogen species (RNS), such as superoxide radical, hydrogen peroxide, hydroxyl radical, and peroxynitrite (Aoshiba and Nagay, 2003). The highly reactive radicals can act as initiators of carcinogenesis, causing DNA damage, activate procarcinogens and alter the cellular antioxidant defense system. This antioxidant system includes superoxide dismutase, glutathione peroxidase, catalase and Glucose-6-phosphate dehydrogenase enzymes, which work in a sequential manner to dispose the free radicals (Carnevali, *et al.*, 2003; Avti *et al.*, 2006).

Despite the social, religious, and current medical argument against the use of tobacco, still the habit of smoking is finding acceptance through out the world.

1.1. Specific aims

- 1- Developing a modified digital smoking machine which supplies fresh air to prevent animal anoxia.
- 2- To study the effect of cigarette smoke on specific activity of antioxidant enzymes including catalase, Glucose-6-phosphate dehydrogenase (G6PD) and glutathione peroxidase enzymes in the lung, liver and kidney.
- 3- To study the recovery of antioxidant enzymes activity three months after stopping the rat exposure to mainstream cigarette smoke.
- 4- To examine the histopathological changes that may occur during chronic exposure of rats to mainstream cigarette smoke, using a developed smoking machine. In this investigation; selected tissues of the cardiovascular and respiratory systems (trachea, lung alveoli, aorta, and heart ventricles) would be examined by light and transmission electron microscopy (TEM), with special emphasis focusing on changes in the epithelium and muscle fibers.
- 5- To study the recovery of histopathological changes by light and transmission electron microscopy, three months after stopping rat exposure to mainstream cigarette smoke.
- 7- To detect the presence of apoptotic nuclei in the previously mentioned selective tissues, using Dead End Colorimetric TUNEL system (DeadEnd kit, Promega).
- 8- To evaluate the response of isolated precontracted- aortic and tracheal tissues to cigarette smoke extract (CSE) and to pure L-nicotine, under isometric conditions by using force transducer and pen recorder.

- 9- To study the isometric contractions of isolated perfused heart, treated with cigarette smoke extract (CSE) and pure L-nicotine.
- 10- To determine nicotine concentration in cigarette smoke extract by spectrophotometry.

2. Literature review

2.1. Normal histology of studied tissues:-

2.1.1. Trachea

Trachea or windpipe is a tubular passageway for air, which extends from the larynx to about the middle of the thorax, where it divides into the two main bronchi. The layers of tracheal wall, from luminal to the superficial side include the mucosa, submucosa, hyaline cartilage and adventitia. The mucosa comprises two parts, the epithelium and lamina propria mucosa. The epithelium is pseudostratified ciliated columnar (Ross *et al.*, 2011). Each of the ciliated cells has 300 cilia in the apical surface; numerous small mitochondria are located beneath the cilia. The second most abundant cell in the mucosal epithelium is the mucous goblet cell, which contains mucous droplets in its apical portion. The third type of columnar cells is the brush cells, which contain numerous microvilli in their apical surface. The basal cells do not extend to the luminal surface of the epithelium. All cells of the ciliated pseudostratified columnar epithelium touch the basement membrane. Lamina propria is located beneath the basement membrane, which contains elastic reticular fibers. The second layer is submucosa, which is composed of areolar connective tissue that contains numerous seromucous glands plus their ducts. The incomplete horizontal ring of hyaline cartilage is important for keeping the tracheal lumen open. The adventitia consists of areolar connective tissue (Young *et al.*, 2006; Janqueira and Carneiro, 2005).

2.1.2. Alveoli of the lung

Alveoli are saclike evagination of the respiratory bronchioles, alveolar ducts, and alveolar sacs (Ross *et al.*, 2011). The wall of alveoli contains two types of alveolar epithelia cells. Type I alveolar cells make up 97% of the alveolar surface. In this cell, the organelles are grouped around the nucleus to reduce the cell thickness. The thin portion contains abundant pinocytotic vesicles. The important role of these cells is to provide a very thin barrier to gas diffusion. Type II cells are fewer in number (approximately 3%) and are found between type I alveolar cells. These cells are round in shape and are found in groups of two or three along the alveolar surface at points where the alveolar wall forms angles. Type II alveolar cells rest on the basement membrane and they exhibit a vesicular cytoplasm caused by the lamellar bodies (Ross *et al.*, 2011; Janqueira and Carneiro, 2005). The interalveolar septum is composed of two thin squamous epithelial layers between which lie elastic and reticular fibers, capillaries, and connective tissue matrix and cells. The connective tissue and capillaries constitute the interstitium (Janqueira and Carneiro, 2005; Young *et al.*, 2006; Rubins, 2003). Alveolar macrophages or dust cells act to remove fine dust particles and other debris from the alveolar spaces. These cells are found either free in the alveolar space or within the alveolar septa (Ross *et al.*, 2011).

2.1.3. Myocardium cells

Cardiac muscle fibers are shorter in length and less circular than skeletal muscle fibers in transverse section. Mature cardiac muscle cells have appeared as cross-striated banding pattern similar to that of skeletal muscle. However, each cardiac muscle cell may have only one or two centrally located nuclei. Cardiac muscle fibers connect to adjacent fibers by intercalated discs that contain gap junctions and desmosomes. (Ross *et al.*, 2011; Janqueira and Carneiro, 2005). Compared with

skeletal muscle fibers, mitochondria of cardiac myocytes are larger and more numerous, they usually occupy 25% of the cytosolic space compared to about 2% in the skeletal muscle fiber. The structure and function of the contractile proteins in cardiac cells are almost the same as in skeletal muscle. Also, the cardiac muscle cell is characterized by diad which is composed of one transverse tubule and one sarcoplasmic reticulum cisternae. The transverse tubules are wider but less abundant than that of skeletal muscle, while the sarcoplasmic reticulum (SR) of cardiac muscle is smaller than the SR of skeletal muscle fibers (Ross *et al.*, 2011; Janqueira and Carneiro, 2005).

2.1.4. Aorta

Aorta is the largest artery, its wall consists of three layers:

1- Tunica intima:

Tunica intima consists of a single layer of flattened endothelial cells, supported by a layer of collagenous tissue rich in elastin. The sub endothelial supporting tissue contains scattered fibroblasts and myointimal cells (Ross *et al.*, 2011; Janqueira and Carneiro, 2005).

2- Tunica media:

Tunica media is particularly broad and extremely elastic; it consists of fenestrated sheets of elastin called elastic lamellae. Between the elastic laminae are smooth muscle cells, reticular fibers, proteoglycans and glycoproteins. In the absence of stretch, the elastic fibers have wavy appearance. In rat, the media comprises 7 to 11 elastic laminae separated by interlaminar spaces which contain smooth muscle cells and collagen (Keech, 1960).

3-Tunica adventitia:

Tunica adventitia consists primarily of elastic fibers, collagen, and a small vasa vasorum. This layer gradually becomes continuous with the connective tissue of the organ through which the vessel runs (Ross *et al.*, 2011; Janqueira and Carneiro, 2005; Young *et al.*, 2006)

2.2. Smooth muscle:

Smooth muscle, is so called because it lacks the sarcomeric banding characteristic of striated muscle. This resulted from the relative lack of organization of protein filaments within smooth muscle cells. They are widely distributed in various hollow organs and tubes, including stomach, intestinal tract, blood vessels, and airway. Smooth muscle is responsible for involuntary contractions of uterus, blood vessels, stomach and intestine (Laporte *et al.*, 2004; Janqueira and Carneiro, 2005; Young *et al.*, 2006).

2.2.1. Structure of smooth muscle cell

Smooth muscle cells contain thick myosin filaments and thin actin –filaments. There are specialized cytoskeleton regions known as dense bodies like Z-lines of striated muscle fibers. Concentrated around the nucleus are mitochondria, lysosomes, centrioles and microtubules. Smooth muscle cells also contain a rudimentary sarcoplasmic reticulum responsible for Ca^{+2} storage and release. However, t-Tubules are not present. A small invagination of the cell membrane called caveolae, which is similar to the transverse tubule system of striated muscle is seen (Taggart, 2001; Janqueira and Carneiro, 2005).

2.2.2. Morphology and types of smooth muscles

Smooth muscle cells are elongated, fusiform and spindle shaped with two tapering ends. They range in size from 20 μm in small blood vessels to 500 μm in the pregnant uterus. Each smooth muscle cell is enclosed by a basal lamina and network of reticular fibers. There are two types of smooth muscle tissue, unitary visceral smooth muscle and multiunit non visceral smooth muscle. In visceral smooth muscle fibers the nerve supplies one muscle and the contraction impulse is propagated through gap junction, while in multiunit fibers each muscle fiber receives innervations. Muscles present in the iris of the eye are examples of multiunit smooth muscles (Janqueira and Carneiro, 2005; Young *et al.*, 2006).

Based on their mechanical and electrophysiological characteristics, the pattern of contractile activity in smooth muscles can be divided into two extreme varieties: tonic and phasic (Ogut *et al.*, 2007). Tonic smooth muscle is characterized by slowly contracting multiunit which maintains tone via Rho-associated kinase (ROCK) or PKC activation. The phasic smooth muscle is characterized by rapidly contracting single unit, as in the intestinal, rectal smooth muscle; the later is a mixture of both types (Patel and Rattan, 2007; Godoy *et al.*, 2009; Taggart and Wray, 1998; Leguillette *et al.*, 2008).

2.2.3. Excitation-contraction coupling of smooth muscle

The regulation of smooth muscle cell contraction may directly come through neural innervations from the autonomic nervous system (ANS), or indirectly from an adjacent cell via gap junctions. Also, the contractile state of a smooth muscle can be altered due to the binding of different agonists to their expressed receptors on the surface of smooth muscle cells, as well as by the activation of stretch-dependent ion channels in the plasma membrane. The prototypical response of a smooth muscle cell to various agonists is to increase the phospholipase C (PLC) activity via coupling through G protein. The phospholipase C produces two potent second messengers from the membrane lipid phosphatidylinositol 4,5-bisphosphate: diacylglycerol (DAG) and inositol 1, 4, 5-trisphosphate (IP3). The IP3 messenger binds to specific receptors on the sarcoplasmic reticulum, causing release of activator calcium (Ca^{+2}). The DG messenger along with Ca^{+2} activates protein kinase C enzyme (PKC), which can phosphorylate specific target proteins like L-type Ca^{+2} channels or regulatory myosin light chain (rMLC) (Varlamova *et al.*, 2001; Cobine *et al.*, 2007; Mizuno *et al.*, 2008; Lukas, 2004).

The contraction of smooth muscle is initiated by an increase in the intracellular calcium ions concentration, and an enhancement Ca^{+2} sensitization of the contractile proteins, which is signaled by the RhoA/ ROK pathway (Andrea and Walsh, 1992; Webb, 2003). A burst of Ca^{+2} into the cytosol will initiate a sequence of events that lead to increase the ATPase activity of myosin II molecule:

- 1- Four calcium ions bind to acidic protein known as calmodulin (CaM), forming Ca^{+2} .CaM complex.
- 2- The complex then activates the apoenzyme myosin light chain kinase (MLC kinase), forming the ternary complex of Ca^{+2} .CaM.MLC kinase.

Activated MLC kinase phosphorylates the 20-kDa light chain of myosin, altering the conformation of myosin head. This will increase its ATPase activity. The energy released from ATP by myosin ATPase activity results in cycling of the myosin cross-bridges with actin for contraction (Webb, 2003, Loirand *et al.*, 2006).

The frequency of cross-bridge cycling in smooth muscle is only one-tenth that encountered in skeletal muscle. The cross-bridges remain intact for a long period with each cycle, reflecting the lower rate of ADP release from the smooth muscle isoform of myosin (Webb, 2003).

2.2.4. Regulation of smooth muscle contraction

The amplitude of smooth muscle contraction depends on the balance of activities by MLC kinase and myosin light chain phosphatase (MLCP). These enzymes phosphorylate/ dephosphorylate the regulatory light chains of myosin II, respectively (Pfitzer, 2001)

In general, interacting signaling modulates regulation of smooth muscle contraction. The sequences of regulation include: Ca^{+2} / calmodulin-dependent MLC kinase activation, Ca^{+2} -independent regulatory myosin light chain phosphorylation, inhibition of myosin phosphatase activity. Regulation includes also actin filament-based proteins such as caldesmon and calponin, which are known to inhibit the actin-myosin interaction by binding to actin (Pfitzer, 2001; Andrea and Walsh, 1992).

2.2.5. Mechanisms of intracellular Ca^{+2} increase

The force of smooth muscle contraction is dependent on extracellular Ca^{+2} concentrations. Contraction is initiated by increase of Ca^{+2} concentrations inside the cell. Elevation of intracellular Ca^{+2} is mediated by the L-type voltage-dependent calcium channels (VDCCs). There are other mechanisms participating in the calcium transfer from its storage sites inside the cell to the cytosol. The Ca^{+2} releases from sarcoplasmic reticulum is activated by a variety of second messengers, such as IP₃, cyclic adenosine diphosphate ribose (cADPR). Alternatively, this activation is significantly accomplished by direct binding of calcium ions themselves to their respective channels in the SR membrane, a mechanism known as Ca^{+2} -induced Ca^{+2} release (CICR). IP₃ and ryanodine receptors (RyRs) are the major calcium release channels that display CICR (Webb, 2003; Sanders, 2001). Actually, IP₃ receptors and ryanodine receptor contain proteins such as kinases and phosphatases, which serve to regulate the sensitivity of these channels to calcium ions (Pfitzer, 2001). In addition, Ca^{+2} influx can occur by mean of the receptor-operated Ca^{+2} channels that are selective for Ca^{+2} transport (Webb, 2003).

2.2.6. Mechanisms of cytosolic Ca^{+2} removals

The elevated Ca^{+2} concentrations in smooth muscle cell must return to the resting level of about 1×10^{-7} M, in order to be ready for further stimulation. This is accomplished by the operation of different mechanisms. One major mechanism is through the plasma membrane Ca^{+2} - ATPase (PMCA). These high-affinity calmodulin-responsive Ca^{+2} efflux pumps are P-type transport proteins. As an ATPase, PMCA exploits the steep electrochemical gradient of calcium around the membrane, to pump it outward the cell using ATP. The function of PMCA can be regulated by different kinases such as cGMP-dependent protein kinase. PKG and cAMP-dependent protein

kinase (PKA), through phosphorylation of sites near the calmodulin binding site. Another protein spanning the plasmalemma and involved in calcium efflux from the cytosol by Na^+ - Ca^{+2} exchanger. This process utilizes energy from the electrochemical gradient of Na^+ to transport 3 Na^+ into the cell against one Ca^{+2} to the outside. As PMCA providing a fine tuning of resting $[\text{Ca}^{+2}]_i$, the Na^+ - Ca^{+2} exchanger has a role in the regulation of higher, stimulatory $[\text{Ca}^{+2}]_i$. Finally, it is important to mention the translocation of cytosolic Ca^{+2} towards the SR lumen by the sarcoplasmic reticulum Ca^{+2} -ATPase (SERCA) (Webb, 2003; Matthew *et al.*, 2004; Sanders, 2001).

2.2.7. Smooth muscle relaxation

Smooth muscle relaxation occurs either as a result of the direct action of a substance that inhibit the contractile mechanism, or simply by removal of a contracting stimulus. The process of relaxation requires a decreased intracellular Ca^{+2} concentration, and increased MLC phosphatase activity. Several Mechanisms are involved in the removal of Ca^{+2} from the cytosol, including the sarcoplasmic reticulum and the plasma membrane Ca^{+2} influx into the sarcoplasmic reticulum or outside the cells at the expense of ATP hydrolysis. The sarcoplasmic reticular Ca,Mg -ATPase under phosphorylation binds 2 Ca^{+2} , before they are pumped to the luminal side of SR. The plasma membrane also contains Ca,Mg -ATPases, which provides additional mechanism for decreasing the concentration of activator Ca^{+2} in the cell. The $\text{Na}^+/\text{Ca}^{+2}$ exchangers are located on the plasma membrane and further aid in reducing the intracellular Ca^{+2} concentrations. Moreover, calsequestrin and the multifunctional protein calreticulin have been identified as sarcoplasmic reticular Ca^{+2} -binding proteins in smooth muscle, which decrease intracellular Ca^{+2} levels. Many proteins like, phospholamban (PLB), PMCA, IP3 receptor, MLC kinase, and telokin are targets of phosphorylation by cyclic nucleotide-dependent protein kinases including cyclic

adenosine monophosphate (cAMP), and cyclic guanosine monophosphate (cGMP) (Webb, 2003; Andrea and Walsh, 1992).

The two principal intracellular pathways for smooth muscle cell relaxation are believed to be activated by cGMP and cAMP. The cGMP is generated by the soluble form of guanylyl cyclase in response to nitric oxide (NO), or in response to peptides like atrial natriuretic peptide, The cAMP is synthesized from ATP by activated adenylyl cyclase (Peters and Michel, 2003).

Some vasodilators, such as nitric oxide (NO), are an example of important regulator of vascular and nonvascular smooth muscle relaxation, acting via the cGMP-PKG pathway. It induces the relaxing effect by different ways, like inhibiting the release of Ca^{+2} via the IP3 receptor, or through the stimulation of SERCA to enhance Ca^{+2} re-uptake into SR (Sanders, 2001).

Other agonists that elevate cAMP through the activation of adenylyl cyclase stimulatory heterotrimeric G protein (Gs)-protein-coupled receptors. After cAMP production, there will be increase of cAMP-dependent protein kinase A activity. The phosphorylation of MLC kinase by PKA, prevents the activation of Ca^{+2} -CaM complex. Furthermore, cAMP causes PKA-dependent phosphorylation of PLB, which increases Ca^{+2} reuptakes into the sarcoplasmic reticulum (Bai and Sanderson, 2006).

2.3. Cardiac muscle

Although the continuous and rhythmic contractility of the myocardium is affected by a specialized conducting system of modified cardiac myocytes, the rate of this inherent rhythm still needs to be controlled by both autonomic and hormonal stimuli. Therefore, presence of unique organelle arrangement within cardiac muscle fibers is expected to accommodate for its highly organized function (Mohrman and Heller, 2006).

The transverse tubules (t-tubules) of mammalian cardiac ventricular myocytes are invaginations of the surface membrane that occur at the Z line. They have both transverse and longitudinal elements, which occur predominantly in ventricular myocytes. The unique arrangement of this network of narrow tubules with a mean diameter of $\approx 200\text{-}300\text{ nm}$, ensures that Ca^{+2} release occurs synchronously throughout the cell to be extruded rapidly (Soeller and Cannell, 1999). Moreover, t-tubules have a variety of proteins involved in cellular Ca^{+2} cycling which are concentrated at the t-tubule. Thus, t-tubules are important for cardiac cell function. Many studies indicated the presence of Ca^{+2} , Na^{+} , K^{+} , and anion handling proteins, like the long-lasting Ca^{+2} channels (LTCCs), $\text{Na}^{+}\text{-Ca}^{+2}$ exchanger, $\text{Na}^{+}\text{-H}^{+}$ exchanger, $\text{Na}^{+}/\text{K}^{+}$ ATPase, K^{+} -channel TASK-1 (tandem pore domain acid-sensitive K^{+} channel), and $\text{Cl}^{-}\text{-HCO}_3^{-}$ exchanger, in the t-tubule membrane (Scriven *et al.*, 2000; Brette and Orchard, 2003; Orchard and Brette, 2008). Therefore, t-tubules are the most important site for excitation-contraction coupling due to the presence of many proteins, including those involved in cellular Ca^{+2} cycling. In this regard, the Ca^{+2} channels in the t-tubules are highly colocalized with RyRs in the sarcoplasmic reticulum, forming the diad, where the t-tubule is only associated with one terminal cisternae of the sarcoplasmic reticulum (Brette and Orchard, 2003; Orchard and Brette, 2008).

2.3.1. Cardiac excitation-contraction coupling

The contraction of a ventricular myocyte is initiated by an influx of Ca^{+2} from the extracellular space that induces the release of a much larger amount of Ca^{+2} from the sarcoplasmic reticulum. Upon membrane depolarization, Ca^{+2} enters the cytosol through a voltage-gated L type Ca^{+2} current (ICa), which triggers Ca^{+2} release from the SR via Ca^{+2} transport channels (ryanodine receptor) to activate contractile machinery. Then calcium will bind to troponin C (TnC), which transmits information via structural changes throughout the actin-tropomyosin filaments to stimulate myosin ATPase activity and muscle contraction (Korzick, 2003; Scriven *et al.*, 2000).

Relaxation is brought about by removal of Ca^{+2} from the cell cytoplasm by two main routes. The SERCA is regulated by PLB to pump calcium back into the SR, while the Na^{+} - Ca^{+2} exchanger uses the inwardly directed electrochemical gradient of sodium to efflux calcium from the cytosol across sarcolemma (Korzick, 2003; Orchard and Brette, 2008).

2.3.2. Regulation of cardiac excitation-contraction coupling

Although the cardiac muscle is a myogenic tissue, but to function properly, it must be subjected to intrinsic and extrinsic regulatory mechanisms (Mohrman and Heller, 2006). One important example is provided by the removal of Ca^{+2} from the cytoplasm by SERCA and Na^{+} - Ca^{+2} exchanger, which are regulated by second messenger pathways, especially the β -adrenergic pathway. LTCC, SERCA, RyR, and PLB all have been reported to be phosphorylated by PKA and Ca^{+2} -CAM dependent protein kinase II (CaMKII), and Na^{+} - Ca^{+2} exchanger by PKA (Orchard and Brette, 2008).

In this context, it is important to highlight the presence of control mechanisms at the level of the sarcomere, especially those acting via G protein-coupled receptors

(GPCRs), immediately upstream of sarcomeric protein substrates. Major substrates are the thin filament proteins troponin I (TnI), troponin T (TnT) and TM, which contribute to transducing the Ca^{+2} -TnC signal. Besides, the myosin binding protein C (MyBP-C) and rMLC acts to control the radial movement of cross-bridges from the thick filament backbone. A further protein titin (Also known as connectin) is a giant third filament that controls the diastolic tension as well as the length-dependent radial movement of cross-bridges (Fukuda *et al.*, 2001; Hinken and Solaro, 2006; Solaro, 2008).

2.4. Morphological changes caused by cigarette smoking:

Based on the available evidence, cigarette smoking was significantly associated with myocardial infarction (MI), atherosclerosis and death from other diseases (Barnoya *et al.*, 2005; De Rosa *et al.*, 2008). The pathophysiological effects of cigarette smoking on atherosclerosis may include enhancement of platelet aggregation, increase of blood viscosity, protein damage, lipid peroxidation and alternation in the haemostatic systems. The toxicity effect of cigarette smoking on the endothelium is a further possible mechanism for explaining the link between atherosclerosis and smoking (Wannamethee *et al.*, 2005; Winkelmann *et al.*, 2009).

The endothelium forms a living interface between circulating blood in the lumen and the rest of vessel wall. In fact, the endothelial cell (EC) injury caused by cigarette smoking leads to an increase in the number of circulating endothelial cells and decreasing the serum concentration of nitrate plus nitrite temporary. Also, it produces an increase in endothelial permeability and morphological changes of the endothelium (Jorge *et al.*, 1995; Yanbaeva *et al.*, 2007). Lin *et al.* (1992) showed that under chronic exposure to nicotine in rats may increase the frequency of the endothelial cell death. The outcome of this death was enhancement in transendothelial leakage of macromolecules such as LDL that could lead to the acceleration of atherogenesis.

Light and electron microscopic studies of pulmonary arteries from rats exposed to cigarette smoking showed a pronounced muscularization of the small pulmonary arteries. Also, there was an intimal and medial thickening that was associated with the cellular elements and extracellular matrix. The smooth muscle cell proliferated and migrated from media of the artery, their shape was modified and there was an increase in rough endoplasmic reticulum. The endoplasmic surface comprised thick, deep "cable like" ridges, and the endothelial fenestrae become apparent. Besides, there was swelling of the mitochondria as well as an increase in the volume density of microfilament and pinocytic vesicle in the endothelial cells (He, 1991; 1992). Pittilo *et al.*, (1982) used scanning electron microscopy to examine the aortic endothelium from rats exposed to graded doses of fresh cigarette smoking. This examination showed the formation of blebbing and microvillus-like projections from the luminal surface. In guinea pig, similar exposure to cigarette smoke induced selective endothelial dysfunction in pulmonary arteries but not in the aorta. Also, it caused smooth muscle cell proliferation in small pulmonary vessels and reduced lung expression of endothelial nitric oxide synthase (eNOS). These changes appeared after 3 months of exposure and preceded the development of pulmonary emphysema (Ferrer, 2009).

Microtubules (MT) are major cytoskeleton filaments that mediated important cellular properties, such as proliferation, migration, and maintenance of the cellular morphology. These filaments have been adversely affected in dose and time-dependent manner during the smoke extract-treated human lung epithelial (A549) cells and noncarcinoma human lung alveolar epithelial (L132) cells. The damage of MT by the smoke extract may be correlated with the pathogenesis of cigarette smoke induced disorders, which result in cellular apoptosis and tissue damage (Das *et al.*, 2009). Ozbay

et al. (2009) showed that Long-term exposure of rats to smoke was associated with focal small anthracotic accumulations, multiple abscesses, cysts with mucinous fluid and emphysematic changes in the lungs. The lymphocytic, eosinophilic and macrophage infiltrations in varying densities were observed in the interstitium of the lungs. Based on the exposure time, small papillary structures were observed in the airway mucosa. As most apparent in pulmonary veins, the intima and media of the pulmonary vessels were thickened and their lumens were narrowed. The bronchoalveolar lavage from cigarette smokers has increased numbers of alveolar macrophages (AMs) and neutrophils (Adesina *et al.*, 1991; Bosken *et al.*, 1992). These macrophages obtained from cigarette smokers were deficient in phagocytosis and bactericidal activity (Plowman, 1982). Simet *et al.*, (2010) studied the chronic cigarette smoke exposure in a mouse model and found it to decrease airway epithelial cell ciliary beating in a protein kinase C-dependent manner. The chronic cigarette smoke is also associated with airway epithelial mucus cell hyperplasia together with a decrease in number of ciliated cells and their cilia. In another study using Wistar rat, the effect of long-term tobacco smoke on ultrastructure and expression of Transforming growth factor beta-1 (TGF- β 1) in alveolar epithelium was investigated (Ruobao *et al.*, 2008). The tobacco smoke resulted in damaging the ultrastructure of alveolus epithelium, which is conspicuous with the increase in smoking period. They suggested that the pathological changes are correlated with the expression of TGF- β 1. The effect of cigarette smoke on trachea tissue of wistar rat showed several morphological changes including loss of cilia in the epithelial layer, an increase of goblet cells, activation of serous glands in the submucosa, and cell infiltration. These morphological changes were correlated with the amount of toxic substances in the cigarette smoke (Kurus *et al.*, 2009).

The mitochondria have essential roles in cell function including energy production, oxidant signaling, apoptosis, immune response, and thermogenesis. Tobacco smoke exposure, which cause mitochondrial damage and dysfunction will likely play an important role in the development of multiple forms of human diseases including cardiovascular disease (Yang *et al.*, 2007).

Ultrastructural changes of 9-day old mouse embryos following mother smoke inhalation, showed mitochondria elongation in shape with less distinct cristae (Bnait and, Seller, 1995). They suggested that maternal smoking may cause anoxia in the embryo. The initial ultrastructure and expression of surfactant protein A (SPA) in the lung of passive smoking mice was studied. The ultrastructure of type II alveolar cell, showed mitochondrial was vacuolar, multilamellar body was increased and degranuled. Also, the level of surfactant protein A in experimental group was gradually decreased (Hua *et al.*, 2007).

Myocardium of Guinea pigs following filtered and unfiltered smoke inhalation demonstrated evident toxic changes in myocardial mitochondria associated with edema. The alterations in mitochondria involved irregular shape and size together with separation of the outer mitochondrial membrane. In addition to that there was an enhanced autophagolysosomal activity and increased lipid contents (Lough, 1978).

Electron microscopy of ventricular myocardium after chronic exposure to cigarette smoking in dog showed no significant changes in the structures of mitochondria, myofibrils, sarcolmma or nuclei, although an increase in intracytoplasmic glycogen appeared to be present (Ahmed *et al.*, 1976).

2.5. Physiological effects of cigarette smoking

The endothelium is the first layer in the arterial bed that has contact with the blood. Being the largest endocrine organ, endothelium has several functions that involve the regulation of vascular smooth muscle tone, platelet adhesion and aggregation, local clotting and vascular growth. The endothelium serves dual role in the control of vascular tone by secreting relaxing and constricting factors (Glasser *et al.*, 1996). The damage of endothelium leads to decreased vessel dilation, increased contraction, proinflammatory, prothrombotic states and cell proliferation in the arterial wall. Consequently, the endothelial dysfunction may contribute to atherosclerotic plaque formation and a decrease in blood flow because of thrombosis and vasospasm, which is finally leading to cardiovascular disease (Widlansky *et al.*, 2003; Michael, 2000).

Some reports showed that endothelium-dependent arterial relaxation is impaired in smokers (Zeiber *et al.*, 1995; Heitzer *et al.*, 1996; Ambrose and Barua, 2004). Also, they demonstrated that chronic cigarette smokers have decrease in endothelial nitric oxide (NO) activity, leading to the impairment of endothelium dependent relaxation (EDR) (Barua *et al.*, 2001; Barua *et al.*, 2003). Torok *et al.*, (2000) showed that chronic passive smoking impairs endothelium-dependent relaxation of isolated rabbit arteries.

Free radicals in cigarette smoke extract (CSE) induce the impairment in endothelium-dependent relaxation (EDR) of isolated rabbit aortas which may be partly due to the suppression of NO production. The captopril attenuates the CSE-induced endothelial dysfunction partly through the scavenging of free radicals (Ota *et al.*, 1997). Sugiyama *et al.*, (1998) studied the effect of cigarette smoke extracts (CSE) on thoracic aortas of 1.5% cholesterol-fed rabbits and control rabbits. They found that atherosclerotic arteries exhibited supersensitive contractile response to superoxide anion derived from CSE. This susceptibility to oxidative stress by smoking could lead to the

genesis of coronary spasm and acute coronary syndrome in atherosclerotic arteries (Sugiyama *et al.*, 1989). In isolated pig coronary arteries, the cigarette smoke extracts were also involved in stimulating biphasic tension change, initial contraction and subsequent relaxation during stable contraction with prostaglandin F2 α , (Murohara *et al.*, 1994). The initial contraction may be in part mediated through the degradation of nitric oxide by the superoxide anions derived from CSE. However, the water-soluble components of cigarette smoke, can induce relaxations of isolated rat renal arteries, that are independent of endothelium, nicotine and cGMP-related vasomotor mechanisms (such as NO or CO) (Halmai *et al.*, 2009).

D-nicotine and L-nicotine both are nicotine isomers but have different physiological effects. L-nicotine was the main isomer in cigarette smoke which produced a biphasic response in guinea-pig trachea characterized by an initial contraction followed by relaxation (Hummel *et al.*, 1992; Funayama *et al.*, 1995). In tracheal preparation of the same animal, the D-nicotine isomer produced only relaxation in a concentration-dependent manner (Hummel *et al.*, 1992; Funayama *et al.*, 1995). Nicotine may act directly by affecting vascular smooth muscle cells, or through a receptor-mediated response, or by both (Hanna, 2006; Christ and Brink, 2000). However, the relaxation caused by nicotine may be mediated by NO production (Zhang *et al.*, 1998). Acute exposure to CSE leads to airway relaxation, which is partially mediated by nicotine (Streck *et al.*, 2010). Cevit *et al.*, (2007) investigated the mechanism of nicotine effects on isolated trachea preparations from ovalbumin-sensitized and control guinea-pigs. In both sensitized and control animals, they showed that nicotine produced a concentration-dependent relaxation on tracheal preparation which was precontracted by carbachol (10^{-6} M). At least this relaxation is mediated in part by nitric oxide (NO) production, since it was significantly reduced in the presence

of N (w)-nitro L-arginine methyl ester L-NAME which is known inhibitor of NO production. Recently, the effect of nicotine on isolated aorta, trachea and the bronchial resistance, was investigated (Hemmati and Jayhoon, 2011). The nicotine at concentrations of 10^{-8} to 10^{-2} M had no contractile effect in isolated rat aorta and trachea, and also can not elicit bronchoconstriction in rat. Apparently, nicotine alone has no direct effect on isolated bronchus, aorta or bronchial resistance. However, its adverse effect on human health may be due to other components present in cigarette smoke (Hemmati and Jayhoon, 2011). The antioxidant vitamin C improves the impairment of endothelium-dependent vasodilatation observed in chronic smokers. Thus, it seems that oxygen free radical formation by chronic smoking plays an important role in the impaired reactivity of large vessels (Motoyama *et al.* 1997; Heitzer *et al.*, 1996).

Ambrose *et al.*, (2004); Benowitz *et al.*, (2000) and Gottlieb, (1992), showed that nicotine in cigarette smoke is probably the most studied component. The nicotine plays major role in smoking-related increases in cardiac output, heart rate, blood pressure and thus myocardial oxygen demand. On the other hand, Long-term exposure of dogs to cigarette smoke or nicotine exhibited a significant deficit in heart contractility (Ahmed *et al.*, 1976). Furthermore, chronic exposure to nicotine in rat resulted in initial fall in heart rate, then a rise during following weeks (Lin *et al.*, 1992). The treatment of isolated perfused rat heart by one of three solutions: Krebs-Henseleit solution (KHs) containing 10% CO 85% O₂ 5% CO₂, 10 µg/ml nicotine, or CO combined with nicotine produced the following results. The carbon monoxide increased coronary flow by 41% without affecting heart rate; nicotine decreased heart rate by 20% and coronary flow by 28%, while combination of both decreased heart rate by 16% but stimulated coronary flow by 13%. Moreover, the separate effect of each treatment was reversible, but the effect they produced in combination was irreversible (McGrath, 1986; McGrath and

Smith, 1984). Another study by Chen and McGrath, (1985), demonstrated that CO caused a contractile depression as well as a decrease in heart rate of isolated rat hearts perfused with 95% CO 5% CO₂ KHs. In isolated perfused heart, the nicotinic acetylcholine receptors (nAChRs) that mediate the initial decrease in heart rate probably contain $\alpha 7$ subunits, whereas those that mediate the increase in heart rate probably do not contain $\alpha 7$ subunits. This result shows that pharmacologically distinct nicotinic acetylcholine receptors (nAChRs) are responsible for the differential effects of nicotine on heart rate. More specifically, this study suggests that $\alpha 7$ subunits participate in the initial nicotine-induced heart rate decrease, whereas $\beta 4$ subunits help to mediate the subsequent nicotine-induced rise in heart rate (*Ji et al.*, 2002).

2.6. Effect of smoking on antioxidant enzyme activities:

Cigarette smoke contains and generates various reactive oxygen species (ROS) and reactive nitrogen species (RNS), such as superoxide radical, hydrogen peroxide, hydroxyl radical, and peroxynitrite (Aoshiba and Nagay, 2003). The highly reactive radicals can act as initiators of carcinogenesis, cause DNA damage, activate procarcinogens and alter the cellular antioxidant defense system. The antioxidant defense system, which includes superoxide dismutase, glutathione peroxidase, catalase and Glucose-6-phosphate dehydrogenase enzymes, can work sequentially to dispose free radicals (Carnevali, *et al*, 2003; Avti *et al*, 2006). Catalase is a common enzyme present in the peroxisomes of nearly all aerobic cells, which functions in catalyzing the decomposition of hydrogen peroxide to water and oxygen without the production of free radicals (Chelikani *et al.*, 2004). Structurally, all studied catalases are tetrameric molecules composed of 4 polypeptide chains with a total of at least 500 amino acids. Each individual subunit has 60,000-dalton molecular weight polypeptide chain attached to a single molecule of heme prosthetic group. This prosthetic group assists in the

catalysis process by facilitating the interaction of the enzyme with hydrogen peroxide (Deisseroth and Dounce, 1970). The second enzyme is Glucose-6-phosphate dehydrogenase (G6PD), found in animal tissues, plant tissues and microorganisms (Abboud and Al-Awaida, 2010; Igoillo-Esteve and Cazzulo, 2006; Scharte *et al.*, 2009). Glucose-6-phosphate dehydrogenase (G6PD; D-glucose-6-phosphate: NADP⁺1-oxidoreductase, E.C.1.1.1.49) catalyzes the conversion of glucose-6-phosphate to 6-phosphogluconate in the pentose phosphate cycle. This house keeping enzyme provides reductive potential in the form of NADPH, to maintain several cellular biosynthetic pathways (Luzzatto and Battistuzzi, 1985), and monitoring the cellular redox regulation (Salvemini *et al.*, 1999). The isolated clones of defective G6PD gene were very sensitive to oxidizing agents like H₂O₂, indicating the importance of this enzyme in protecting cells against oxidative stress (Pandolfi *et al.*, 1995). The third enzyme is glutathione peroxidase (GPx), which can metabolize a wide range of organic hydroperoxides as well as hydrogen peroxide. This enzyme contains four selenium ions and found in different cell fractions and tissues of the body (Arthur, 2000).

Avti *et al.*, (2006) studied the effect of 32 weeks oral treatment for Male Wistar rats with aqueous extract of smokeless tobacco (AEST) at low dose (96 mg/kg body weight per day). In liver, AEST decreased GSH levels and the activities of superoxide dismutase (SOD), Catalase (CAT), and GPx by 34.6%, 29%, 17.1%, and 17.4%, respectively, but it increased lipid peroxidation (Lpx) by 64%. In kidney, GSH, SOD, CAT, and GPx were decreased by 26.6%, 23%, 33%, and 18%, respectively, with an increase of Lpx by 65%. The AEST decreased the lung GSH, SOD, CAT, and GPx, and increased lung Lpx by 43%, 28.5%, 37%, 40%, and 24%, respectively. This reduction of specific enzymes activity was associated with mild to moderate inflammation in liver and lung tissues. In another study, using Walton reverse-smoking exposure apparatus,

the 21 days exposure of thirty-day-old rats to thirteen cigarettes per day allowed an increase in the activity of glutathione peroxidase, glutathione reductase, and glucose-6-phosphate dehydrogenase 34%, 24%, and 38%, respectively, over control values (York *et al.*, 1976). However, this dose of cigarette exposure did not cause detectable histological changes.

The acute exposure of alveolar epithelial cells from lungs of rabbits and rats to cigarette smoke resulted in reducing the activities of GPx and G6PD (Rahman *et al.*, 1995; Joshi *et al.*, 1988). Mukherjee *et al.*, (1993) studied the effects of chronic exposure of guinea pigs to cigarette smoke under both mainstream (MS) and sidestream (SS) conditions with emphasis on the activities of major antioxidant enzymes and lipid peroxidation of erythrocytes. The smoke-exposed groups had an increase in the activity of superoxide dismutase (SOD), a decrease in the activities of glutathione peroxidase (GPx) and NADPH generating enzymes. In contrast, this smoking treatment caused an increase of the *in vitro* lipid peroxidation for both mainstream and sidestream exposed erythrocytes of animal groups, though such increase was higher in the mainstream exposed group.

2.7. Cigarette smoke-induced apoptosis

There are two types of cell death: apoptosis and necrosis (Zimmermann *et al.*, 2001). Necrotic cell death is considered an accidental type of death, caused by gross cell injury, and results in the death of groups of cells within a tissue. In contrast, apoptotic cell death may be induced or is preprogrammed into death of individual cells (Zimmermann *et al.*, 2001). Apoptotic cells are characterized by certain morphological features, including membrane blebbing, cytoplasmic and nuclear shrinkage as well as chromatin condensation. The morphological changes observed in the nucleus of

apoptotic cells are, in part, due to the generation of DNA fragments through the action of endogenous endonucleases. Typically, the DNA of apoptotic cells is cleaved to 180–200 bp fragments (Arends *et al.*, 1990).

Kuo *et al.*, (2005) demonstrated that the effect of CS-induced lung injury including apoptosis, may be via reactive oxygen species and nitrogen oxides (NO_x) generation. The formation of these oxidizing agents either lead to the phosphorylation of p38/JNK MAPK pathway and then activation of Fas cascades, or to stimulate the stabilization of p53 and increase in the ratio of Bax/Bcl-2. This effect may induce apoptosis and may be an important pathway in the lung pathogenesis of CS. In other studies (Agostini *et al.*, 2001; Aoshiba *et al.*, 2001), the chronic mainstream cigarette smoke (CS) exposure of rat caused significant and time-dependent increase in the proportion of apoptotic cells of bronchial and bronchiolar epithelium. The oxidative stress was the initial event in the lung of guinea pig exposed to cigarette smoke, which was followed by inflammation, apoptosis and lung injury. All these pathophysiological events were reduced when the cigarette smoke-exposed guinea pigs were given black tea infusion as a drink instead of water (Banerjee *et al.*, 2007).

2.8. Smoking machine:

Many smoking machines have been developed for studying the chemical composition of cigarette smoke and its effect on human body (Baeza-Squiban *et al.*, 1999; Baker *et al.*, 2004; Chen *et al.*, 2008; Counts *et al.*, 2005). Rats, guinea pigs, and mice are used as experimental mammalian animals, to study the effect of mainstream smoke on structure and function of many organ systems as well as on antioxidant defense system of tested animals. Liswi, (1988) exposed albino rats to the smoke of three brands of Jordanian cigarettes for 3 months. She used a simple inhalation chamber that was connected to vacuum pump, with a continuous way of mainstream smoking. The inhalation time needs about 5-6 minutes to finish the burning of the cigarettes. Al-Kurd *et al.*, (2002) designed a special smoking machine to study the effect of exposing guinea pigs to cigarette smoke, which measured the timing of puff duration for 2.5 seconds. The smoking period was carried out for 3.5 and 5.5 months. In these machines, the effect of smoking on animal's tissues was not demonstrated. The modified smoking machine took in consideration the prevention of oxygen deprivation and poisoning by toxic gases such as CO poisoning in the inhalation chamber.

Furthermore, smoking machine should be applicable for studying the effects of cigarette smoke on different types of experimental animals (Shraideh *et al.*, 2011).

3. Materials and Methods

3.1. Chemicals

All chemicals were used as analytical grade:

Bovine serum albumin (Sigma-Aldrich, USA), Carbamoylcholine chloride (Sigma-Aldrich, Germany), Diglycidyl ether of polypropylene glycol (Fluka AG, Buchs SG, Switzerland), Dimethyl aminoethanol (Fluka AG, Buchs SG, Switzerland), Eosin Y (Riedel-de Haen, Seelze, Germany), Folin - Ciocalteu phenol reagent (Sigma-Aldrich, USA), Glutaraldehyde (BDH Chemicals, England), Glutathione reductase (Sigma-Aldrich, USA), Hydrogen peroxide 37% (Gainland chemical company, UK), L-Glutathione (Sigma-Aldrich, Japan), Lithium carbonate (Sigma-Aldrich, USA), LM brand (Jordan cigarettes company), L-nicotine (Merck Chemicals, Germany), NADPH (Sigma-Aldrich, USA), Neonyl succinic anhydride (Ted Pella, USA), Osmic acid (BDH Chemicals, England), papaverine (BDH Chemicals, England), Paraformaldehyde 4% (Fluka AG, Buchs SG, Switzerland), Phenylephrine hydrochloride (Sigma-Aldrich, Germany), Sodium azide (Research organic, USA), Sodium potassium tartarate (Scharlau chemie, European union), β -NADP (Sigma-Aldrich, USA), Vinyl cyclohexane dioxide (Fluka AG, Buchs SG, Switzerland).

3.2. Experimental design

Sixty male albino rats (*Rattus norvegicus*), obtained from the animals room/ Department of biological science/ University of Jordan, with an average weight of 100-150 g were divided into two groups. The first group (test) was exposed to cigarette smoke while the second group (control) was left untreated. The exposure to smoking was carried out as one dose daily for a period of 90 days, followed by a period of three months of non-exposure to smoking as a recovery stage from the effects of cigarette smoking. Following each period, a histological and biochemical studies were performed. Control animals were placed in the chamber and were exposed to fresh air instead of cigarette smoke.

3.3. The digital smoking machine

Exposure of animals to cigarette smoke has been done using a modified digital smoking machine (Shraideh *et al.*, 2011).

3.4. The effects of cigarette smoke on histology of the cardiovascular and respiratory systems: Light microscopy

3.4.1. Protocol of light microscopy

Following an overnight recovery from the last smoke exposure, rats were sacrificed by ether anesthesia and tissues of interest (trachea, alveoli of the lung, aorta, and ventricles of the heart), were gently dissected out, washed well with normal saline (0.9% NaCl), and fixed in 10% saline buffered formalin for at least 24 hrs. To ensure adequate fixation, the formalin fixative was used at volume 10-20 times more than the volume of tissue pieces. Dehydration was achieved by passing tissues through a graded series of alcohol followed by two changes of xylene. After infiltration in paraffin wax, tissues were embedded in pure paraffin wax (Avti *et al.*, 2006).

Sections (5µm thick) were obtained by a microtome (Spencer 50). Finally sections were mounted on glass slides and stained with hematoxylin and eosin. Sections were examined and photographed using Zeiss photomicroscope1, equipped with Moticam 2300 digital camera/ 3.0 Mega pixels.

3.5. The effects of cigarette smoke on tissue ultrastructure

3.5.1. Procedure of transmission electron microscopy

3.5.1.1. Preparation of blocks

Tissues of trachea, lung, aorta, and heart ventricles were directly cut into tiny pieces, approximately (1 mm³), and then immersed in the Karnovsky's fixative for 2 hr at room temperature. Tissue specimens were then washed with washing buffer (pH 7.2) for 30 min (3 changes), and then post-fixed with 1% osmium tetroxide in distilled water for 1 hr. at room temperature specimens were washed again three times, 10 min each with the washing buffer. Dehydration was done by immersing the tissues for 5 min once, in acetone concentrations of 30%, 50%, 70%, 95% and twice in 100% acetone. The specimens were infiltrated in a solution of 50% spurr's medium in acetone for 2 hr, followed by two successive changes of 100% spurr's medium, and left overnight with continuous smooth agitation. The samples were then embedded in pure spurr's medium and left in an oven at 60 °C overnight; to allow full polymerization of the resin (Alarifi *et al.*, 2004; Reynolds, 1963; Karnovsky, 1965).

3.5.1.2 Sectioning, Staining and Microscopy

Before sectioning, each tissue block was trimmed, to expose a suitable area of the tissue section. Silver-gold thin sections were obtained using the ultramicrotome (Reichert-Jung Ultracut E) and a diamond knife, and then mounted on a 200 mesh copper grids. Sections were stained with aqueous uranyl acetate in the dark for 20 min, and washed with boiled distilled water, and then post stained with lead citrate for 10 min. Finally, the stained sections were studied at 60 kilovolts, using Zeiss 10B transmission electron microscope (Alarifi *et al.*, 2004).

3.6. Detection of apoptosis in tissue sections

The presence of apoptotic cell death in tissue sections of trachea, alveoli of the lung, aorta, and ventricles of the heart, was examined using Dead End Colorimetric

TUNEL (TdT-mediated dUTP Nick-End Labeling) kit (Promega, USA)

3.6.1. TUNEL assay procedure (TUNEL kit, Promega)

1- Five Micrometer paraffin-embedded tissue sections obtained by a microtome (Spencer 50) were loaded on glass slides and then placed on a hot plate just to soften paraffin and directly transferred to xylene to be deparaffinized.

2- The slides were immersed in absolute ethanol for 10 min and then rehydrated in 95%, 85%, 70% and 50% ethanol, respectively, for 3 min each.

3- Two washing steps, 5 min each, with 0.85% NaCl, and phosphate buffered saline (PBS) (0.1M/pH 7.4), respectively.

4- Tissue sections were then fixed in 10% buffered formalin with PBS (0.1M/pH 7.4) for 15 min, and then immersed in PBS again for 10 min.

5- Tissue sections were put on a flat surface, and permeabilized with proteinase K for 10 min.

6- Two washing steps with PBS (0.1M/pH 7.4), 5 min each were carried out before and after the re-fixation of tissue sections for 5 min in 10% buffered formalin.

7- Tissue sections were equilibrated for 10 min using an equilibration buffer provided with the TUNEL (Promega kit).

8- Tissue sections were then incubated with TdT (Terminal deoxynucleotidyl

Transferase) reaction mixture provided with the TUNEL (Promega kit) at 37 °C for 1 hr.

9- The reaction was terminated by immersing the slides in saline-sodium citrate (SSC) buffer provided with the TUNEL (Promega kit) for 15 min.

10- In order to remove unincorporated biotinylated nucleotides (Biotinylated nucleotide is incorporated at the 3'-OH DNA ends using the enzyme Terminal deoxynucleotidyl

Transferase (TdT)), slides were immersed in PBS for 15 min.

11- To block endogenous peroxidases, tissue sections were immersed for 6 min in PBS solution containing 0.3% hydrogen peroxide.

12- Slides were washed in PBS for 15 min.

13- Slides were immersed in streptavidin HRP solution (bound to biotinylated nucleotides), and incubated for 30 min.

14- Slides were washed in PBS for 15 min.

15- Each tissue section was then immersed in the DAB solution. When a light brown background was observed by the naked eye, slides were gently rinsed several times with distilled water, mounted in glycerol, and photographed under a photomicroscope.

Tissue sections from control rats were considered as controls.

3.7. *In Vitro* physiological studies

Fifty male albino rats (*Rattus Norvegicus*), obtained from the animals room/ Department of biological science/ University of Jordan, weighing 200–250 g were used.

3.7.1. Isolated, perfused heart system

3.7.1.1. Protocol

Male rats (200–250 g) were pretreated with heparin (500 U/100 g) approximately 20 min before rat decapitation. Whole heart was carefully excised with the main trunk of the aorta remaining attached. The excised heart sample was transferred to a Petri-dish containing ice-cold physiological saline solution (PSS) buffer in order to trim of excess fat. After that the heart was transferred to the perfusion apparatus (Langendorff), where the aorta was tied onto a glass cannula connected to a reservoir located 70 cm above the heart. The reservoir contained PSS

which was continuously aerated, with a mixture of 95% O₂ and 5% CO₂. The temperature was maintained at 37 °C by temperature-controlled chamber. The perfusion was carried out at a constant flow rate of 5 to 7 ml/min. A small light stainless steel hook was inserted into the heart apex and connected by a thread to a force transducer (FT-302, CB Sciences, USA). This was further connected to a pen recorder (Cole Parmer, Chicago, IL). The isometric contractions of the beating heart were recorded under a tension of approximately 1 g. A syringe with needle attached to the side of the glass cannula was used to inject the test solution at specific concentrations immediately above the heart (Abdalla *et al.*, 1992; Donald and Davida, 1997; Zhang *et al.*, 1998; Ji *et al.*, 2002).

3.7.1.2. Preparation of cigarette smoke extracts (CSE)

CSE was prepared by bubbling mainstream smoke of one filter cigarette into 2 ml phosphate-buffered saline during 2.5 minutes (0.1M/pH 7.4) (Murohara, 1994).

3.7.1.3. The effect of cigarette smoke extract and L-nicotine on the isolated perfused heart

An equilibration period of 20-30 min with fresh PSS perfusate was performed to stabilize the heart rate. Then, various concentrations of cigarette smoke extract and L-nicotine (beginning with the lowest concentration) were individually injected through a needle located immediately above the aorta. The heart was perfused with aerated PSS before the injection of next compound concentration to ensure reaching a stable record. Changes in the heart rate as well as the force of contraction were examined, and the results were expressed as a percentage value relative to the control value obtained immediately before the addition of the test compound.

3.7.2. Tissue bath experiments

3.7.2.1. Protocol

A slight anesthetization of the animal by inhaling diethyl ether was rapidly followed by decapitation. Then, either aortic or tracheal tissue was dissected out and immediately transferred into warm aerated PSS (pH 7.4) before the clearing of adherent fat and connective tissue performance. One ring (2-3 mm in length) was obtained, and suspended in a water-jacketed tissue bath, filled with 9 ml fresh PSS. The ring was horizontally oriented and suspended by two wire clips passed through the lumen; one clip was anchored inside the tissue bath, while the other was connected to a force transducer (FT-302, CB Sciences, USA) (Schramm, 2000; Ignaz *et al.*, 1994). The tissue was then progressively stretched (approximately 1g for both aorta and trachea). The tissue bath solution was aerated with 5% CO₂ and 95% O₂ gas mixture, and the temperature was maintained at 37 °C by temperature-controlled chamber throughout the experiment. Rings of either aorta or trachea were then allowed to equilibrate at their optimal length for about 60 min and 90 minutes, respectively. To protect against interfering metabolites, buffer replacements were carried out every 15 minutes prior to further exposure for any test solution. Isometric tension was measured and recorded on a pen recorder (Cole Parmer, Chicago, and 1L) (Schramm, 2000; Martin *et al.*, 1997; Ignaz *et al.*, 1994).

3.7.2.2. Concentration-effects of CSE and pure L-nicotine on the contractility of aortic and tracheal smooth muscles

After an equilibration period (section 3.6.1.2), the aortic rings were precontracted with 0.01 mM phenylephrine (PE). Then various concentrations of CSE (0.1, 0.3, 1, 3, 10, 30, 60 and 100 µl/ml), or pure L-nicotine (2.4, 7, 24, 70, 240, 700, 2400 µg/ml), were added in a cumulative manner to the tissue bath. This was followed by addition of the non-specific relaxant papaverine (Pap) at 1 mM to induce maximum relaxation. The magnitude of the response induced by each added aliquot was calculated from the recorder and expressed as a percentage of the maximum response induced by papaverine. Each concentration was not added until the

tissue response to the previous concentration reached a plateau. Tracheal rings were treated similarly by CSE ($\mu\text{l/ml}$), and pure L-nicotine ($\mu\text{g/ml}$), except that the initial pre-contraction was achieved by 0.02 mM carbachol (CCh) (Lotriet *et al.*, 2007).

3.8. Biochemical studies

3.8.1. Cell extraction

Rat tissues of liver, lung, and kidneys were excised and perfused with ice-cold perfusion solution (0.15 M KCl, 2 mM EDTA, pH-7.4). Tissues were homogenized in Tris-HCl buffer (50 mM, pH 7.4), and the homogenates were centrifuged at 10,000 x g and 4°C for 30 min to obtain the supernatant. The latter was used for measurement of enzyme activities and estimation of protein concentration (Avti *et al.*, 2006).

3.8.2. Assay of catalase (CAT) activity

Catalase activity was measured in the tissue supernatant by the method of Luck, (1963). The reaction mixture contained 0.05 M Tris-buffer, 5 mM EDTA (pH 7.0), and 10 mM H_2O_2 (in 0.1 M potassium phosphate buffer, pH 7.0). The supernatant was added to the above mixture in a final reaction mixture of 3 ml. The rate of change in absorbance per minute was recorded at 240 nm. Catalase activity was calculated by using the molar extinction coefficient of $43.6 \text{ M}^{-1} \text{ cm}^{-1}$ for H_2O_2 . The level of CAT was expressed in terms of $\mu\text{moles H}_2\text{O}_2$ consumed/min /mg of protein.

3.8.3. Assay of glucose-6-phosphate dehydrogenase (G6PD) activity

The G6PD activity was measured by the method of Tian *et al.*, (1994). The supernatant was added to a mixture of 1 mM MgCl_2 , 1 mM sodium azide, 50 mM Tris-HCl buffer (pH 7.6), and 0.25 mM NADP in a final volume of 3 ml. The reaction was started in cuvette at 37°C by adding glucose 6-phosphate (0.6 mM). The increase in absorbance per min at 340 nm due to

reduction of NADP^+ to NADPH was measured in a spectrophotometer. Enzyme units were expressed as number of μmoles NADPH formed using the extinction coefficient $6.22 \times 10^3 \text{ M}^{-1} \text{ cm}^{-1}$ in 1-cm path at 340 nm. The levels of G6PD activity were expressed in terms of μmoles NADPH produced/min /mg of protein in crude extract.

3.8.4. Assay of glutathione peroxidase (GPx) activity

The GPx activity was measured by the method of Paglia and Valentine, (1967). The reaction mixture contained 50 mM potassium phosphate buffer (pH 7.0), 1 mM EDTA, 1 mM sodium azide, 0.2 mM NADPH, 1 U glutathione reductase, and 1 mM reduced glutathione. The mixture (2.9 ml) was allowed to equilibrate for 5 min at 25°C before initiating the reaction with 0.1 ml of 2.5 mM H_2O_2 . The-linear activity was recorded as absorbance at 340 nm. Units of enzyme activity were expressed as μmoles of NADPH oxidized to NADP by using the extinction coefficient of $6.22 \times 10^3 \text{ M}^{-1} \text{ cm}^{-1}$ at 340 nm. The levels of GPx were expressed in terms of μmoles NADPH consumed/min/ mg of protein in crude extract.

3.9. Spectrophotometric determination of nicotine in CSE

3.9.1. Method principle

This method is based on the development of a green color; due to the reduction of potassium permanganate to the manganate, which is equivalent to the oxidation of nicotine in the presence of sodium hydroxide. The green product absorbs strongly at wavelength of 610 nm (Al-Tamrah, 1999).

3.9.2. Protocol

The following procedure was adopted to a 25 ml volumetric flask:

- 1- Adding 1 ml of 0.0125 M potassium permanganate, followed by 2 ml of 6.25 M NaOH.
- 2- After a gentle mix, the desired amount of phosphate-buffered saline alone, phosphate-buffered saline with nicotine, or that of a CSE was added, and the volume was made up to about 20 ml with distilled water.
- 3- Then, the mixture was heated in a water bath at 100 °C for approximately 7.5 min.
- 4- The solution was cooled to room temperature, then, the volume was adjusted to 25 ml with distilled water.
- 5- Finally, sample of this solution was transferred to UV-9200 spectrophotometer to measure the absorbance at 610 nm against a reagent blank (Al-Tamrah, 1999).

3.10. Protein content determination

The protein concentration in the tissue homogenates was determined using Lowry method (Lowry et al., 1951).

3.11. Statistical analysis

All data in the physiological part are presented as means \pm SEM. Student's t-test for independent samples was used to determine whether differences between the mean values of the responses of the control and the experimental tissues, were significant. The differences were considered significant if the probability was less than 0.05 ($P < 0.05$).

Values for both specific enzyme activity and inflammatory cell count in BAL are expressed as mean \pm SEM. Statistical analysis was performed by the unpaired Student's t-test. A p-value < 0.05 was considered significant.

4. RESULTS

4.1. Spectrophotometric determination of L-nicotine

4.1.1 Calibration curve (Results are shown in appendix (B)).

4.1.2. L- nicotine content in CSE

One gram of cigarette tobacco produces an equivalent of 57 mg L-nicotine in CSE.

Table 1 provides the L-nicotine content in different CSE concentrations.

Table 1: L-nicotine content in the different CSE concentrations.

CSE ($\mu\text{l/ml}$ reaction mixture)	L-nicotine content ($\mu\text{g/ml}$ reaction mixture)
0.1	2.4
0.3	7
1	24
3	70
10	240
30	700
100	2400

4.2. Calibration curve for Lowry's protein assay using bovine serum albumin (BSA) as standard.

4.2.1. Calibration curve

This method gave linear relationship over the entire concentration range (0-100 µg/ml), with a correlation coefficient ($R^2 = 0.995$), which is used to determine protein concentration in tissues homogenates to calculate specific enzyme activity. Results are shown in appendix (C).

4.3. Results of *In Vitro* physiological studies

4.3.1. Tissue bath experiments

4.3.1.1. Effect of cigarette smoke extract (CSE) on isolated smooth muscle preparations

CSE, in concentrations ranging from 0.1-100 $\mu\text{l/ml}$ caused biphasic tension change in carbachol-precontracted trachea ($P < 0.05$) (Figures 1 and 5). Also, CSE in concentrations ranging from 0.1-100 $\mu\text{l/ml}$ induced biphasic tension change in isolated rat aorta during stable contraction to phenylephrine ($P < 0.05$) (Figures 2 and 5). The maximum contractant and relaxant effect of CSE on isolated aorta and trachea are shown in Table 2.

Table 2: The maximum response induced by CSE on rat isolated aorta and trachea preparations^a.

Tissue	N ^b	Maximum contraction effect (% of papaverine maximum)	Maximum relaxant effect (% of papaverine maximum)
Aorta	6	106.8 \pm 1.5	11.9 \pm 3.3
Trachea	6	115.9 \pm 5.8	12.2 \pm 3

^a Values are expressed as means \pm SEM.

^b Number of experiments.

4.3.1.2. Effect of pure L-nicotine on isolated smooth muscle preparations

L-nicotine, in concentrations ranging from 2.4-2400 µg/ml induced a biphasic tension change in carbachol-precontracted tracheal rings ($P < 0.05$) (Figures 3 and 6). Also, L-nicotine in concentrations ranging from 2.4-2400 µg/ml caused a biphasic tension change in phenylephrine-precontracted aortic rings ($P < 0.05$) (Figures 4 and 6). The maximum contracting and relaxant effect of L-nicotine on isolated aorta and trachea are shown in Table 3.

Table 3: The maximum response induced by L-nicotine on rat isolated aorta and trachea preparations^a.

Tissue	N ^b	Maximum contraction effect (% of papaverine maximum)	Maximum relaxant effect (% of apaverine maximum)
Aorta	6	117.1±2.8	58.6±3.7
Trachea	6	104.9 ± 1.3	29.8 ±4.3

^a Values are expressed as means ± SEM.

^b Number of experiments.

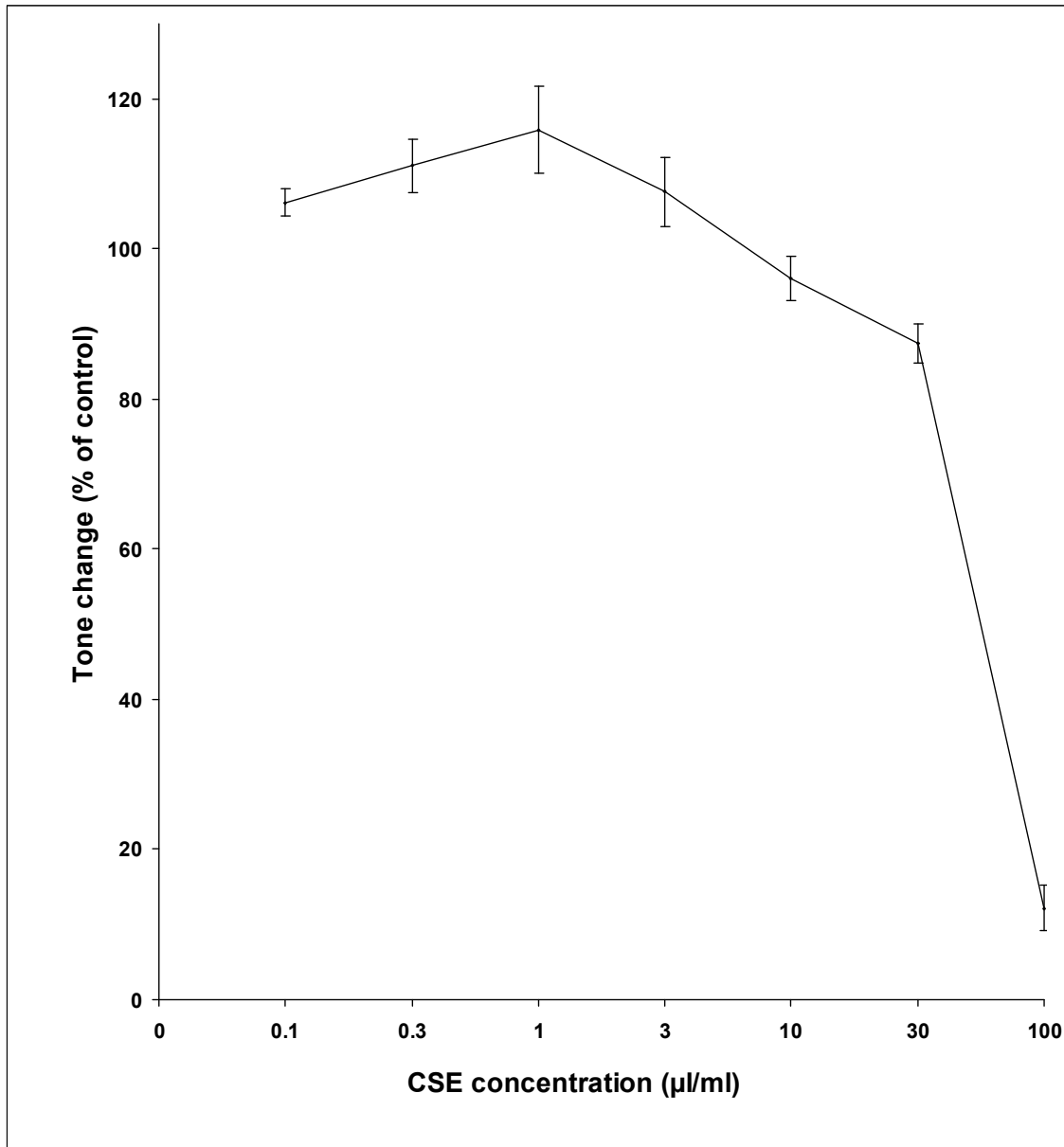


Figure 1: Cumulative concentration-effect curve of CSE on carbachol-precontracted tracheal rings. Tone change is given as the means \pm SEM of 6 experiments.

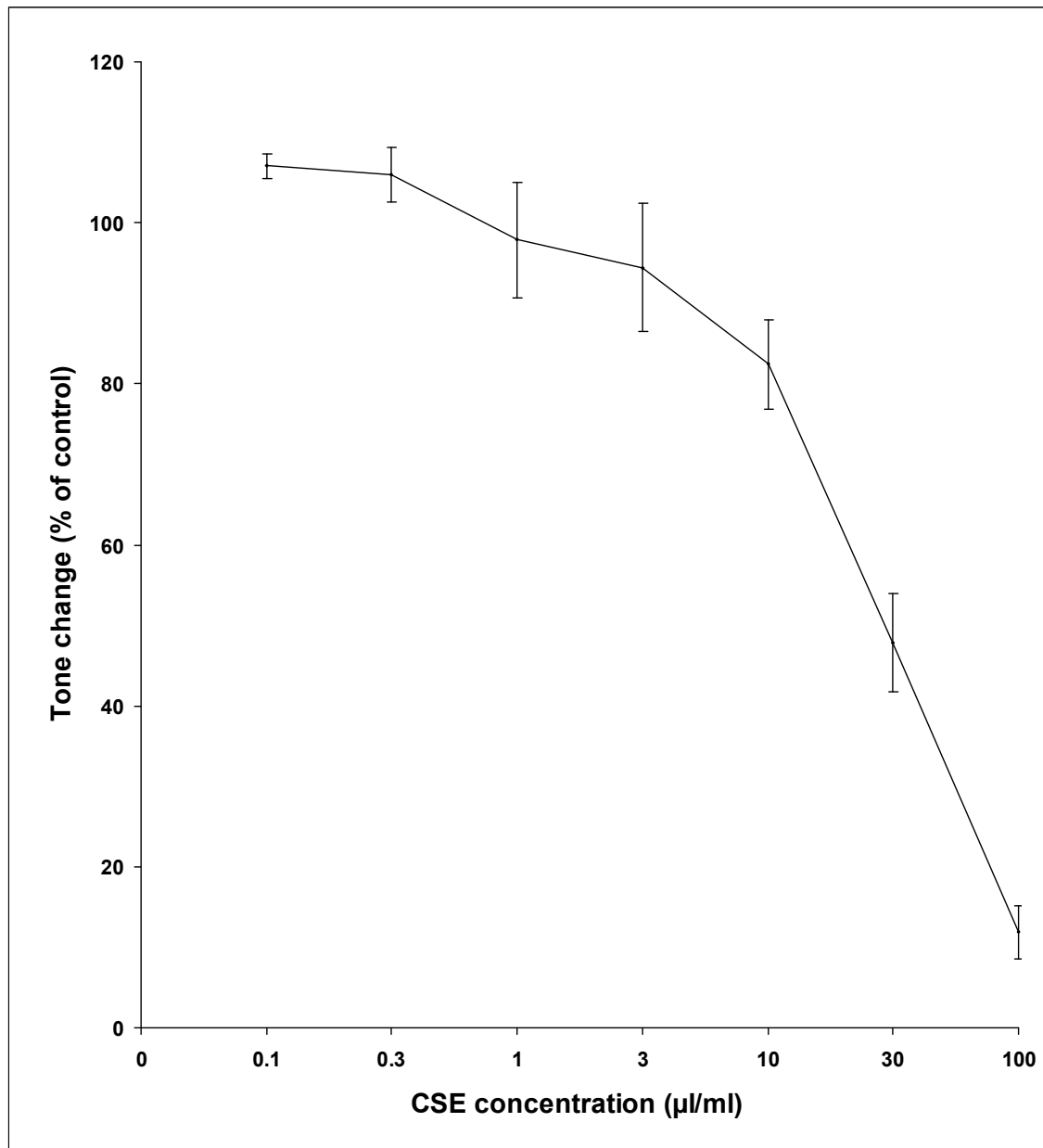


Figure 2: Cumulative concentration-effect curve of CSE on rat phenylephrine-precontracted aorta. Tone change is given as the means \pm SEM of 6 experiments

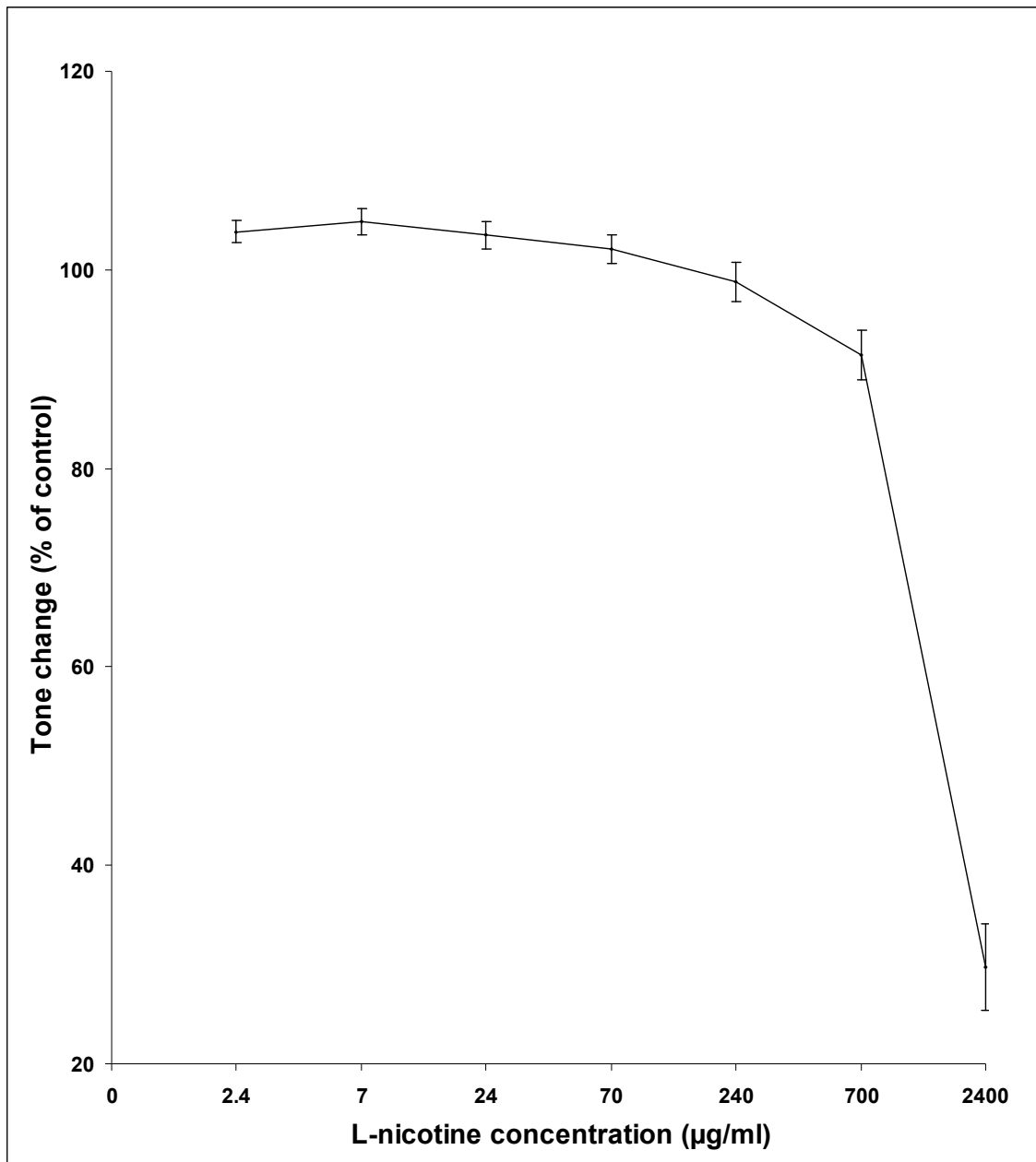


Figure 3: Cumulative concentration-effect curve of L-nicotine on carbachol-precontracted tracheal rings. Tone change is given as the means \pm SEM of 6 experiments.

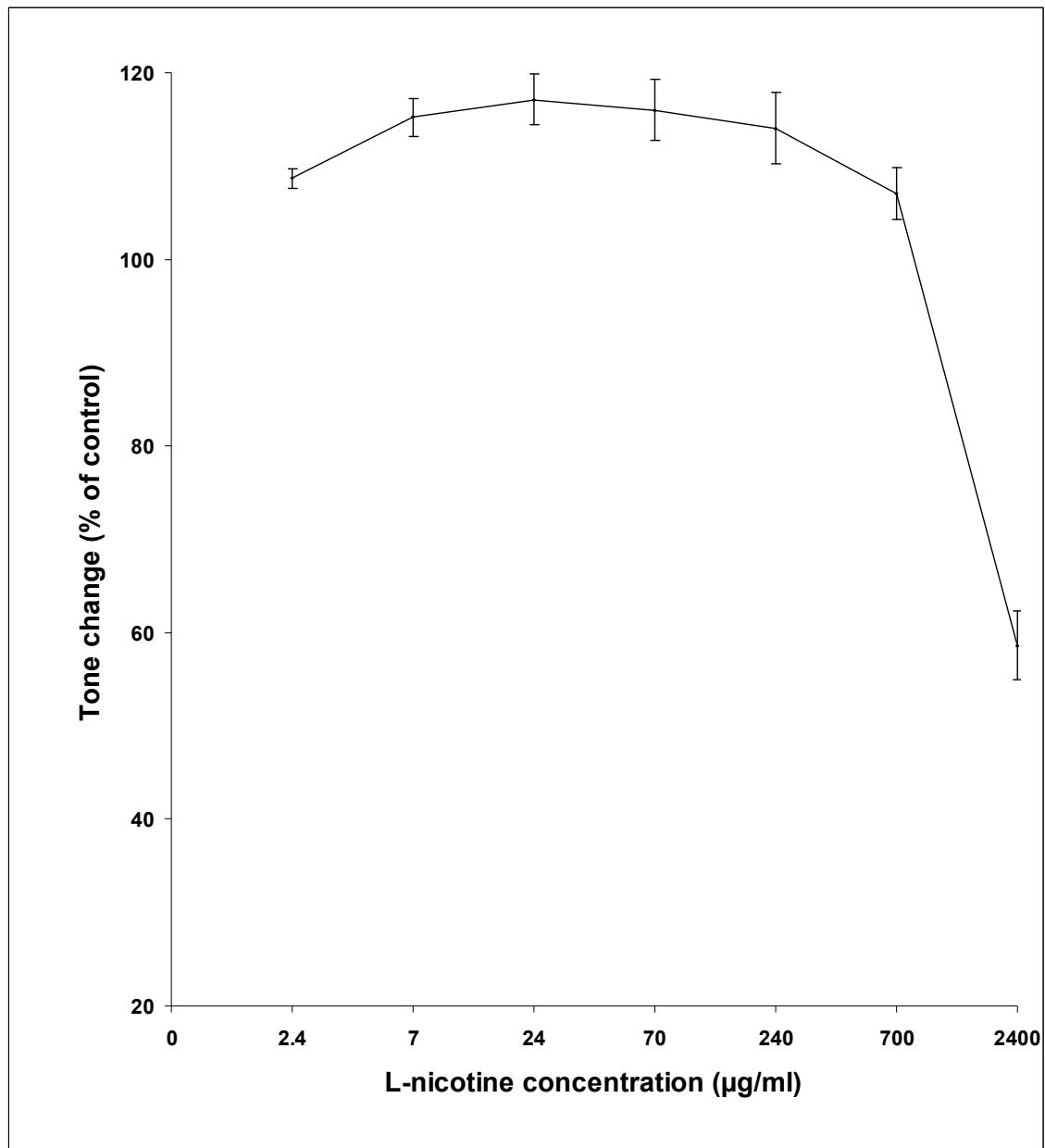
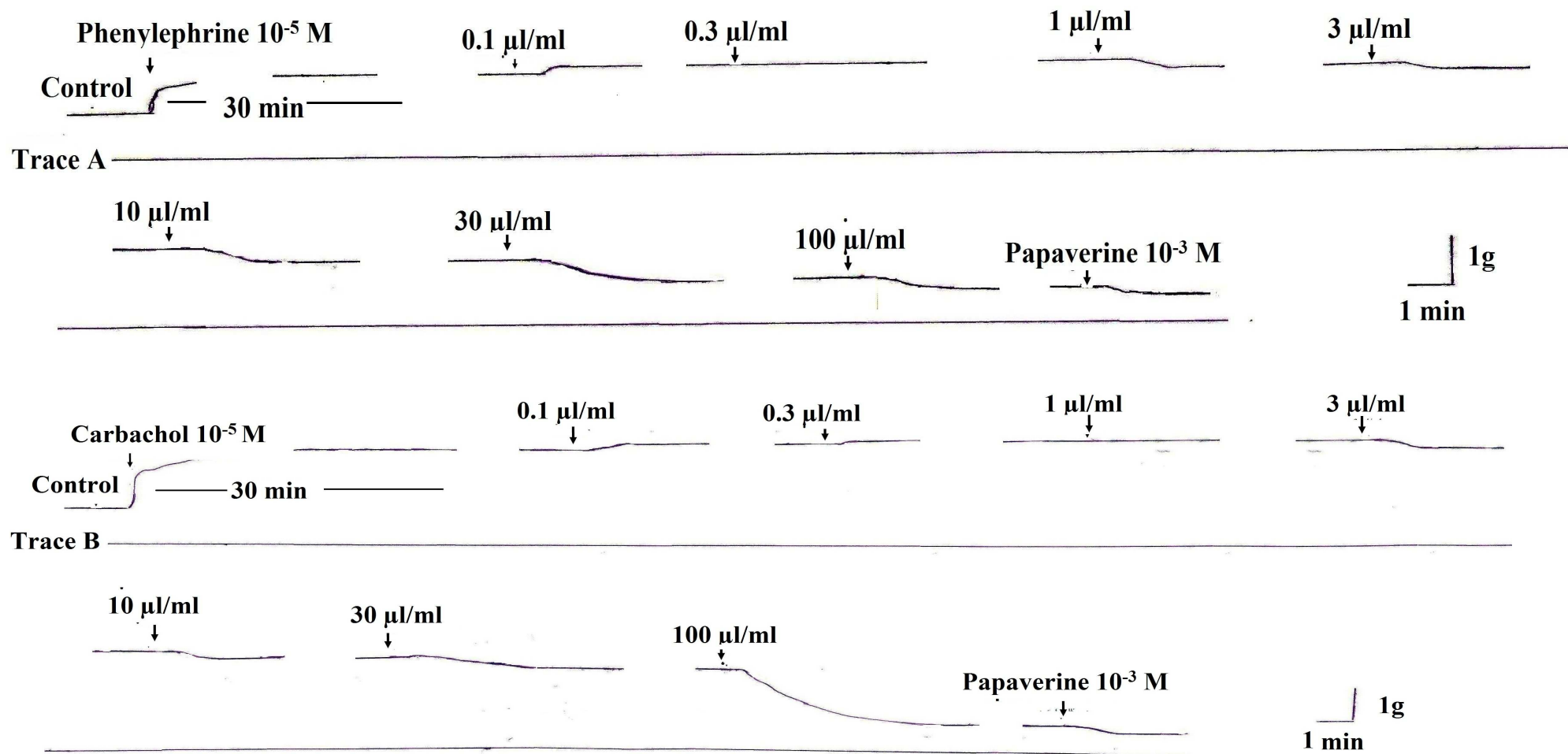


Figure 4: Cumulative concentration-effect curve of L-nicotine on rat phenylephrine-precontracted aorta. Tone change is given as the means \pm SEM of 6 experiments.



Figures 5: Effects of various concentrations of cigarette smoke extract (CSE) on rat isolated phenylephrine-precontracted aorta (trace A), and carbachol- precontracted trachea (trace B). (Times scale is not applicable to intervals of the traces).

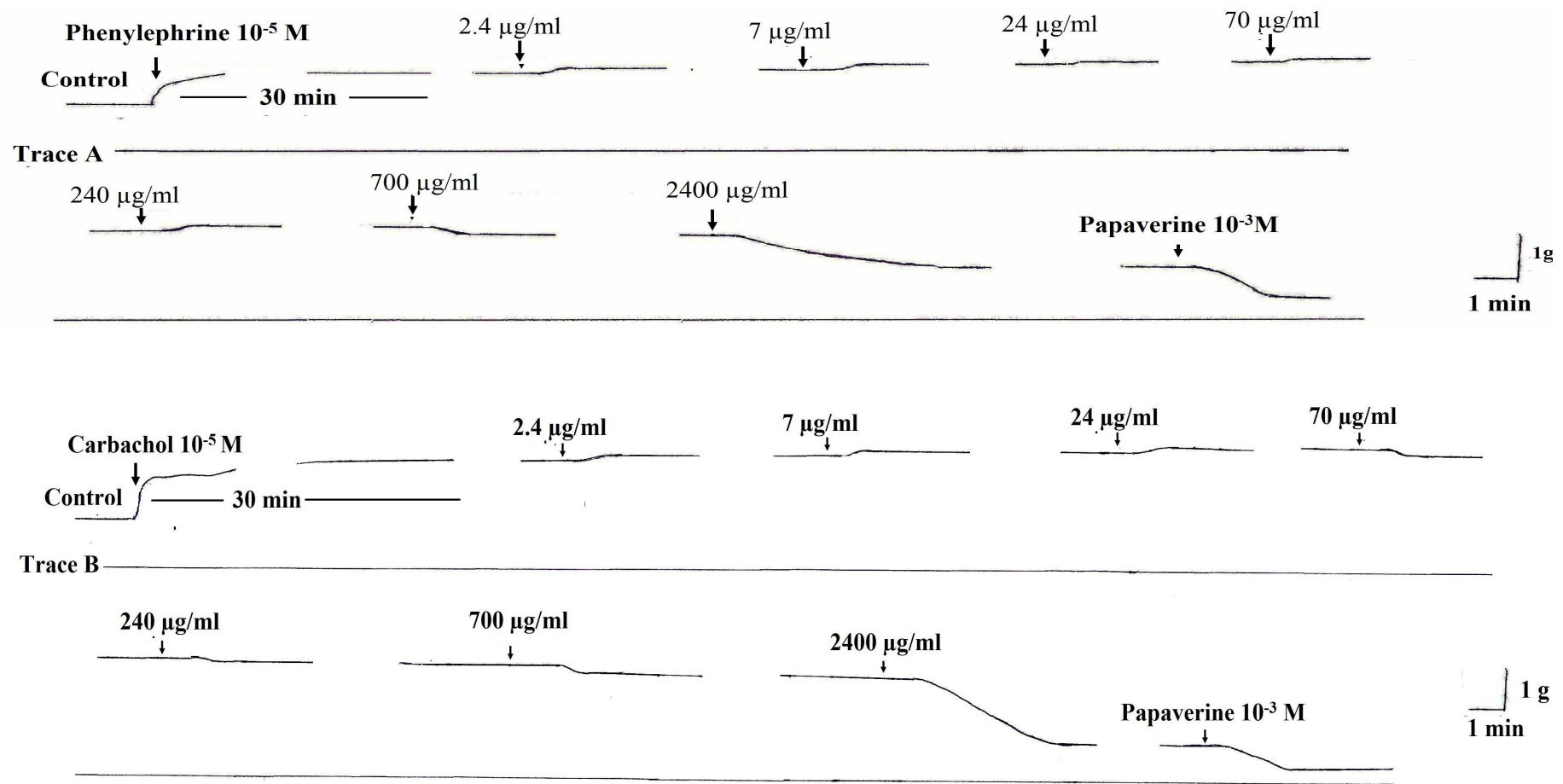


Figure 6: Effects of various concentrations of L-nicotine on rat isolated phenylephrine-precontracted aorta (trace A), and carbachol-precontracted trachea (trace B). (Times scale is not applicae to intervals of the traces).

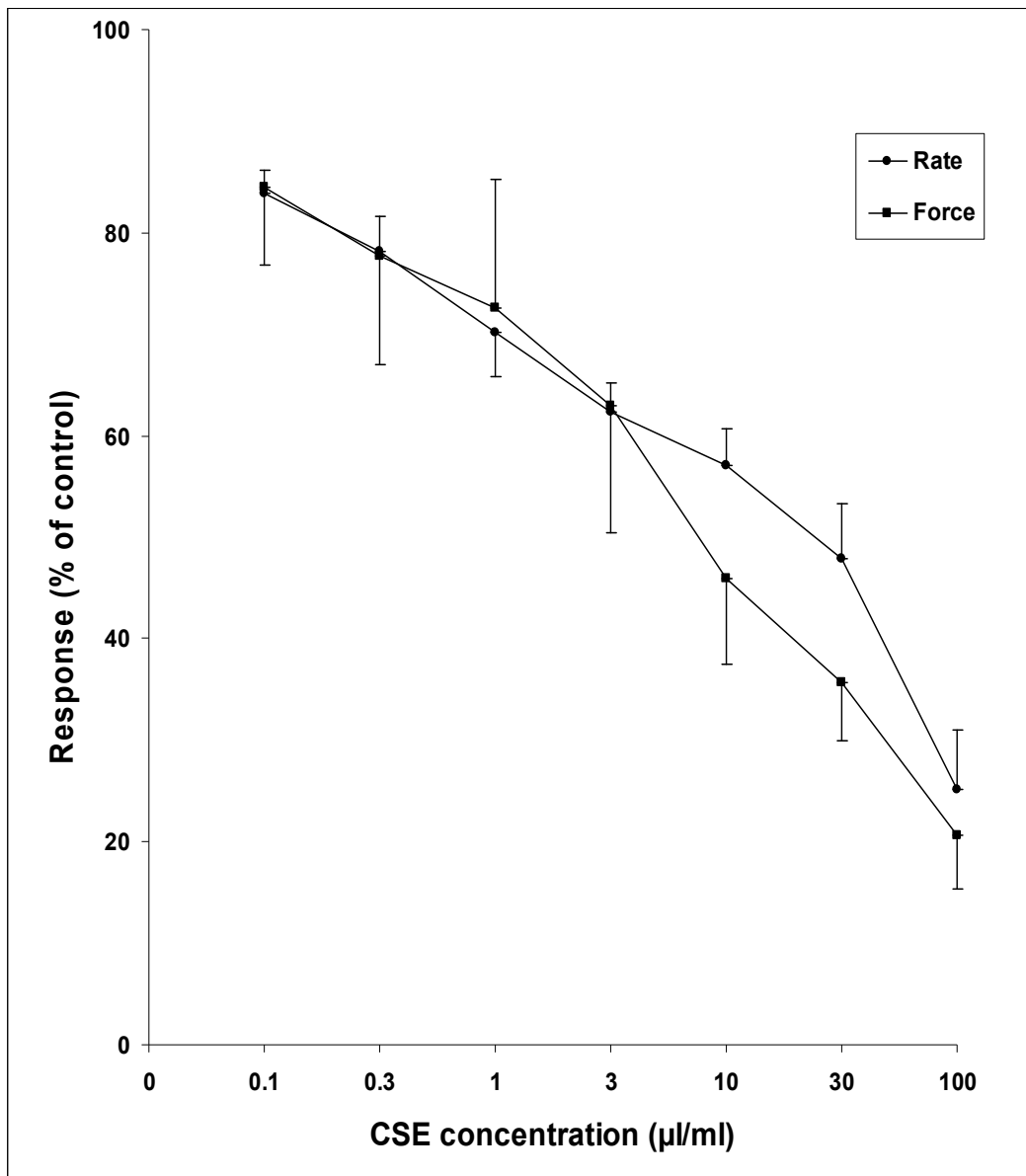
4.3.2. Isolated perfused heart experiments

4.3.2.1. Effect of CSE on the isolated perfused heart

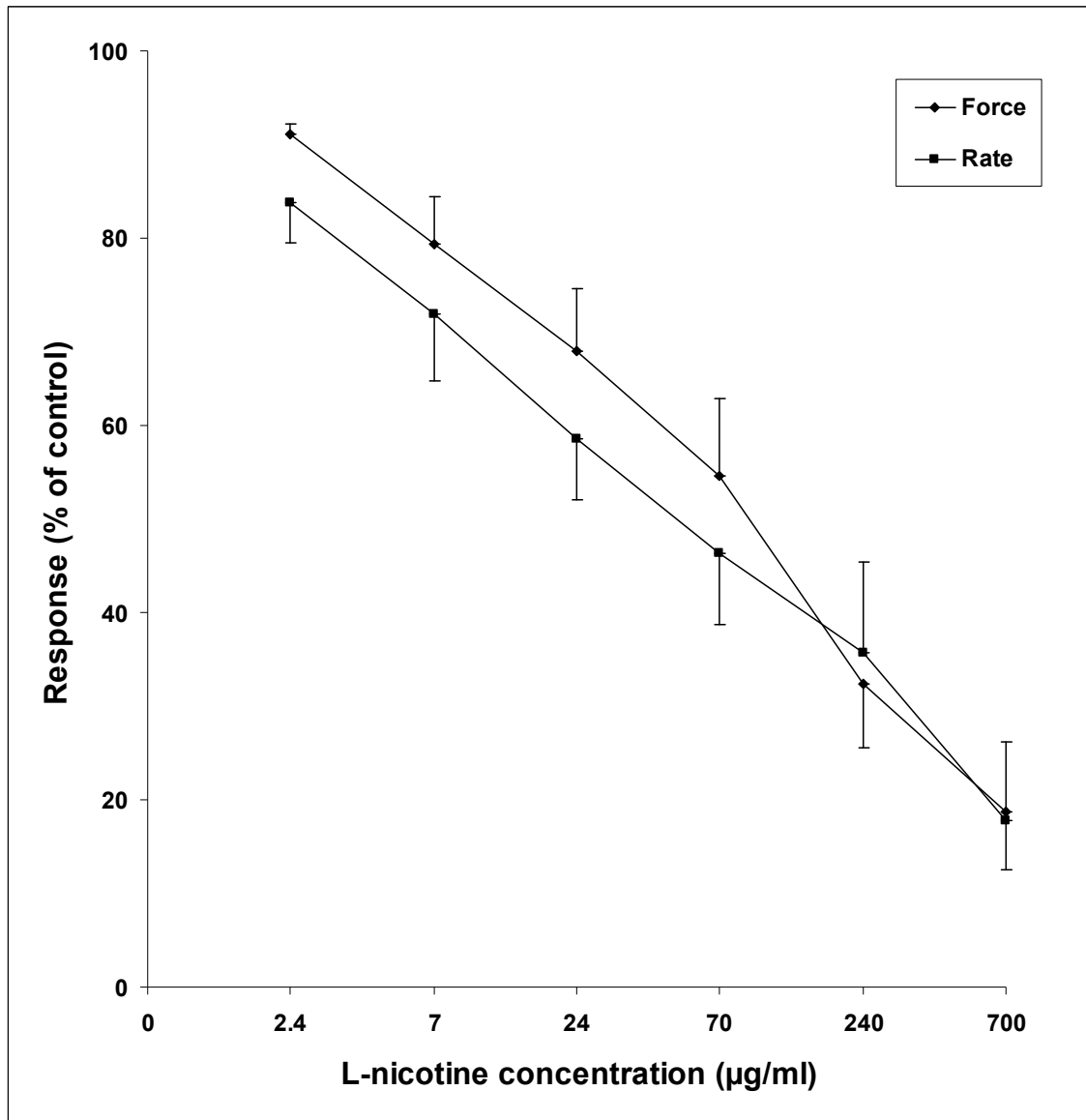
CSE, in concentrations ranging from 0.1-30 $\mu\text{l/ml}$ induced a significant concentration-dependent reduction of both the force and rate of the contractions of perfused heart ($p < 0.05$) (Figures 7 and 9).

4.3.2.2. Effect of L-nicotine on the isolated perfused heart

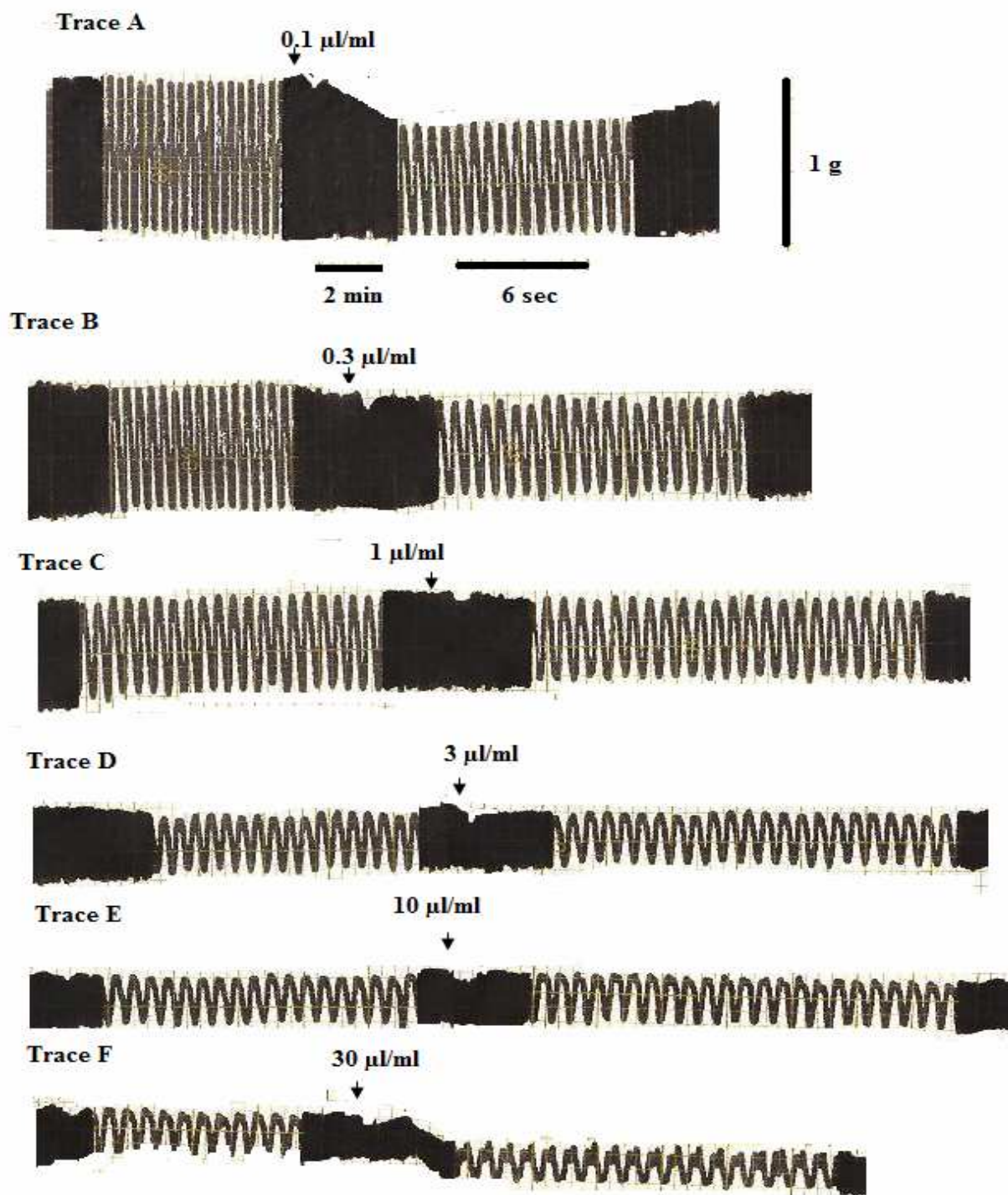
L-nicotine, in concentrations ranging from 2.4-700 $\mu\text{l/ml}$ caused a significant concentration-dependent decrease in the force and rate of the contractions of perfused heart ($p < 0.05$) (Figures 8 and 10).



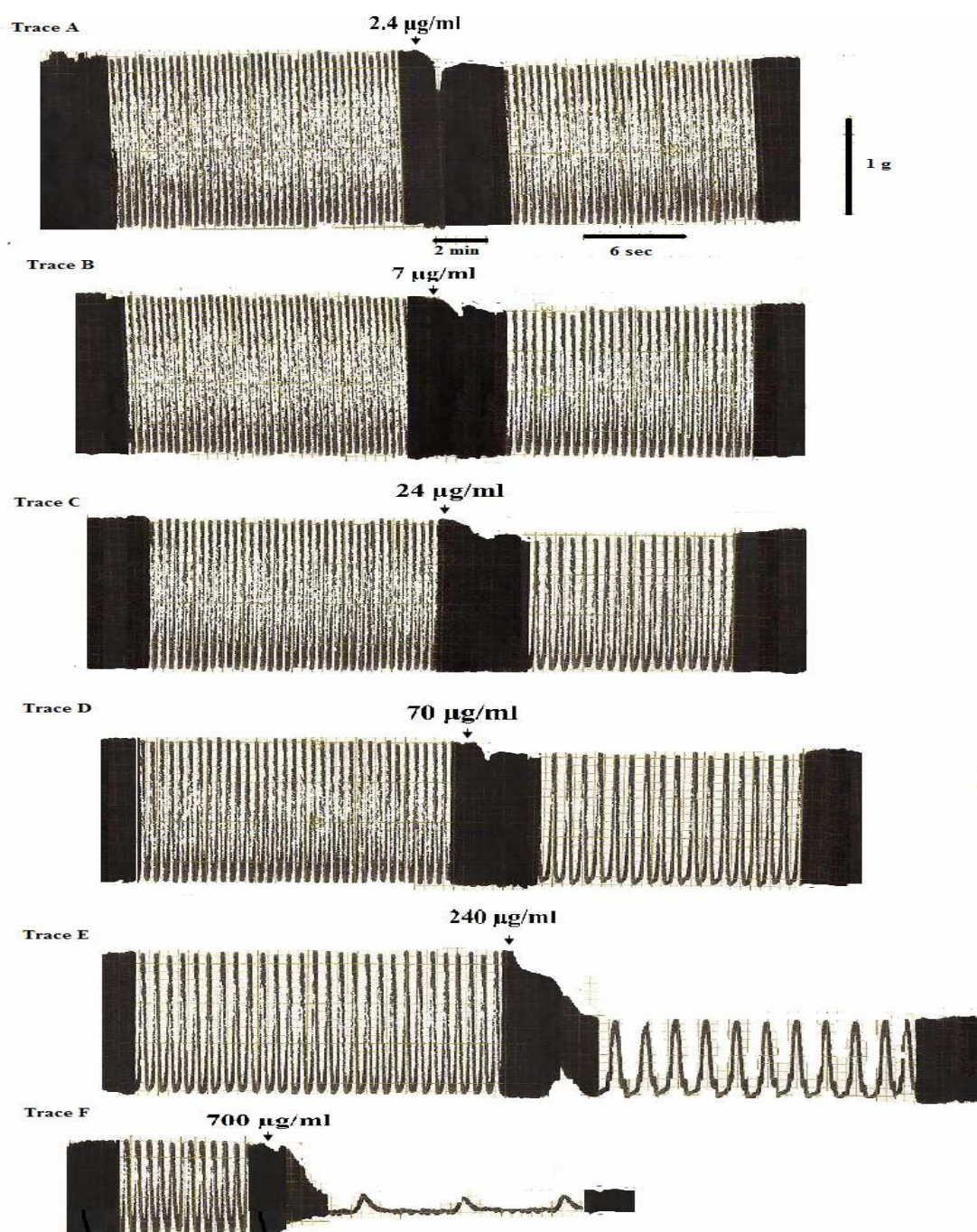
Figures 7: Concentration-effect curve of CSE on the rate and force of rat isolated perfused heart. The force and rate of the contractions of perfused heart is given as the means \pm SEM of 6 experiments



Figures 8: Concentration-effect curve of L-nicotine on the rate and force of rat isolated perfused heart. The force and rate of the contractions of perfused heart is given as the means \pm SEM of 6 experiments.



Figures 9: Effects of increasing concentrations of cigarette smoke extract (CSE) on rat isolated perfused heart, (trace A-F). All traces from the same preparations. The small depression immediately after the addition indicates an artifact due to rapid injection of the compound.



Figures 10: Effects of increasing concentrations of L-nicotine on rat isolated perfused heart, (trace A-F). All traces from the same preparations. The small depression immediately after the addition indicates an artifact due to rapid injection of the compound.

4.4. Results of correlation of antioxidant enzyme activities with tissues inflammation during smoke exposure of rats.

4.4.1. Catalase specific activity of cigarette smoke-exposed rats and recovery rats.

The cigarette smoke exposure caused a significant decrease in catalase specific activity compared to control by 23 %, 18 % and 50% in liver, kidney and lung tissues, respectively. However, during the recovery period this enzyme activity retained almost normal levels by 97%, 99% and 95% respectively. Smoking has more severe inhibition effects on catalase specific activity in the lung (Table 4).

Table 4: Catalase specific activity compared to control in the cigarette smoke-exposed rats and after recovery period in liver, kidney and lung tissues of rats^a.

^a Values are expressed as means \pm SEM of 6 experiments. * Significant value ($P < 0.05$).

^b The level of CAT activity was expressed in terms of $\mu\text{moles H}_2\text{O}_2$ consumed/min /mg of protein in crude extract.

Tissues	Control rats ^b	Smoke exposed rats ^b	Smoke recovered rats ^b
Liver	475 \pm 24	365 \pm 16.2	463 \pm 20
Kidney	89.5 \pm 5.3	73 \pm 2.8	88.4 \pm 4.8
Lung	19.5 \pm 1.9	9.6 \pm 0.8	18.2 \pm 2.1

4.4.2. Glutathione peroxidase specific activity of cigarette smoke-exposed rats and recovery rats.

Smoke exposure caused a significant reduction in glutathione peroxidase (GPx) specific activity compared to control by 16 %, 13% and 35% in liver, kidney and lung tissues, respectively. After the recovery period glutathione peroxidase (GPx) activities in liver, kidney and lung retained almost normal levels 97%, 99% and 96% respectively. Smoking showed severe inhibition effects on glutathione peroxidase specific activity in lung (Table 5).

Table 5: Glutathione peroxidase specific activity compared to control in the cigarette smoke-exposed rats and after recovery period in liver, kidney and lung tissues of rats^a.

^a Values are expressed as means \pm SEM of 6 experiments.* Significant value ($P < 0.05$).

^b The levels of GPx activity were expressed in terms of μ moles NADPH consumed/min/mg of protein in crude extract.

Tissues	Control rats ^b	Smoke exposed rats ^b	Smoke recovered rats ^b
Liver	1.29 \pm 0.04	1.09 \pm 0.06	1.25 \pm 0.05
Kidney	0.53 \pm 0.023	0.45 \pm 0.021	0.52 \pm 0.019
Lung	0.35 \pm 0.025	0.22 \pm 0.016	0.33 \pm 0.021

4.4.3. G6PD specific activity of cigarette smoke-exposed rats and recovery rats.

Smoke exposure caused a significant reduction in G6PD specific activities compared to control by 29 %, 18 % and 38% in liver, kidney and lung tissues, respectively. However, during the recovery period, the enzyme activity retained almost normal levels in liver, kidney and lung by 98%, 97% and 96 % respectively. Smoking showed severe inhibition effects on G6PD specific activity in the lung (Table 6).

Table 6: G6PD specific activity compared to control in the cigarette smoke-exposed rats and after recovery period in liver, kidney and lung tissues of rats.

^a Values are expressed as means \pm SEM of 6 experiments. * Significant value ($P < 0.05$).

^b The levels of G6PD activity were expressed in terms of μ moles NADPH produced/min /mg of protein.

Tissues	Control rats ^b	Smoke exposed rats ^b	Smoke recovered rats ^b
Liver	0.051 \pm 0.003	0.036 \pm 0.002	0.05 \pm 0.0024
Kidney	0.037 \pm 0.0017	0.035 \pm 0.0019	0.036 \pm 0.002
Lung	0.0227 \pm 0.0016	0.0135 \pm 0.0006	0.0209 \pm 0.0011

4.4.4. Tissues inflammation during smoke exposure and recovery in liver, lung, and kidney.

Long period smoking exposure of rats, produced inflammatory changes in liver, lung, and kidney tissues. These changes involved interstitial inflammation involving lymphocytes and plasma cells in lung (Figure 12), portal area inflammation in liver (Figure 15) and mesangial cell proliferation in corpuscles (Figure 18). After the recovery period, all these inflammatory changes from smoking effects almost diminished in tissues (Figure 13, 16 and 19).

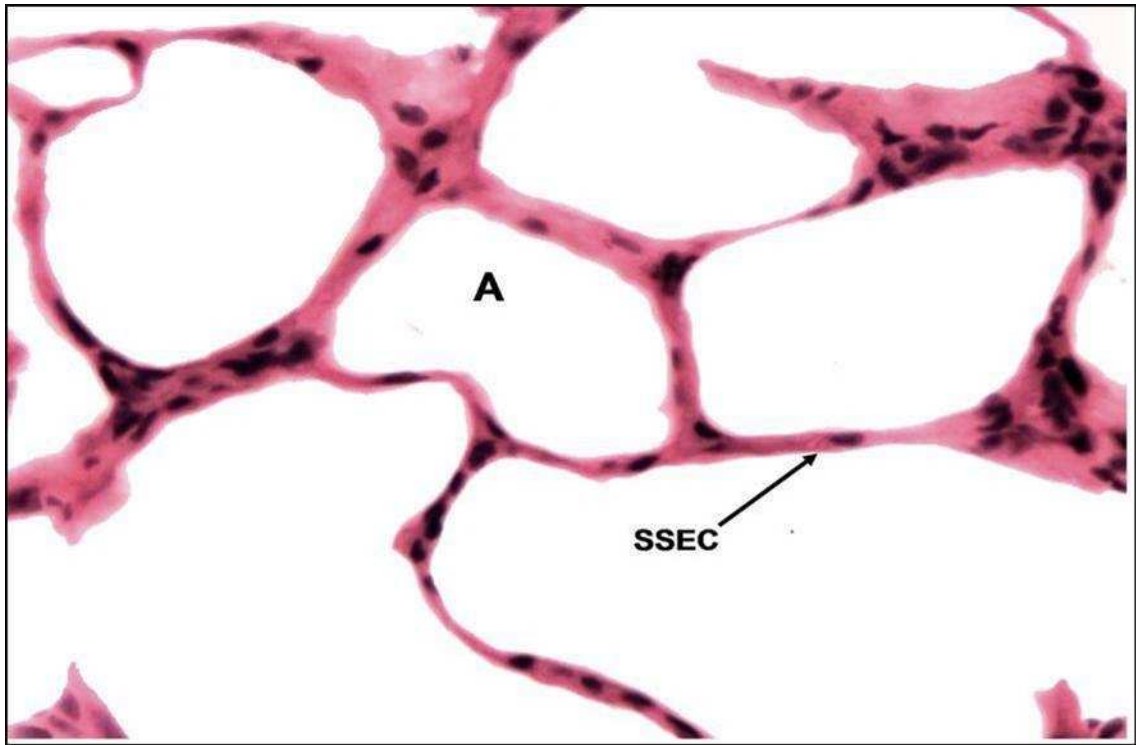


Figure 11: Normal morphology of lung alveoli in a control rat. A: alveolus, SSEC: simple squamous epithelial cell. Magnification: 815x. H&E stain.

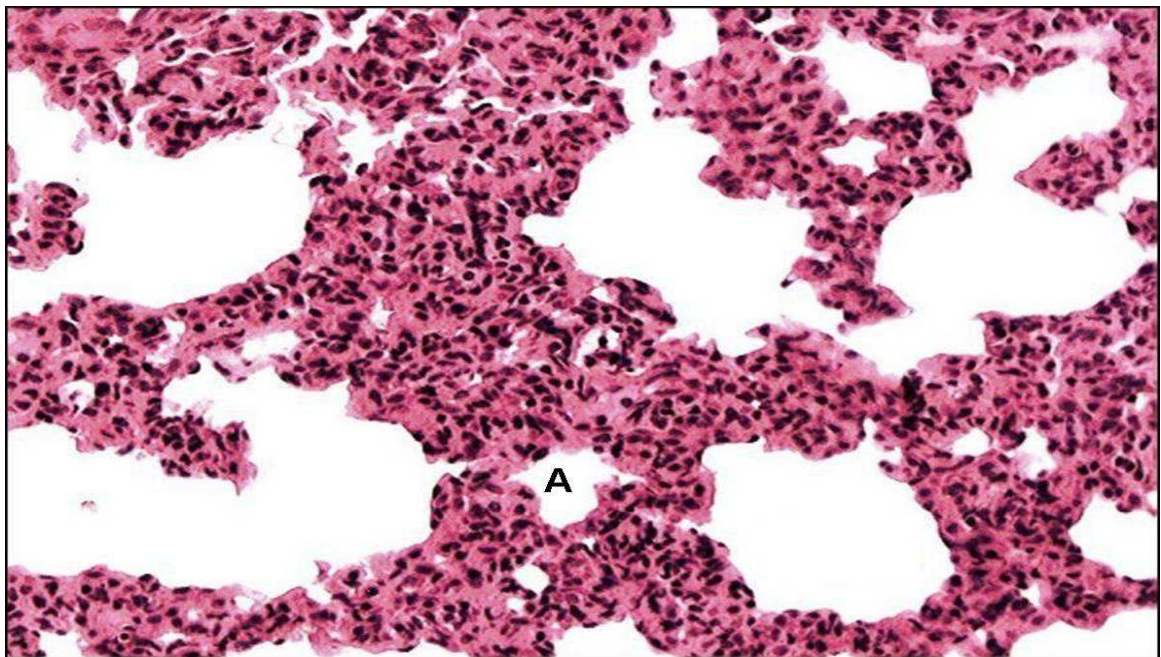


Figure 12: Lung alveoli of cigarette smoke-exposed rat, showed infiltration of different inflammatory cells, some degree of collapsed alveoli and deposition of collagen fibrils in the alveolar walls. A: alveolus. Magnification: 435x .H&E stain

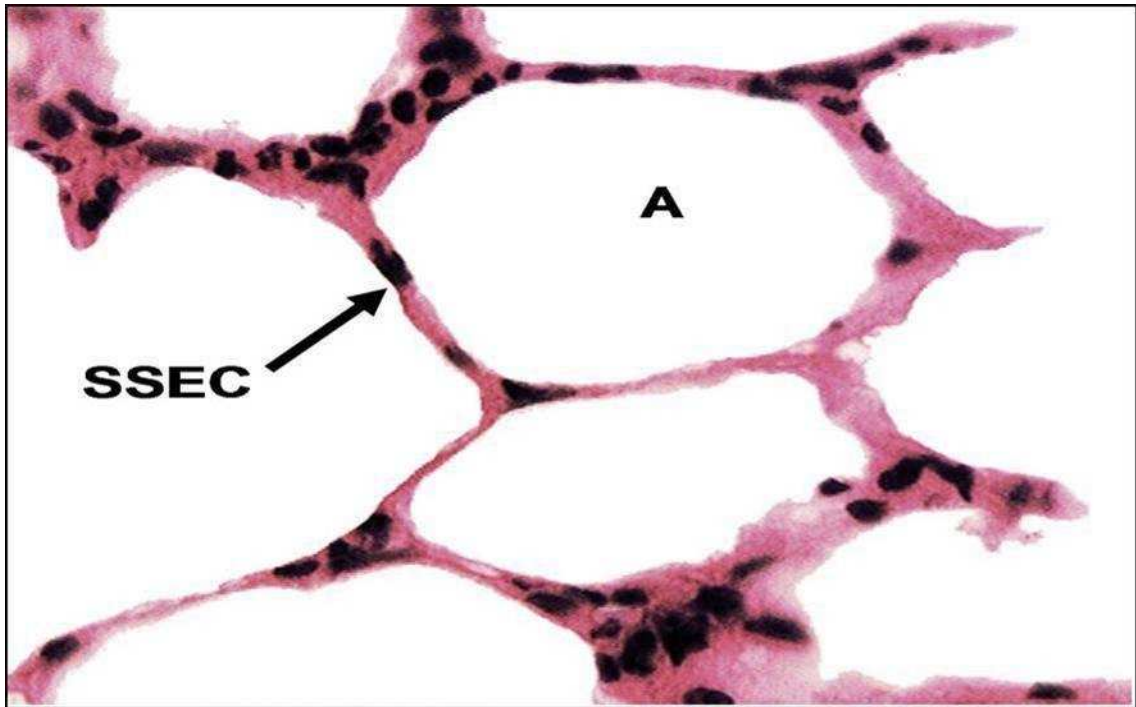


Figure13: Lung alveoli of cigarette smoke-exposed rat after the recovery period. Much less thickening in the alveolar wall and no inflammatory cell infiltration was observed. A: alveolus, SSEC: simple squamous epithelial cell. Magnification: 1380x . H&E stain.

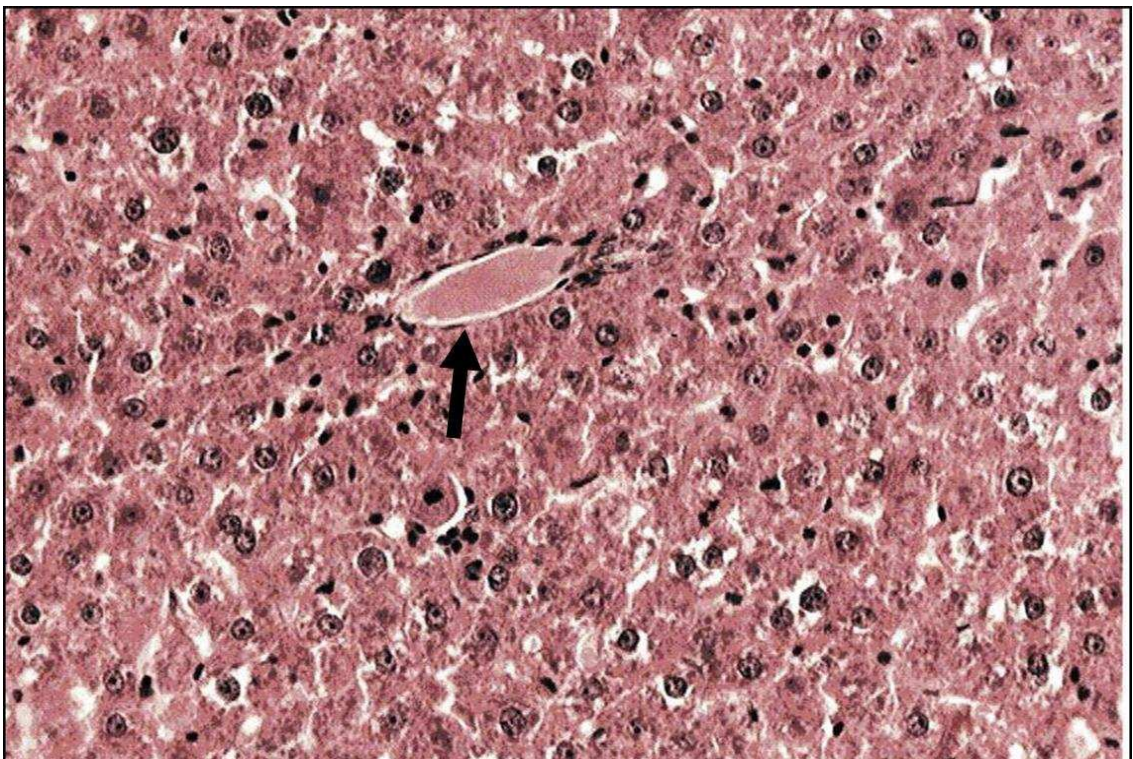


Figure 14: Normal morphology of liver in a control rat. Arrow: Portal area. Magnification: 375x .H&E stain.

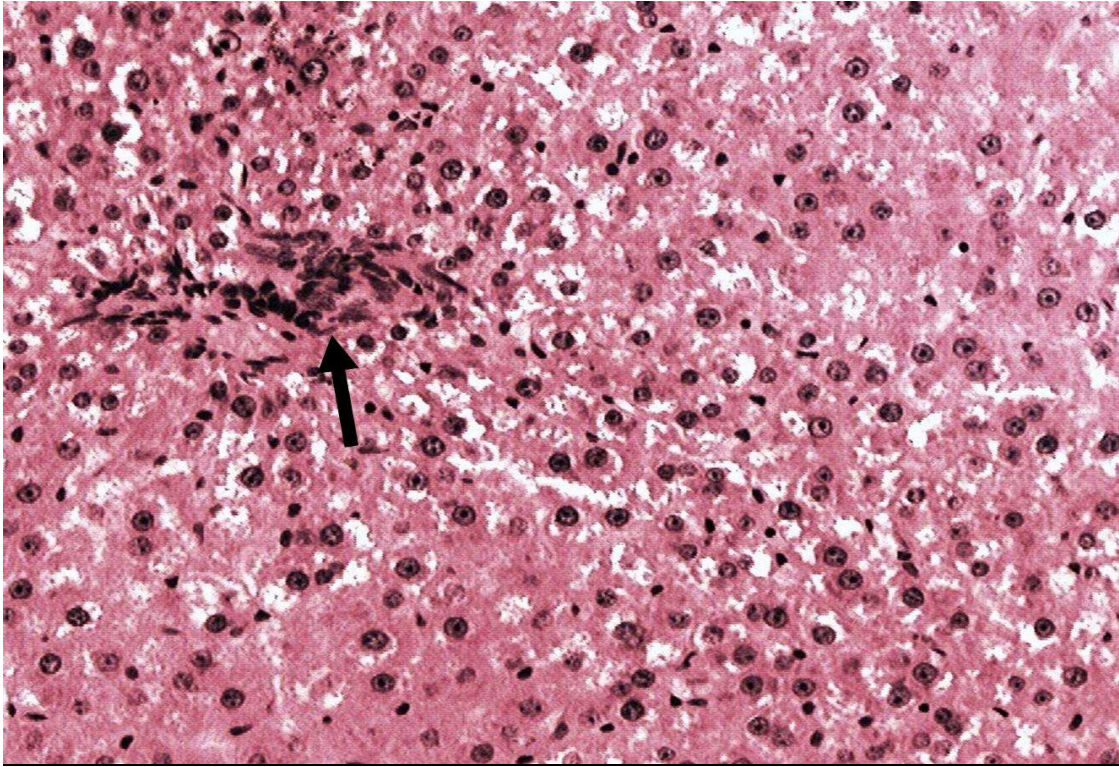


Figure 15: Liver tissue of cigarette smoke-exposed rat. Showing inflammatory change around the portal area. Arrow: portal area. Magnification: 400x.H&E stain.

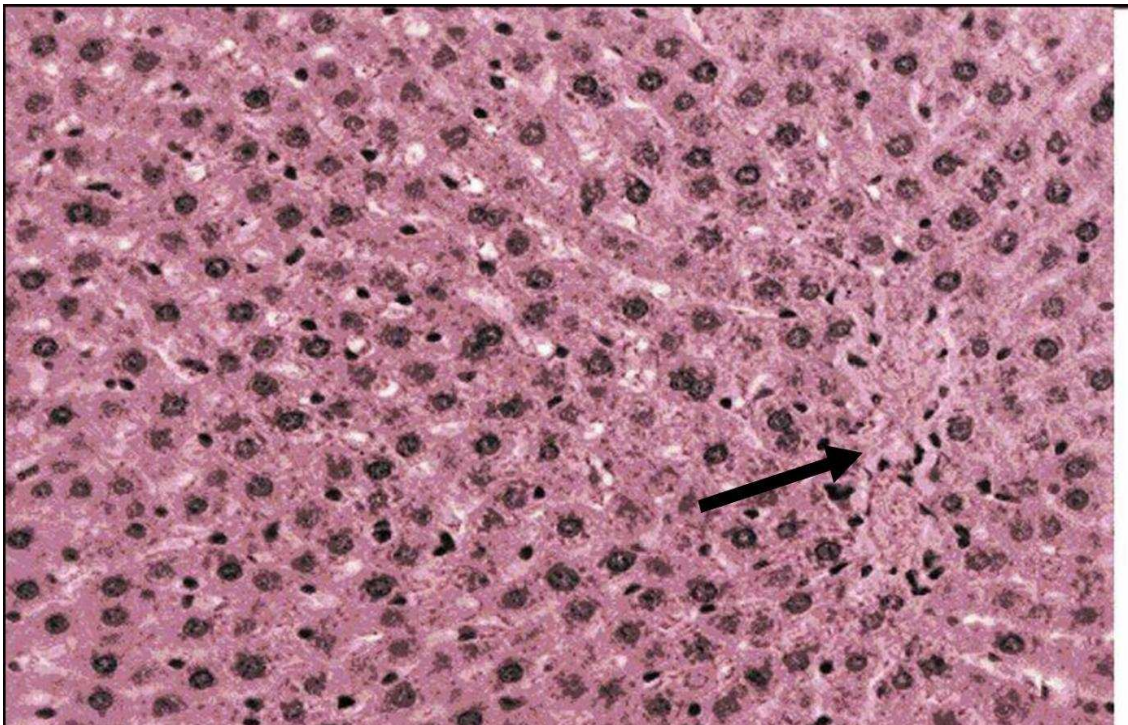


Figure 16: liver tissue of cigarette smoke-exposed rat after the recovery period showing the absence of portal area inflammation. Arrow: Portal area. Magnification: 440x. H&E stain.

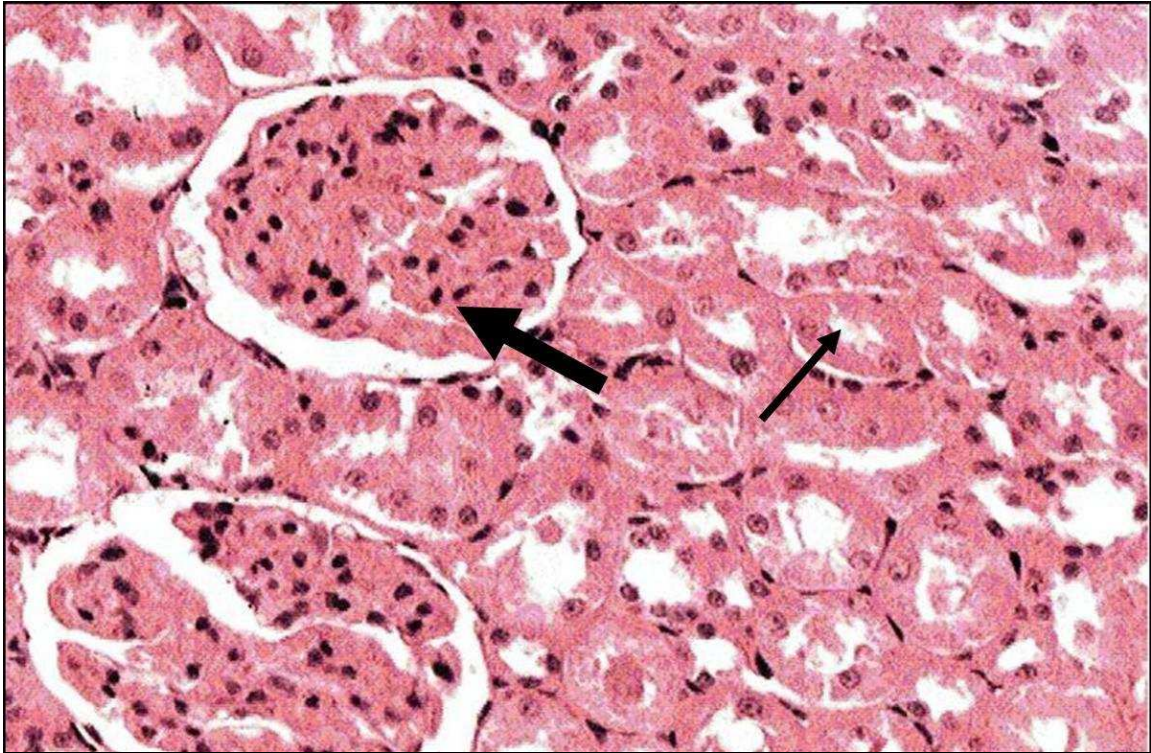


Figure 17: Normal morphology of the cortical area in the kidney of a control rat. Thick arrow: Renal corpuscle .Thin arrow: Proximal tubule. Magnification: 440x. H&E stain.

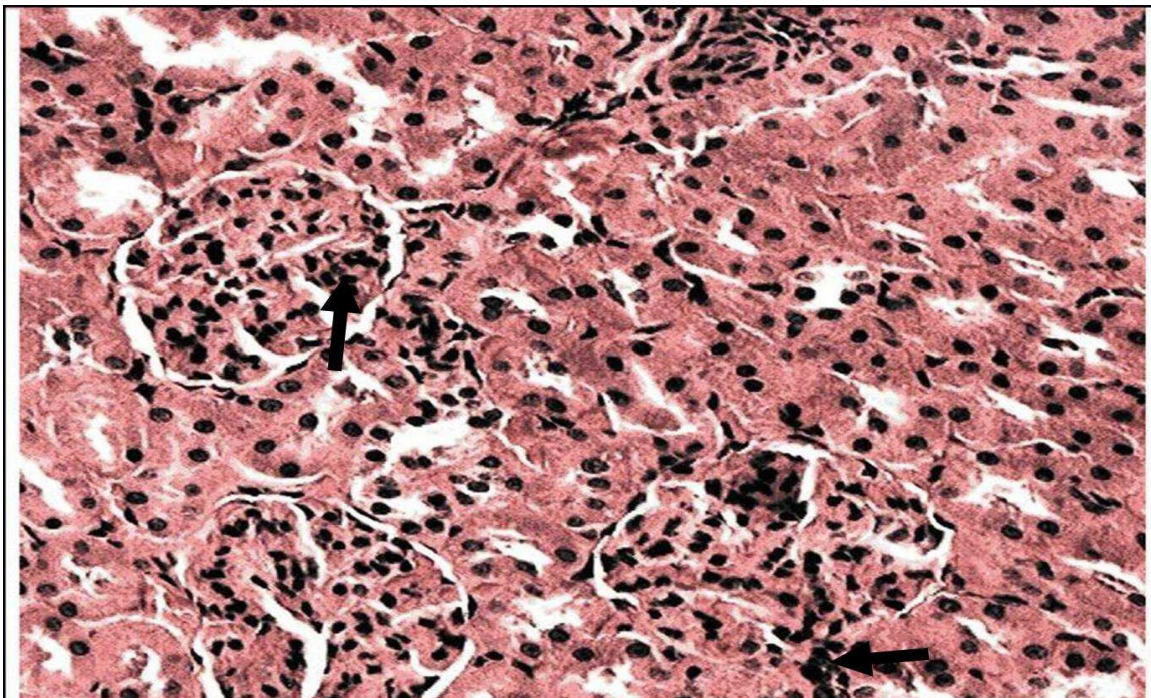


Figure 18: Kidney tissue of cigarette smoke-exposed rat. Showing mesangial cell proliferation. Arrow: mesangial cell. Magnification: 440x. H&E stain.

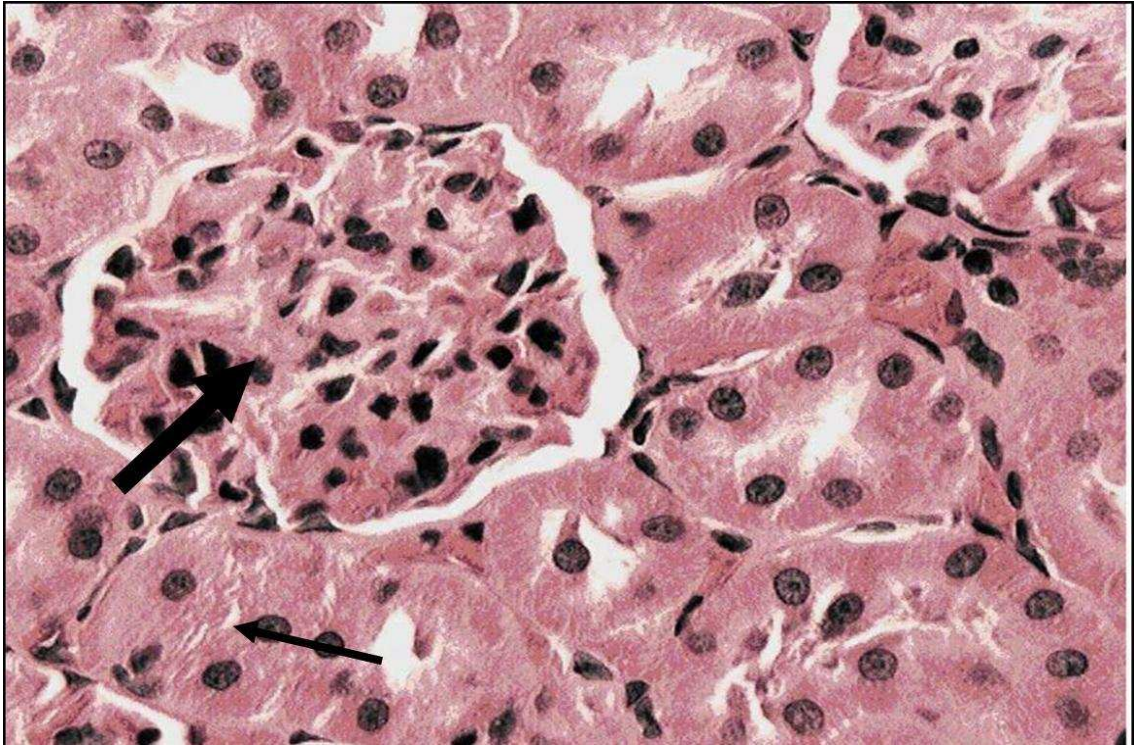


Figure 19: Kidney tissue of cigarette smoke-exposed rat after the recovery period, showing return of the renal corpuscle into the normal appearance. Thick arrow: Renal corpuscle. Thin arrow: Proximal tubule. Magnification: 900x. H&E stain.

4.5. The ability of cigarette smoke to induce apoptosis in tissue sections

4.5.1. Effect on the trachea

Cigarette smoke didn't induce apoptosis in the tracheal epithelium of rats after three months of exposure (Figures 20 and 21).

4.5.2. Effect on the aorta

Cigarette smoke didn't induce apoptosis in the aortic tissue after three months of exposure (Figures 22 and 23).

4.5.3. Effect on heart ventricles

Cigarette smoke didn't induce apoptosis in heart ventricles after three months of exposure (Figures 24 and 25).

4.5.4. Effect on the lung

Cigarette smoke induced apoptosis in alveoli and epithelial bronchiole of the lung. There were characteristic dark-brown apoptotic nuclei in the examined sections (Figures 26, 27, and 28)

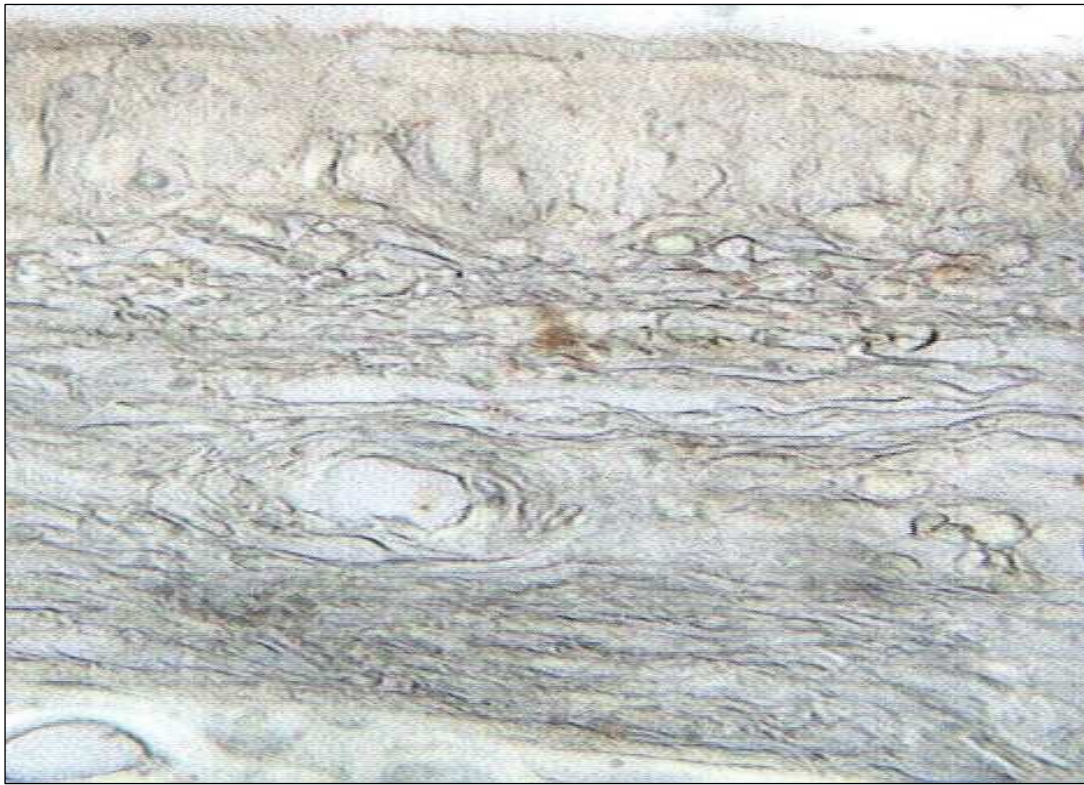


Figure 20: Normal tracheal tissue (TUNEL staining, original magnification: 160x).

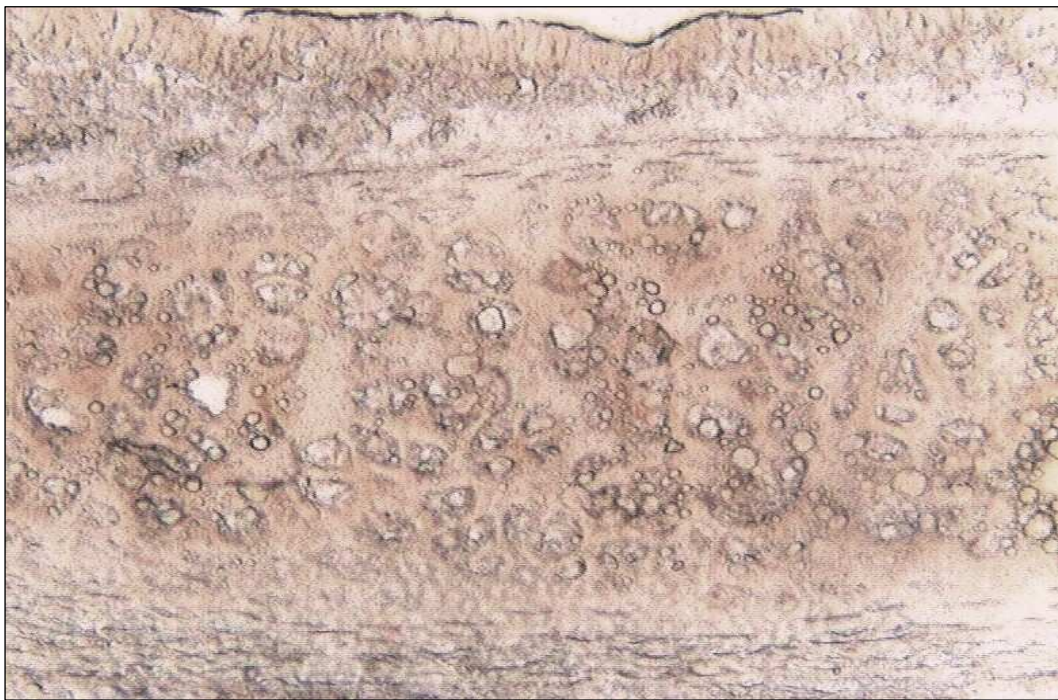


Figure 21: Tracheal tissue from cigarette smoke-exposed rat; no dark-brown apoptotic nuclei (TUNEL staining, original magnification: 160x).

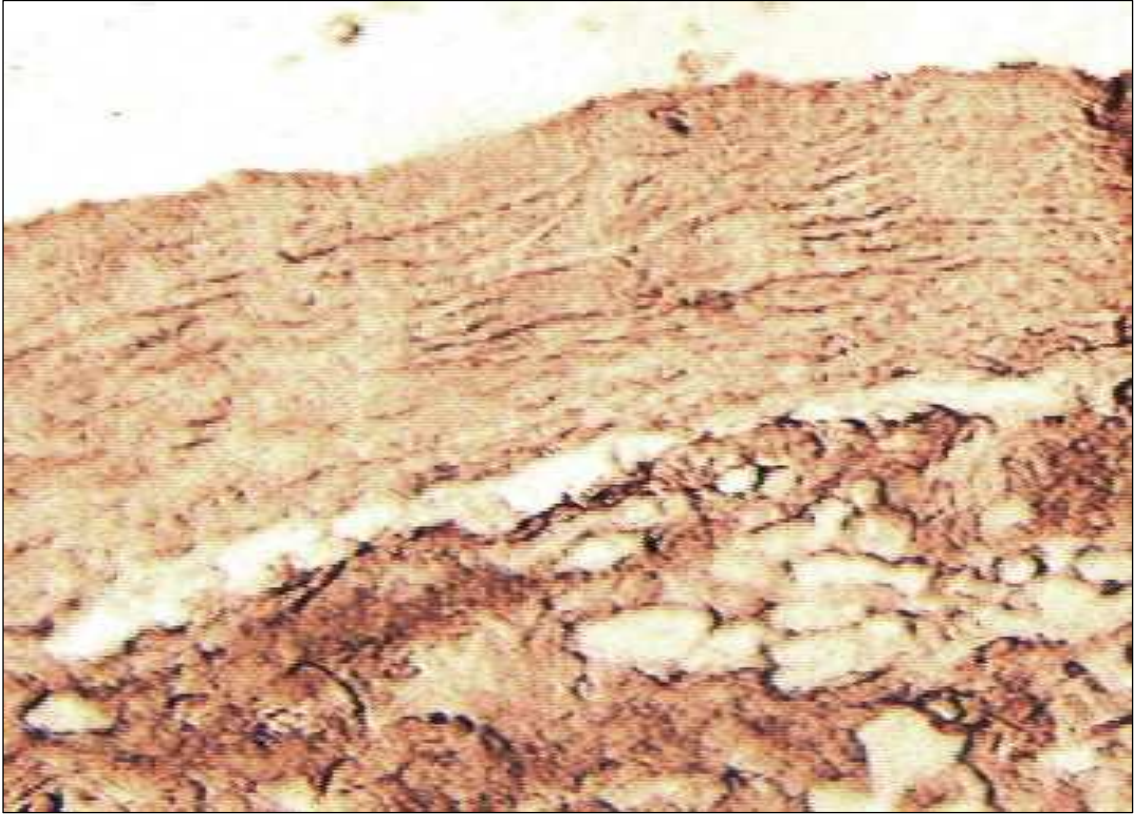


Figure 22: Normal aortic tissue (TUNEL staining, original magnification: 160x).

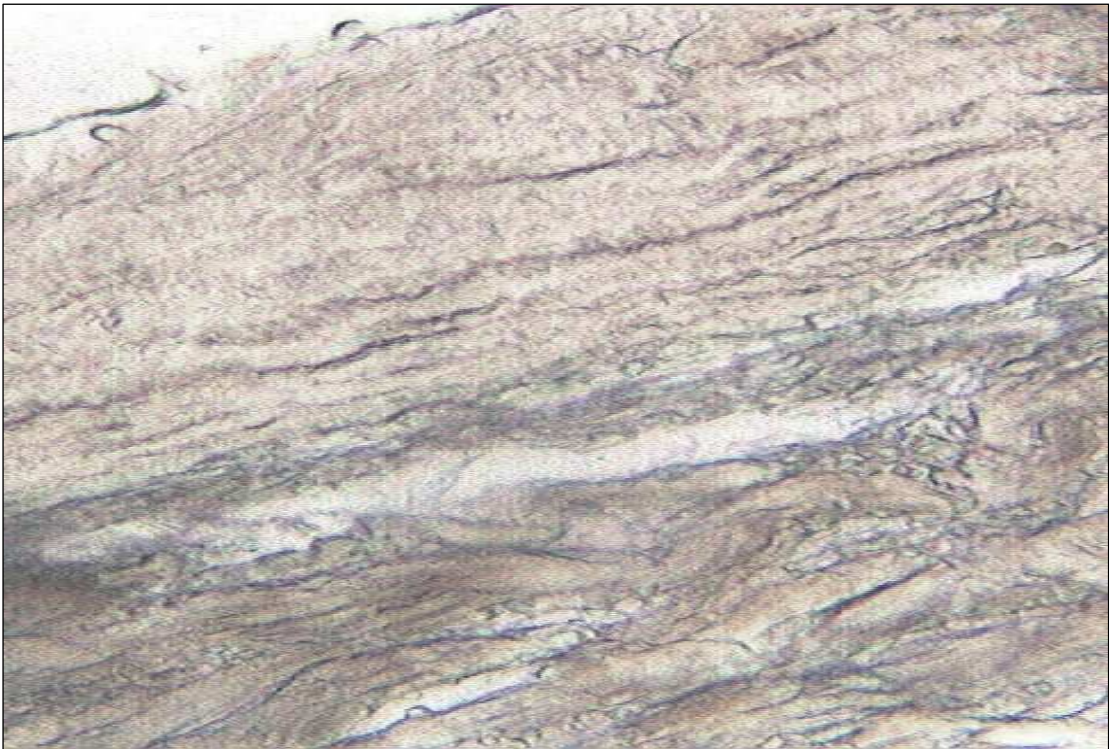


Figure 23: Aortic tissue from cigarette smoke-exposed rat; no dark-brown apoptotic nuclei (TUNEL staining, original magnification: 160x).



Figure 24: Normal heart ventricular tissue (TUNEL staining, original magnification: 160x).

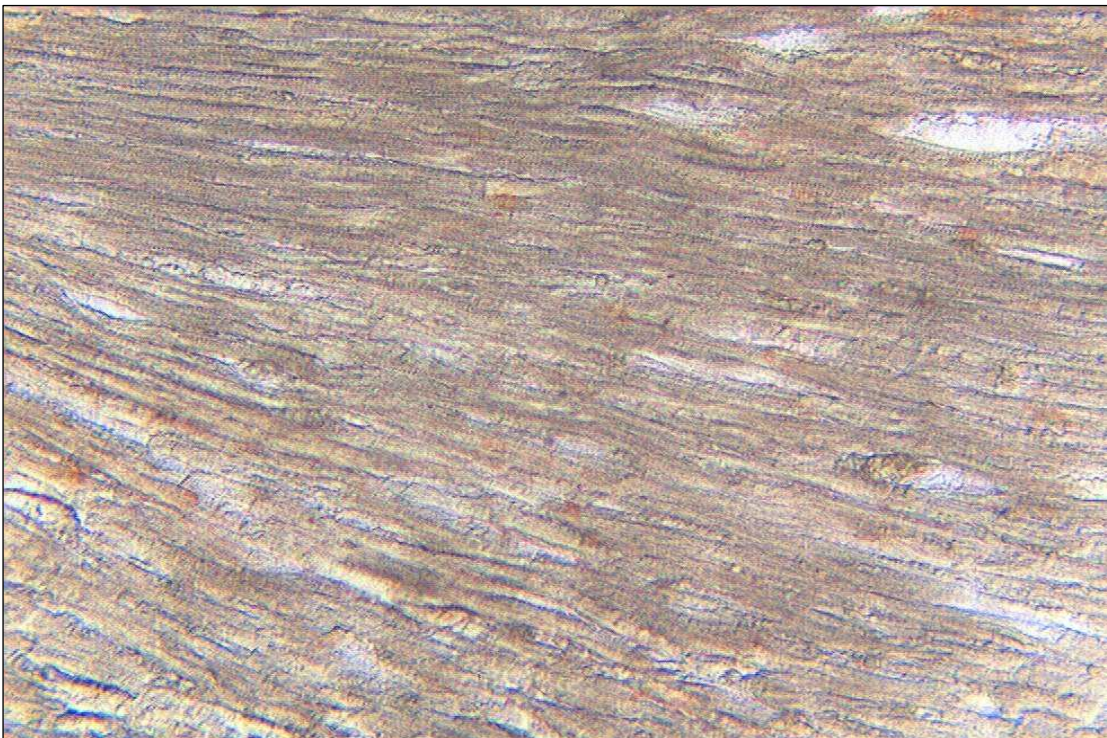


Figure 25: Heart ventricular tissue from cigarette smoke-exposed rat; no dark-brown apoptotic nuclei (TUNEL staining, original magnification: 160x).

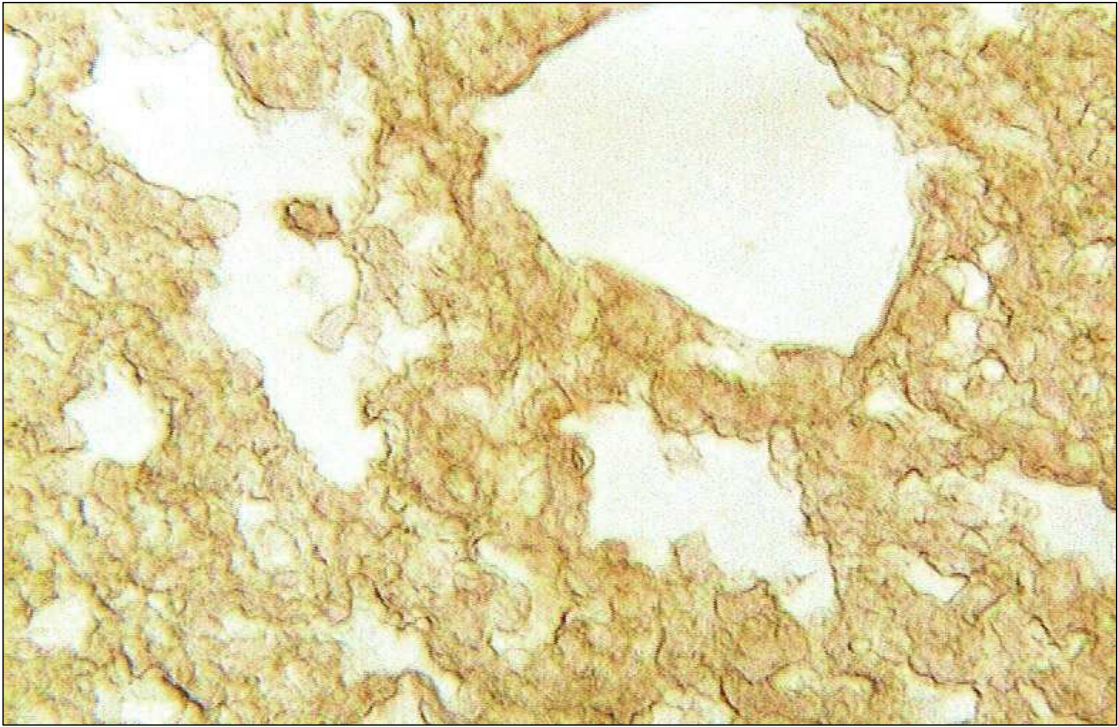


Figure 26: Normal lung alveoli (TUNEL staining, original magnification: 160x).

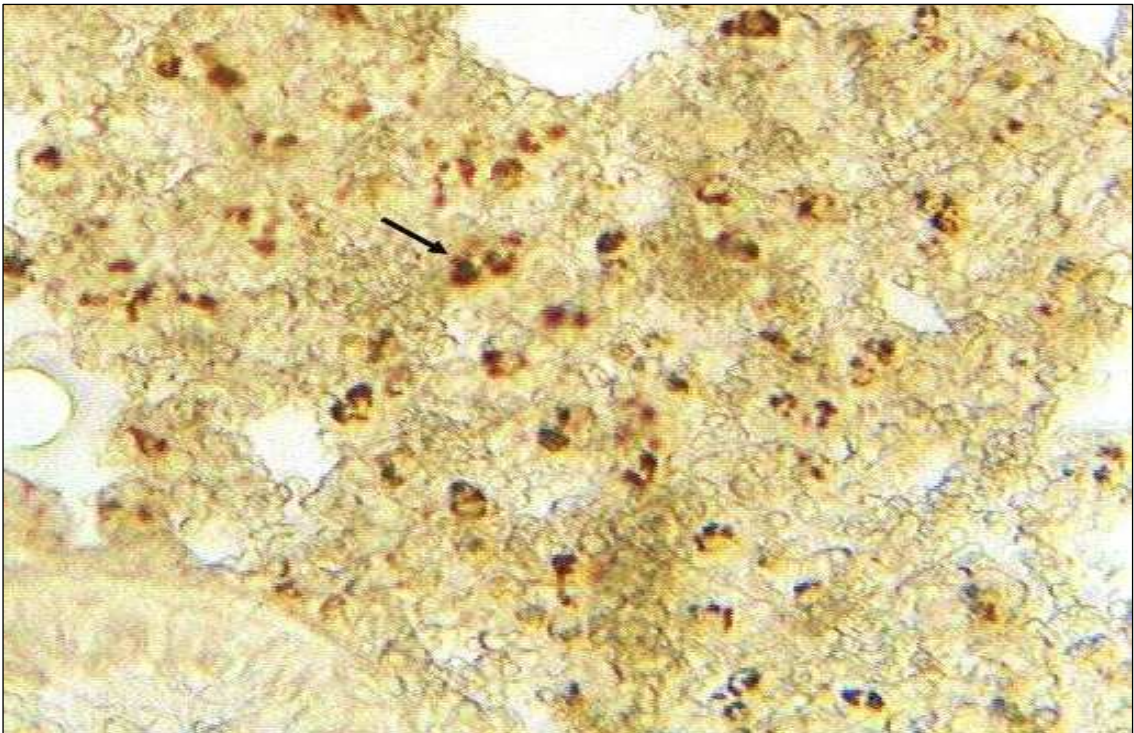


Figure 27: Lung alveoli from cigarette smoke-exposed rat, with the presence of many dark-brown apoptotic nuclei. The arrow indicates one apoptotic nucleus (TUNEL staining, original magnification: 160x).

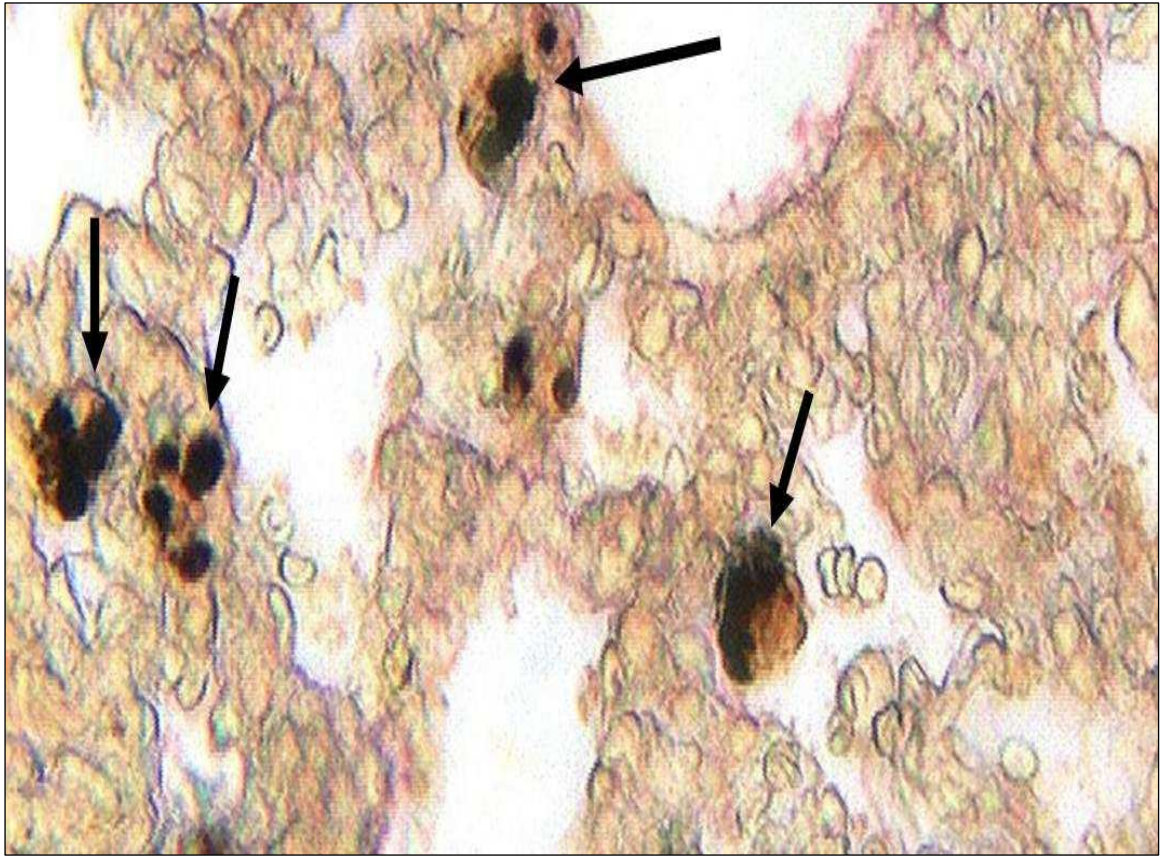


Figure 28: Magnified picture of several typical apoptotic cells, as observed in tissue sections of lung alveoli from cigarette smoke-exposed rat. The arrows indicate typical apoptotic nucleus (TUNEL staining, original magnification: 400x).

4.6. Histological studies

4.6.1. Studying the effect of Cigarette smoke and its recovery by light microscopy

4.6.1.1. Effect on the trachea

Control sections showed healthy ciliated pseudostratified columnar epithelium, mucosal and fibroelastic layers normally seen in tracheal tissue (Figures 29 and 30). The tracheal mucosa of cigarette smoke-exposed was adversely affected; showing an epithelial cellular hyperplasia with ciliary amalgamation, presence of inclusion bodies, and inflammatory cell infiltration (Figures 31, 32 and 33). After the recovery period, the tissue showing partial recovery (Figures 34 and 35).

4.6.1.2. Effect on alveoli of the lung

Photomicrographs of lung alveoli from control animals revealed the normal appearance of their characteristic simple epithelium and terminal bronchiole (Figures 36, 37 and 38). Lung alveoli of cigarette smoke-exposed rats showed clear thickening in the alveolar wall tissue, collapsed alveoli, inflammatory cell infiltration and blood extravasations (Figures 39, 40, 41, 42 and 43). After the recovery period, the high degree of proliferating cells was relatively reduced (Figures 44, 45, 46, 47 and 48).

4.6.1.3. Effect on the aorta

Control sections showed normal layers of aorta: intima, media and adventitia (Figure 49). Aortic tissue sections of cigarette smoke-exposed rats showed thickening in internal elastic lamina and elastic lamellae in the tunica media, elastic lamellae more obvious in the tunica media, elongated nuclei, slightly contraction of smooth muscle, and endothelial cells disruption (Figure 50, 51 and 52). After the recovery period, the tissue showing partial recovery, nuclei are still elongated (Figures 53 and 54).

4.6.1.4. Effect on heart ventricles

Photomicrographs of control sections showed normal cardiac muscle fibers (Figures 55 and 56). Heart ventricular tissue of cigarette smoke-exposed showed some degree of separation between cardiac muscle fibers (Figure 59), elongated nuclei, congested blood vessels (Figure 57 and 60), and inflammatory cell infiltration (Figure 58).

After the recovery period, the tissue showing partial recovery, nuclei are still elongated (Figures 61, 62 and 63).

4.6.2. Studying the effect of cigarette smoke and its recovery by transmission electron microscopy

4.6.2.1. Effect on the trachea

Thin sections of trachea from control animals showed normal ciliated pseudostratified columnar epithelium and goblet cell (Figures 64 and 65). The examined thin section of cigarette smoke-exposed, showed low number of cilia, a high degree of cytoplasmic vacuolization, and some boundaries between cells can't be distinguished. Mitochondria aggregates in the apical portion of epithelial cells, inclusion bodies are present, and disrupted endoplasmic reticulums were also observed (Figure 66, 67 and 68).

After the recovery period, tracheal epithelium showing partial recovery (Figures 69).

4.6.2.2. Effect on alveoli of the lung

Thin sections of lungs from control rats revealed normal morphology of type II pneumocytes (Figure 70), and type I pneumocytes (Figure 71). The alveolar epithelium of cigarette smoke-exposed rats showed damaged multilamellar bodies of type II pneumocyte, together with cytoplasmic vacuolization and chromatin condensation, membrane blebs projecting from the cytoplasm, and degeneration of alveolar epithelium (Figure 72, 73, 74, 75 and 76).

After the recovery period, thin sections in the alveolar epithelium showed condensed chromatin and increase in number of mitochondria (Figure 77).

4.6.2.3. Effect on heart ventricles

Control photomicrographs revealed normal sarcomeres and mitochondria (Figures 78 and 79). Thin sections of ventricular cardiomyocytes of cigarette smoke-exposed rats revealed mitochondria with deteriorated and partially disrupted or disappeared cristae. Also it showed areas with a partial disruption of the myofibrils (Figures 80, 81 and 82).

Thin section of heart ventricles tissue of cigarette smoke-exposed rats after the recovery period, showed partial recovery of cardiac muscle fibers. Enlarged mitochondria with partial disruption cristae (Figures 83 and 84).

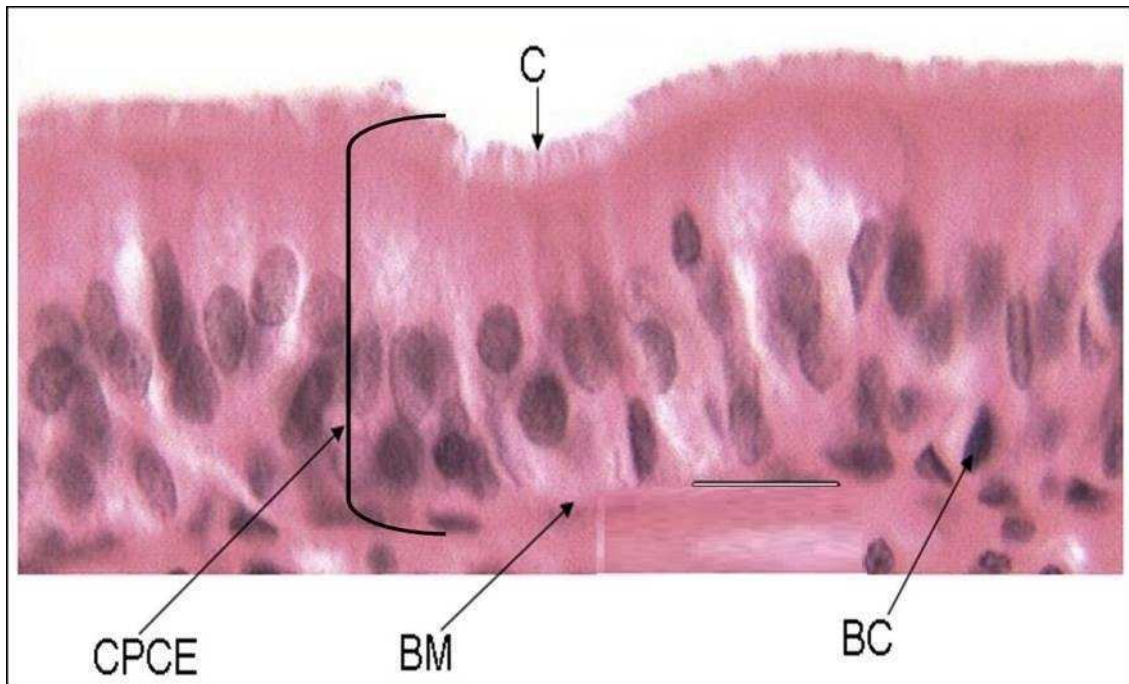


Figure 29: Section of normal tracheal tissue. CPCE: ciliated pseudostratified columnar epithelium, C: cilia, BM: basement membrane, BC: basal cell. Magnification: 1120x .H&E stain.

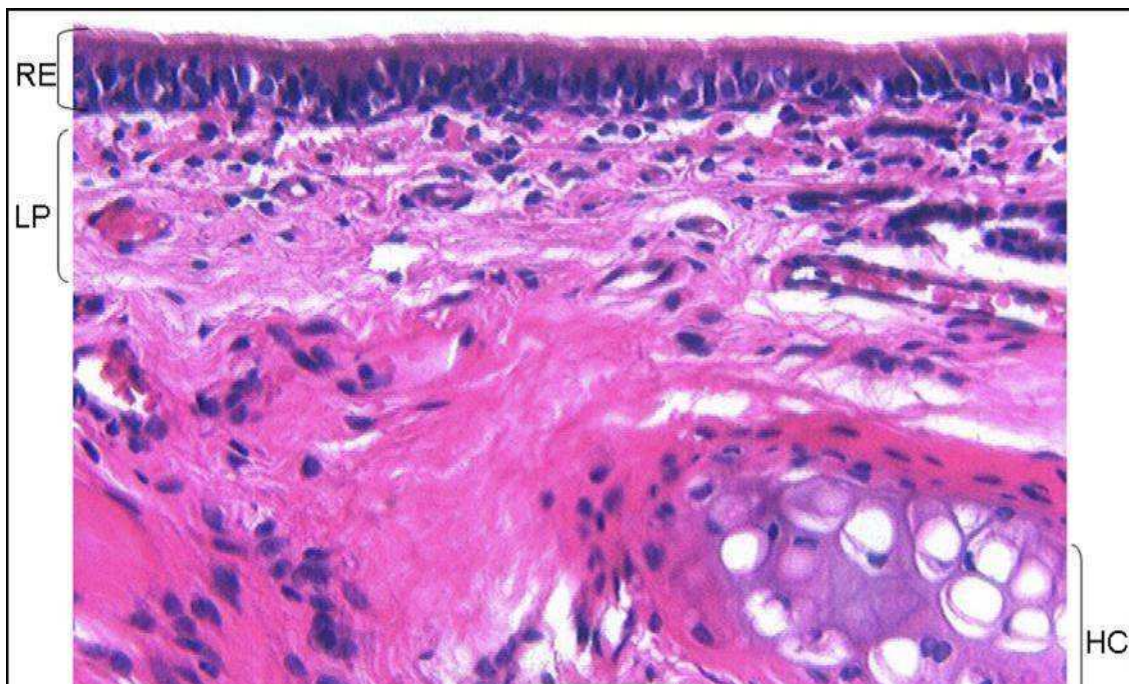


Figure 30: Section through normal trachea showing its parts. RE: respiratory epithelium, LP: lamina propria, HC: hyaline cartilage. Magnification: 450x .H&E stain.

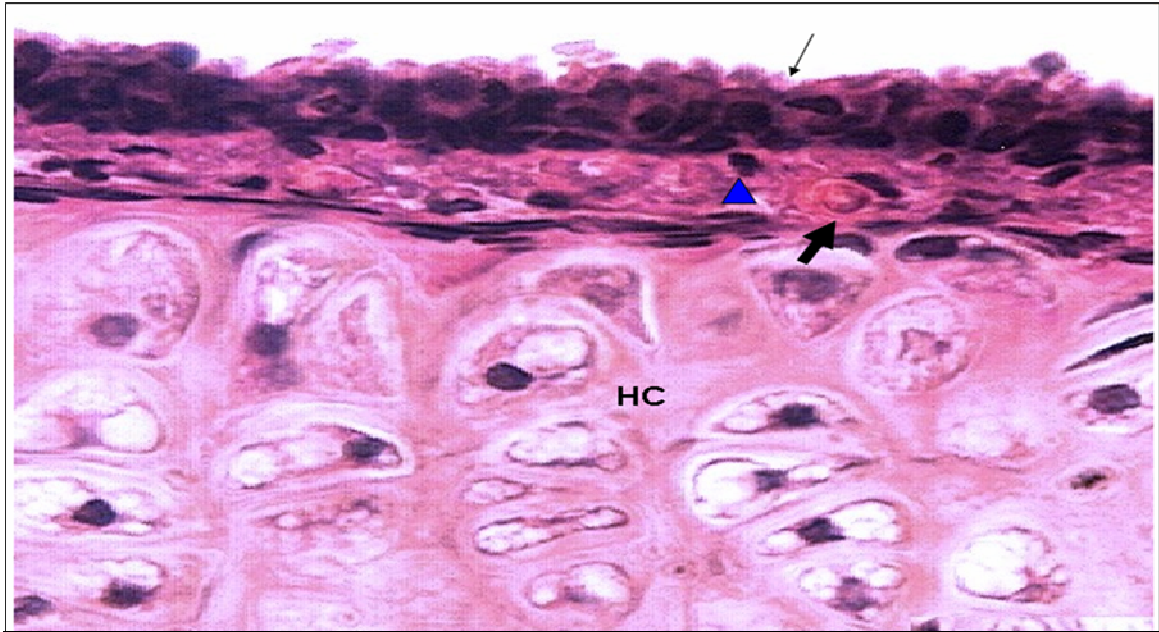


Figure 31: Trachea of cigarette smoke-exposed rat, showing an epithelial cellular hyperplasia and inflammatory cell infiltration (triangles) with ciliary amalgamation. Thick arrow: blood vessel. Thin arrow: a profound loss of the cilia. Magnification: 1260x H&E stain.

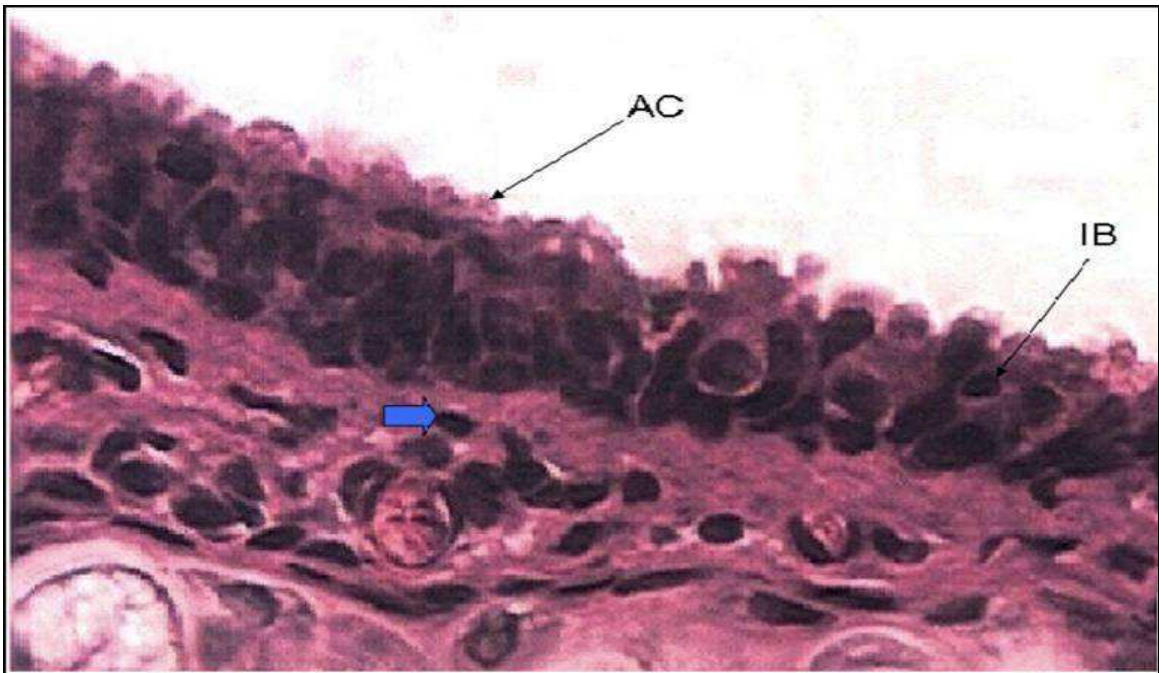


Figure 32: Section from the tracheal mucosa of cigarette smoke-exposed rat, showing inflammatory cell infiltration (Thick arrows). IB: inclusion body, AC: amalgamated cilia. Epithelial cells are highly proliferated. Magnification: 1185x. H&E stain.

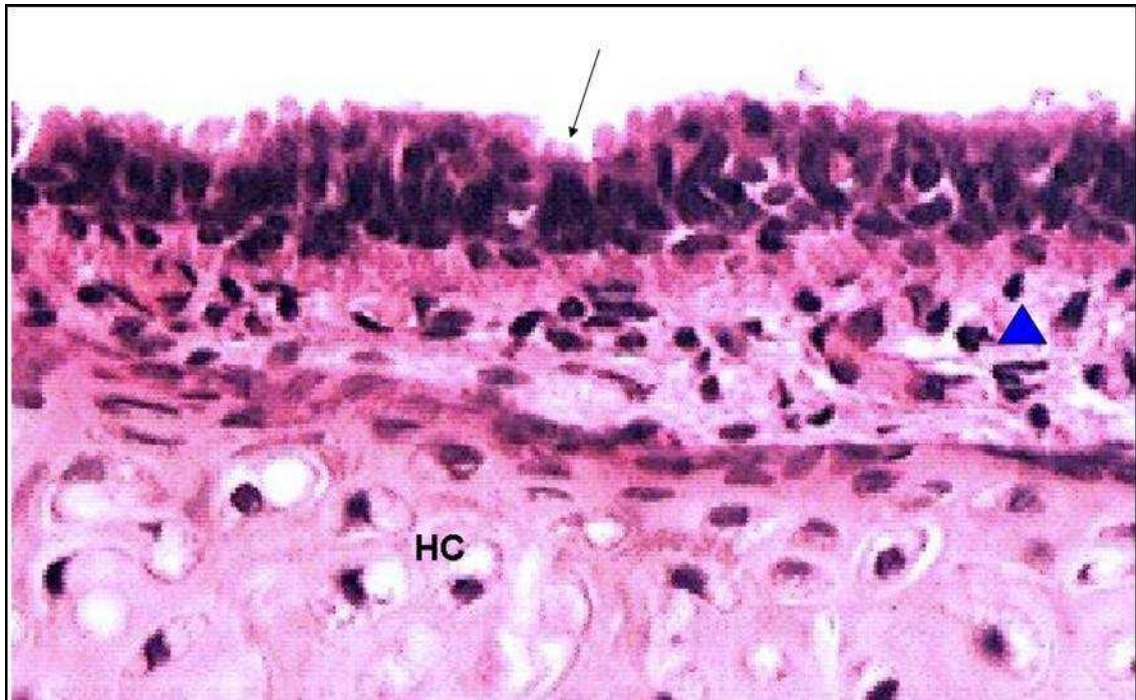


Figure 33: Trachea of cigarette smoke-exposed rat, showing a high degree of epithelial cellular hyperplasia. Thin arrow: a profound loss of the cilia. Triangle: inflammatory cell infiltration. Magnification: 620x. H&E stain.

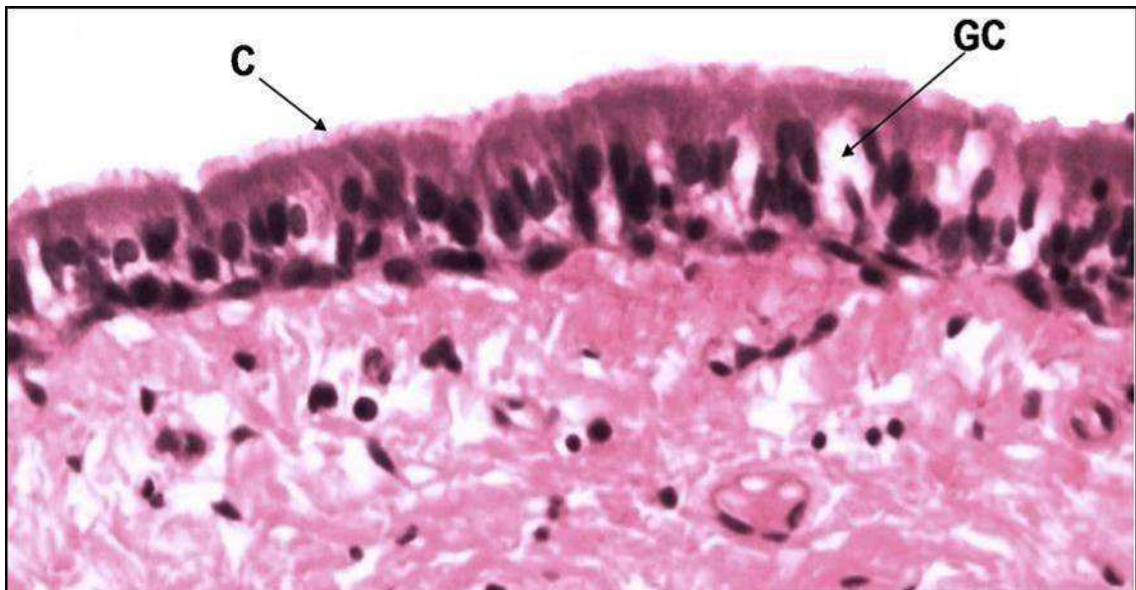


Figure 34: Section from tracheal mucosa of cigarette smoke-exposed rat after the recovery period, showing returns of cilia nearly toward normal morphology, together with a fewer number of cell proliferation in the epithelium. GC: goblet cell. C: cilia. H&E stain. Magnification: 1250x. H&E stain.

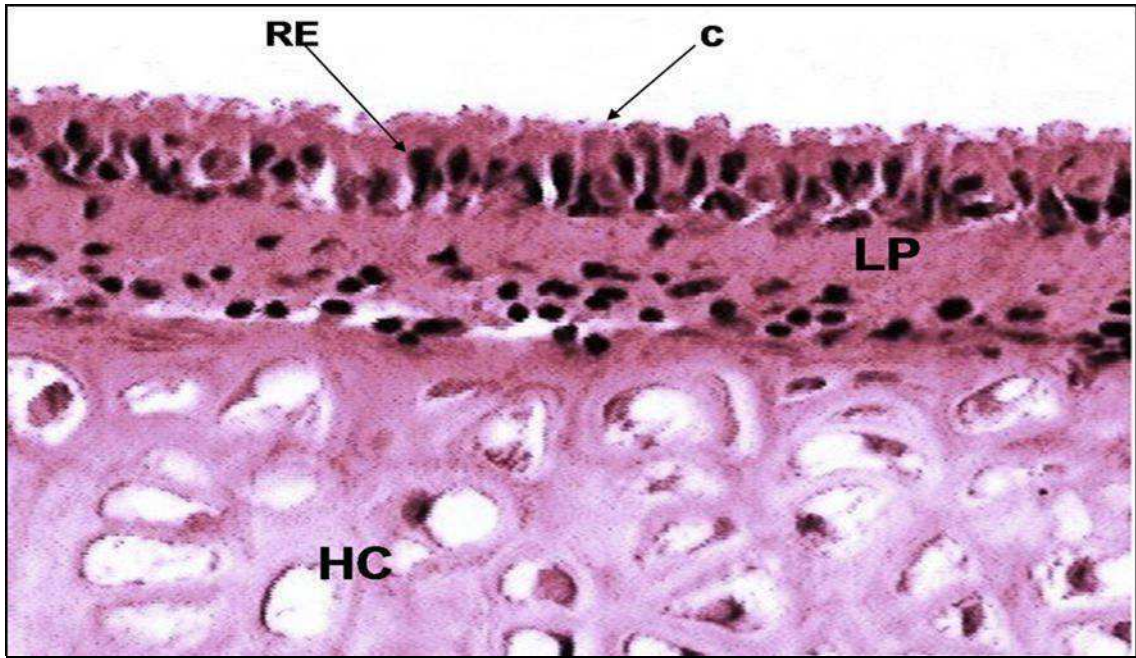


Figure 35: Trachea of cigarette smoke-exposed rat after the recovery period. Showing partial recovery of tracheal epithelium. RE: respiratory epithelium, LP: lamina propria, HC: hyaline cartilage. C: cilia. Magnification: 1060x. H&E stain.

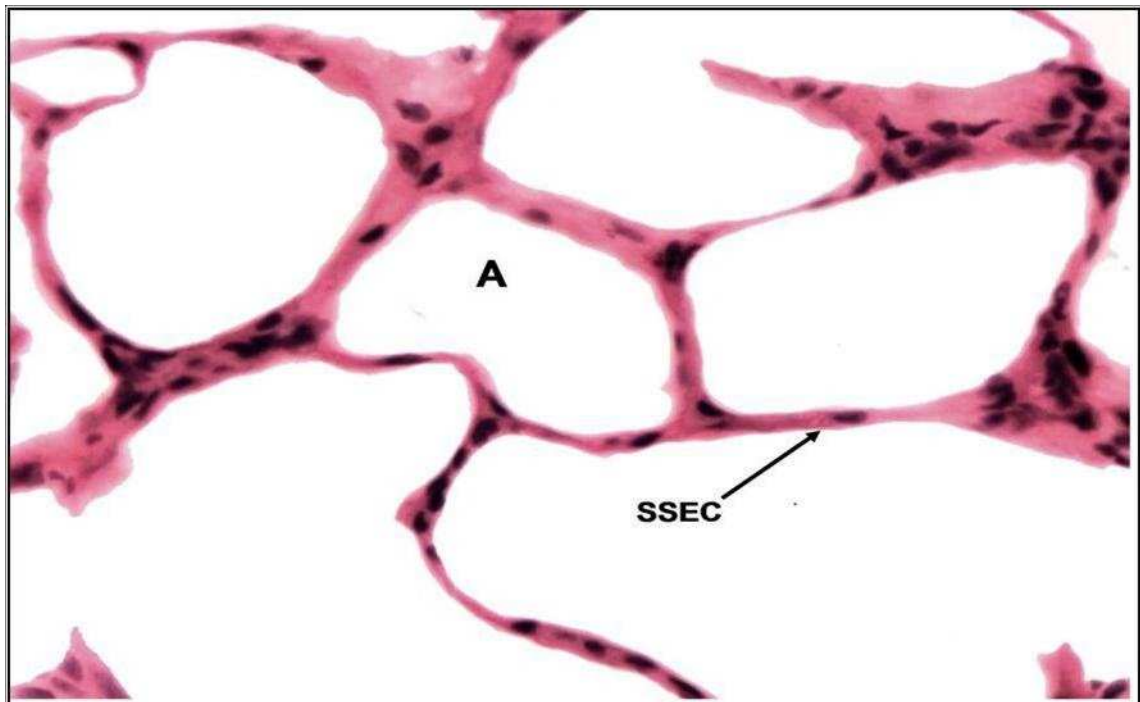


Figure 36: An enlarged image of a normal lung alveolus. A: alveolus, SSEC: simple squamous epithelial cell. Magnification: 815x .H&E stain.

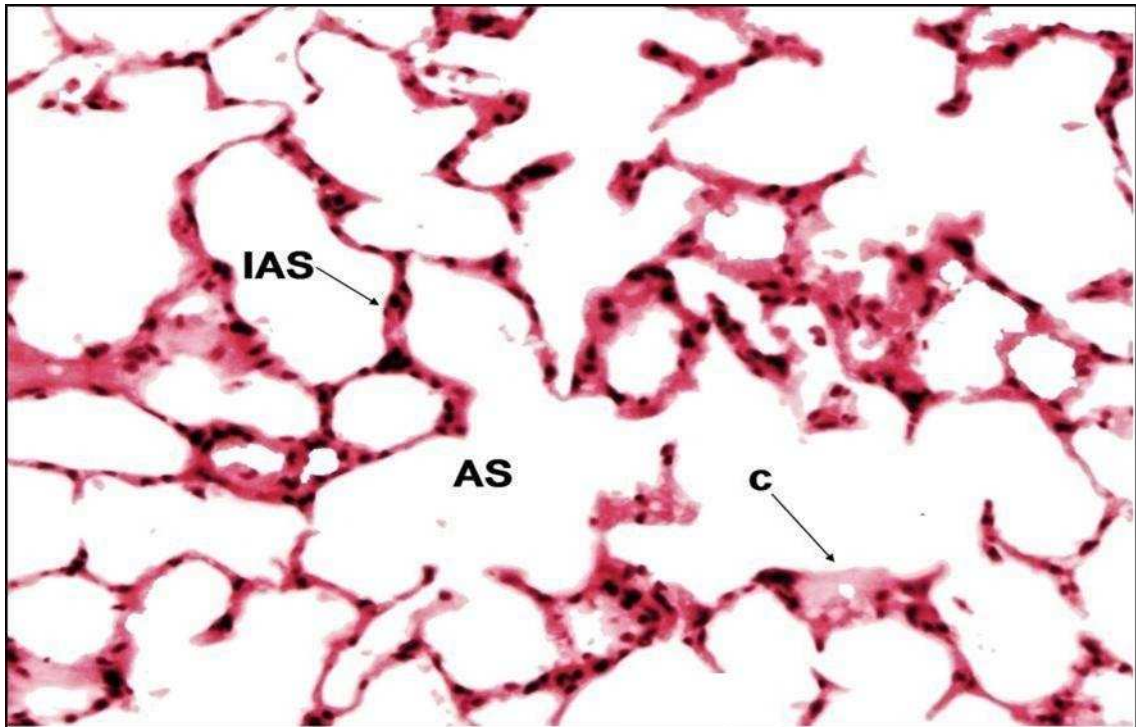


Figure 37: Control lung alveoli, IAS: interalveolar septum, AS: alveolar sac, C: capillary. Magnification: 270x. H&E stain.

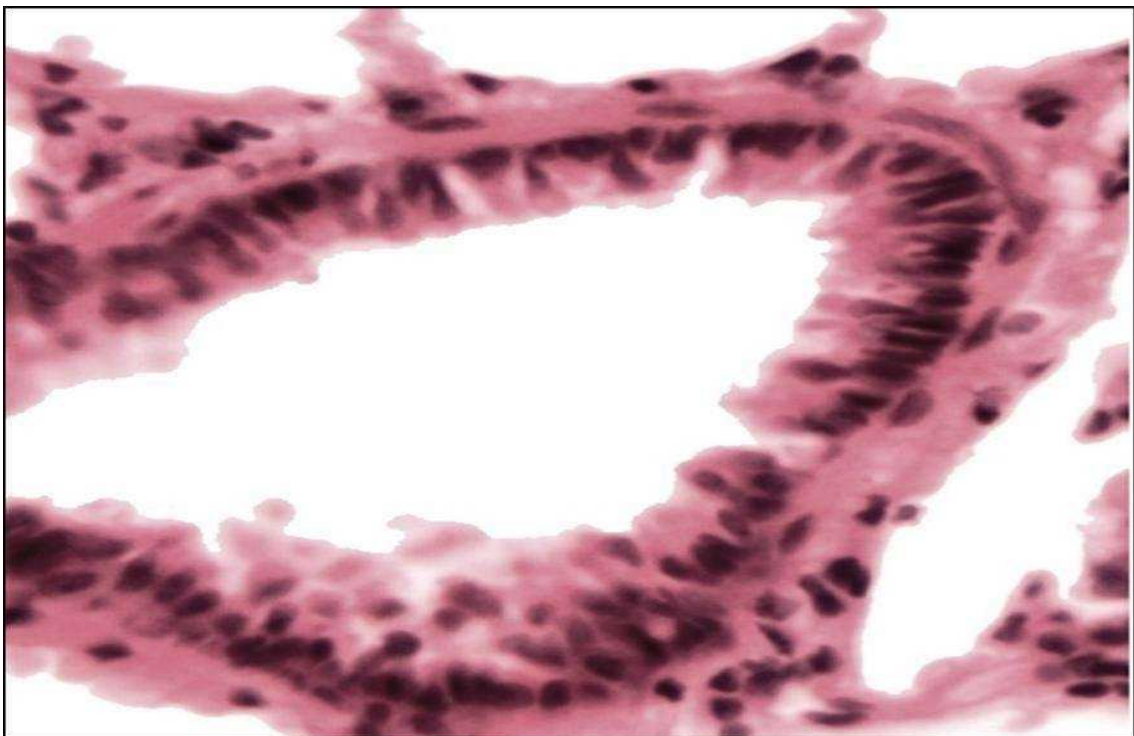


Figure 38: An enlarged image of a normal terminal bronchiole, showing continuous respiratory epithelium not interrupted by alveoli opening. Magnification: 1350x.H&E stain.

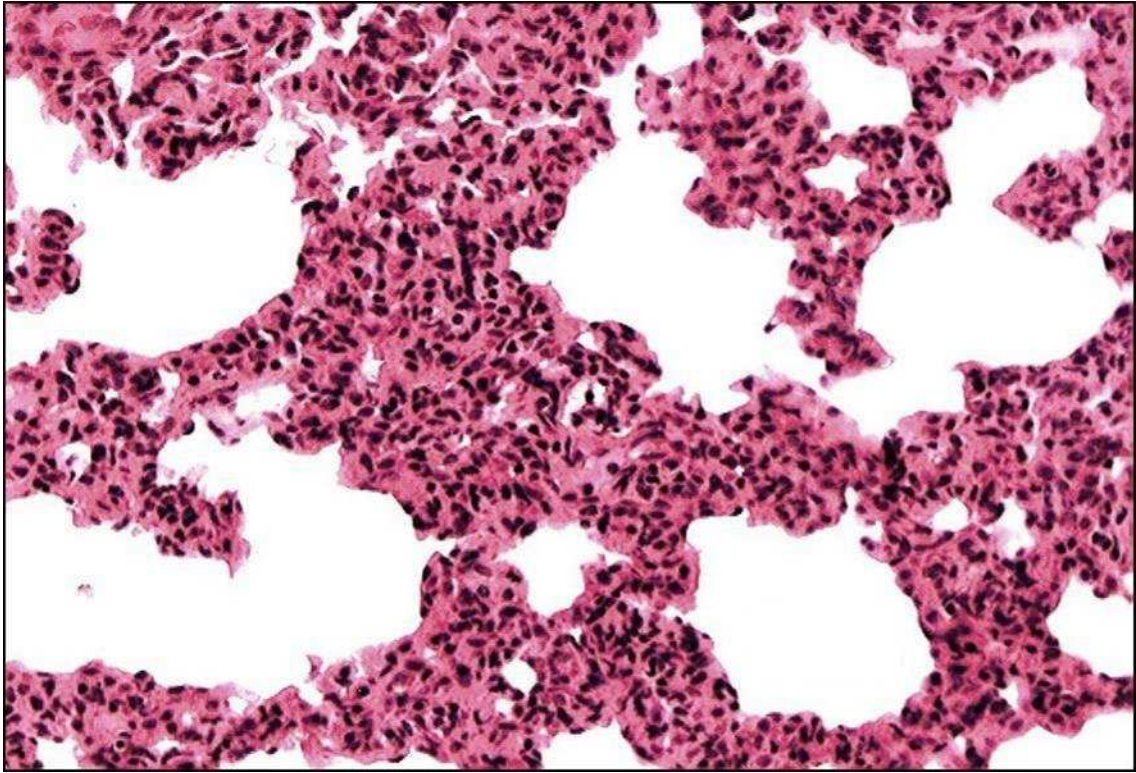


Figure 39: Lung alveoli of cigarette smoke-exposed rat, showed infiltration of different inflammatory cells, some degree of collapsed alveoli and deposition of collagen fibrils in the alveolar walls. Magnification: 435x .H&E stain

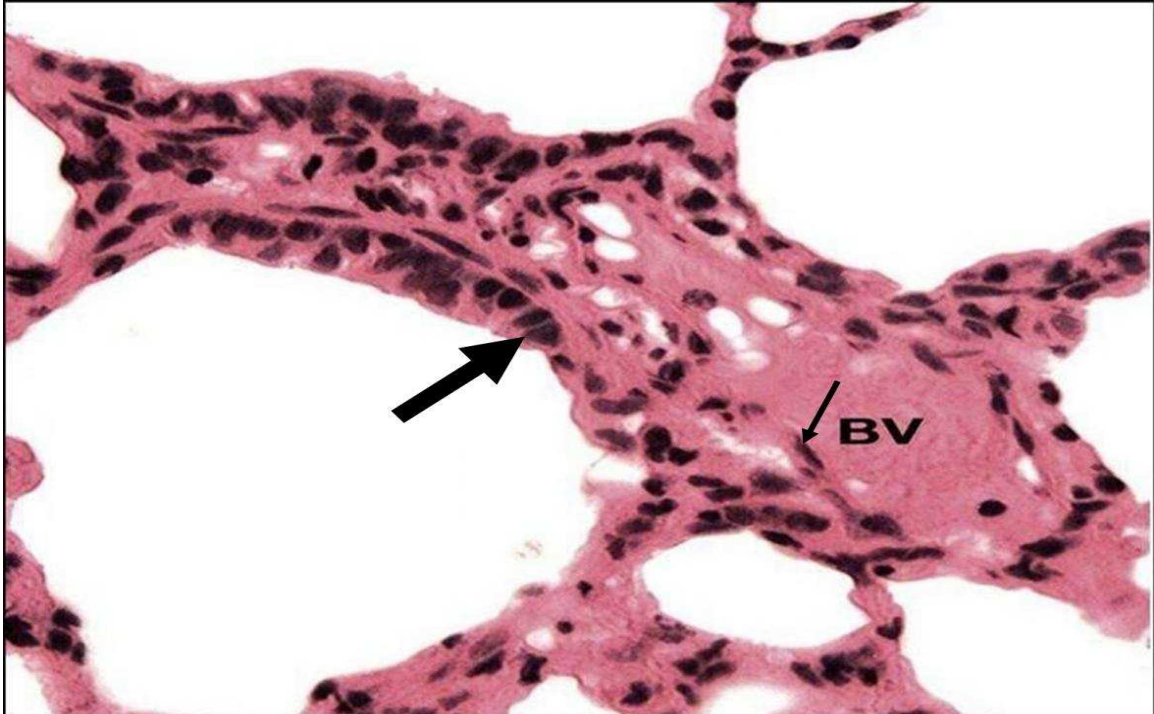


Figure 40: Lung alveoli of cigarette smoke-exposed rat, showing some degree of thickening in the blood-air barrier. BV: Blood vessel. Thick arrow: type I alveolar epithelial cell. Thin arrow: Endothelial cell. Magnification: 1160x .H&E stain.

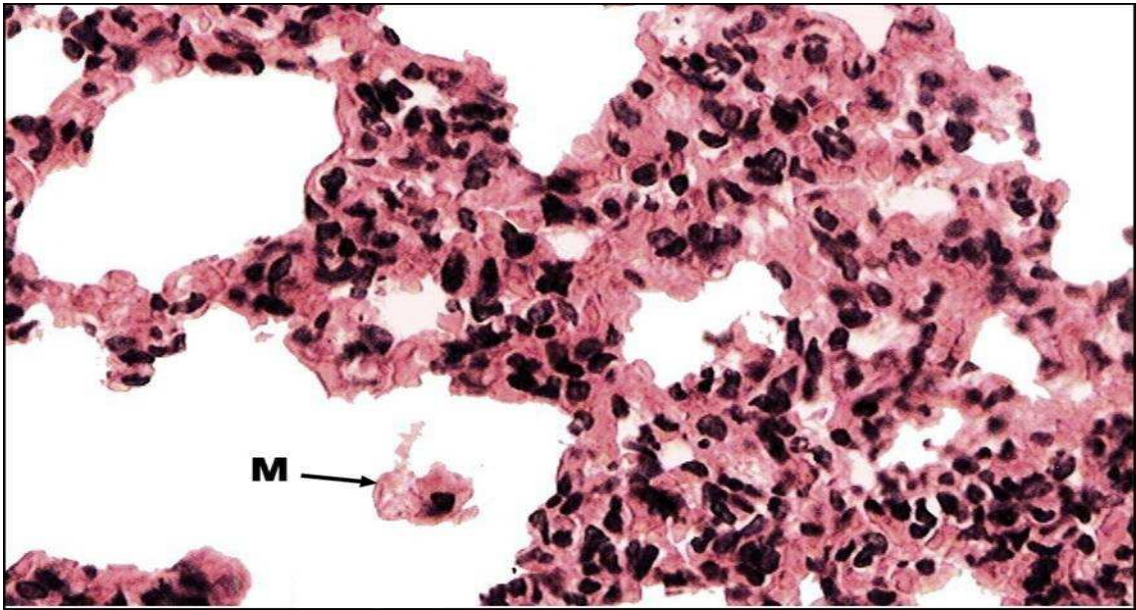


Figure 41: Lung alveoli of cigarette smoke-exposed rat, showing thickening in the alveolar wall and macrophage is not filled with inclusion bodies (deficient in phagocytosis). M: alveolar macrophage (dust cell). Magnification: 750x. H&E stain.

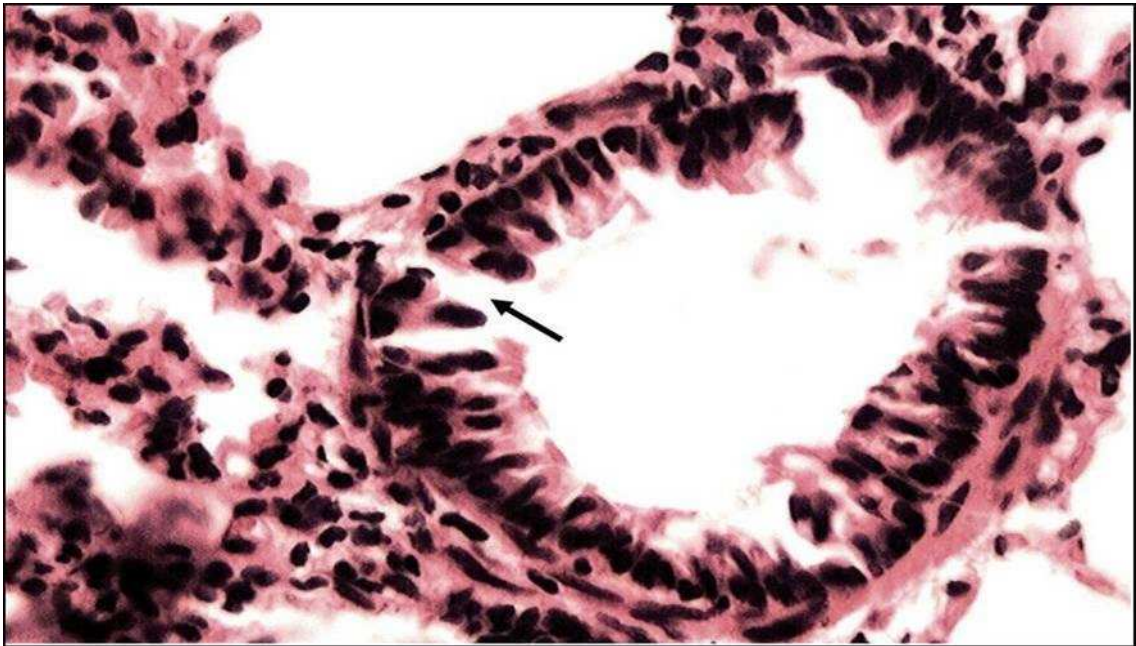


Figure 42: An enlarged image of a terminal bronchiole of cigarette smoke-exposed rat, showing disturbed respiratory epithelium, and an epithelial cell hyperplasia. Magnification: 900x. H&E stain.

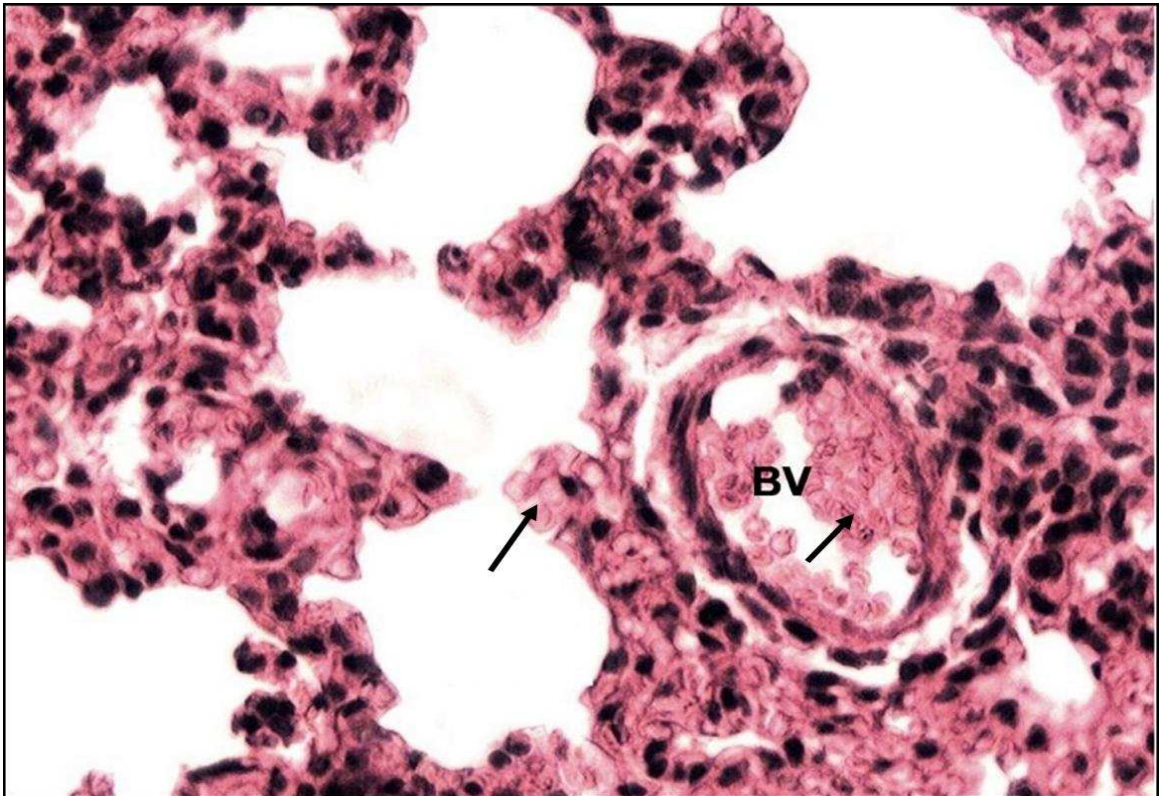


Figure 43: Lung alveoli of cigarette smoke-exposed rat, showing blood extravasation. Arrow: Erythrocyte .Magnification: 750x.H&E stain.

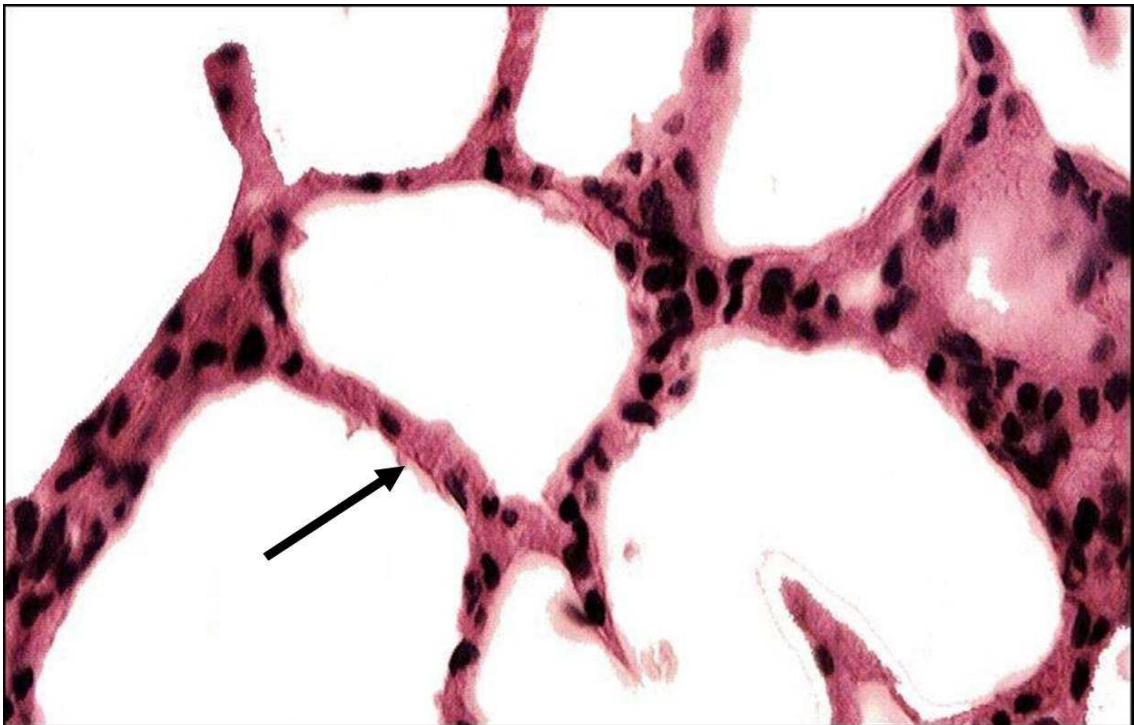


Figure 44: Lung alveoli of cigarette smoke-exposed rat after the recovery period. Showing partial recovery of lung alveoli. Arrow showing thickening in the alveolar wall Magnification: 780x .H&E stain.

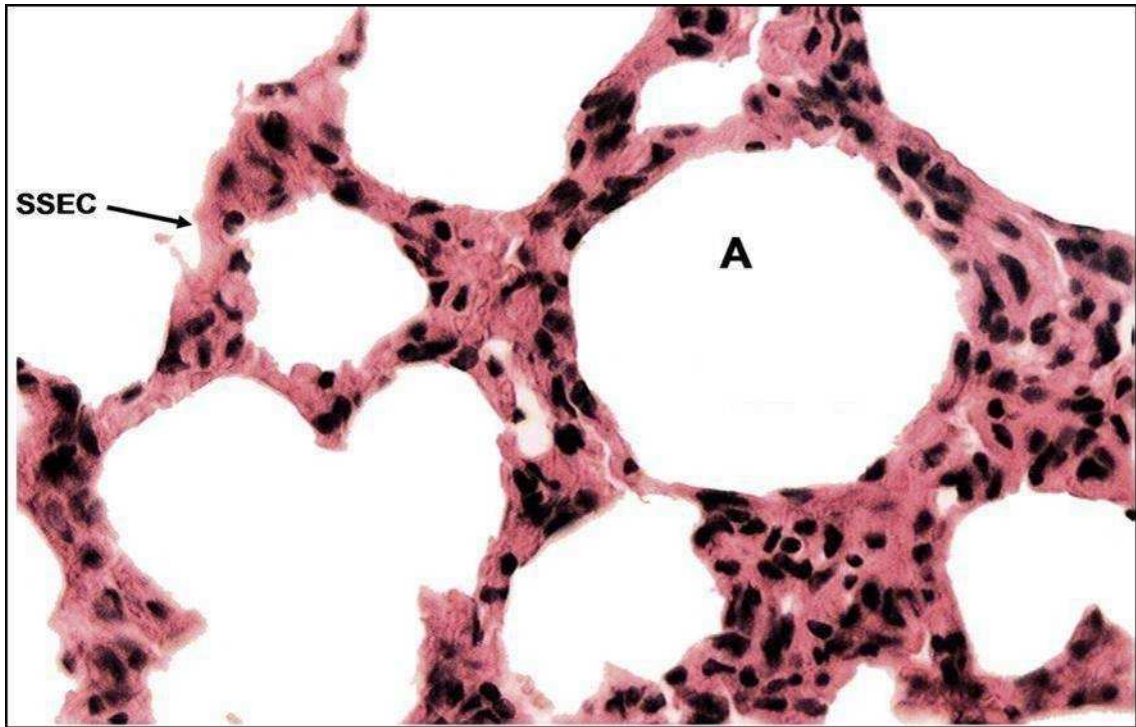


Figure 45: Lung alveoli of cigarette smoke-exposed rat after partial recovery. Showing less thickening in the alveolar wall. A: alveolus, SSEC: simple squamous epithelial cell. Magnification: 745x.H&E stain.

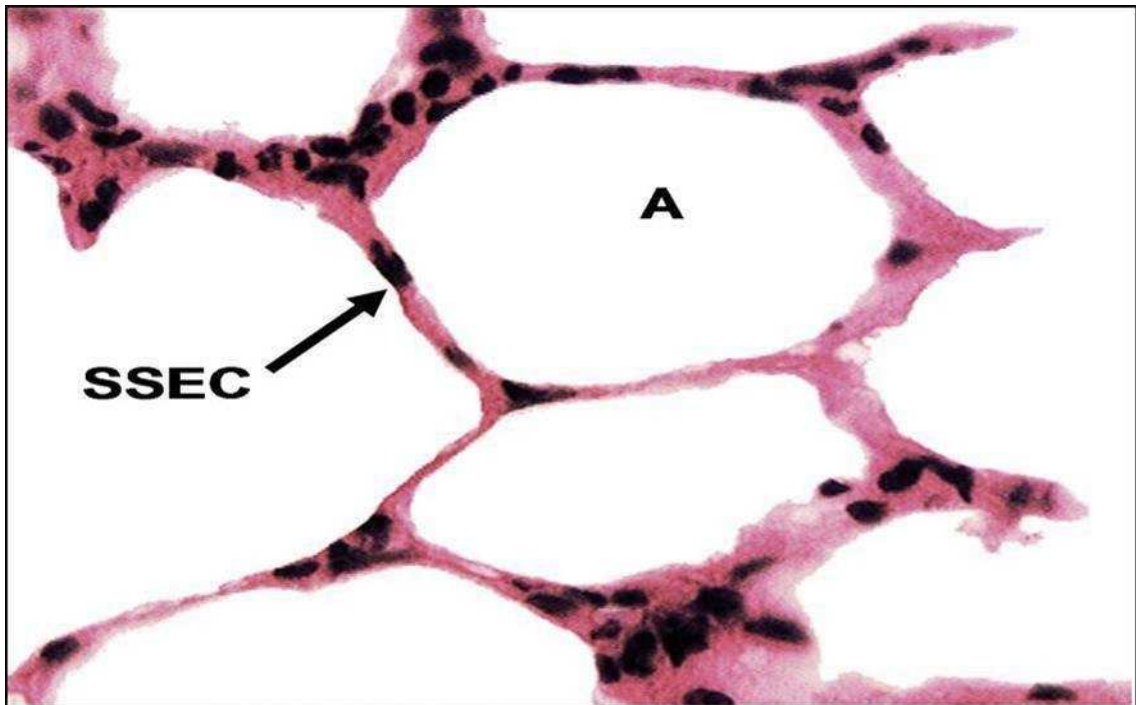


Figure 46: Lung alveoli of cigarette smoke-exposed rat after the partial recovery. Much less thickening in the alveolar wall and no inflammatory cell infiltration was observed. A: alveolus, SSEC: simple squamous epithelial cell. Magnification: 1380x . H&E stain.

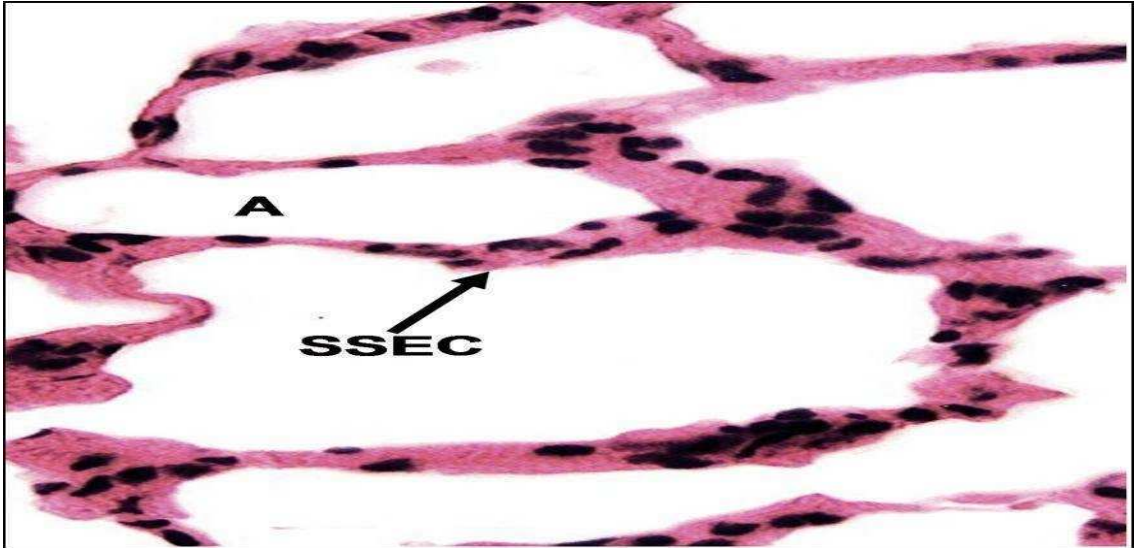


Figure 47: Lung alveoli of cigarette smoke-exposed rat after the partial recovery, showing less thickening in the alveolar wall. A: alveolus, SSEC: simple squamous epithelial cell. Magnification: 1750. H&E stain.

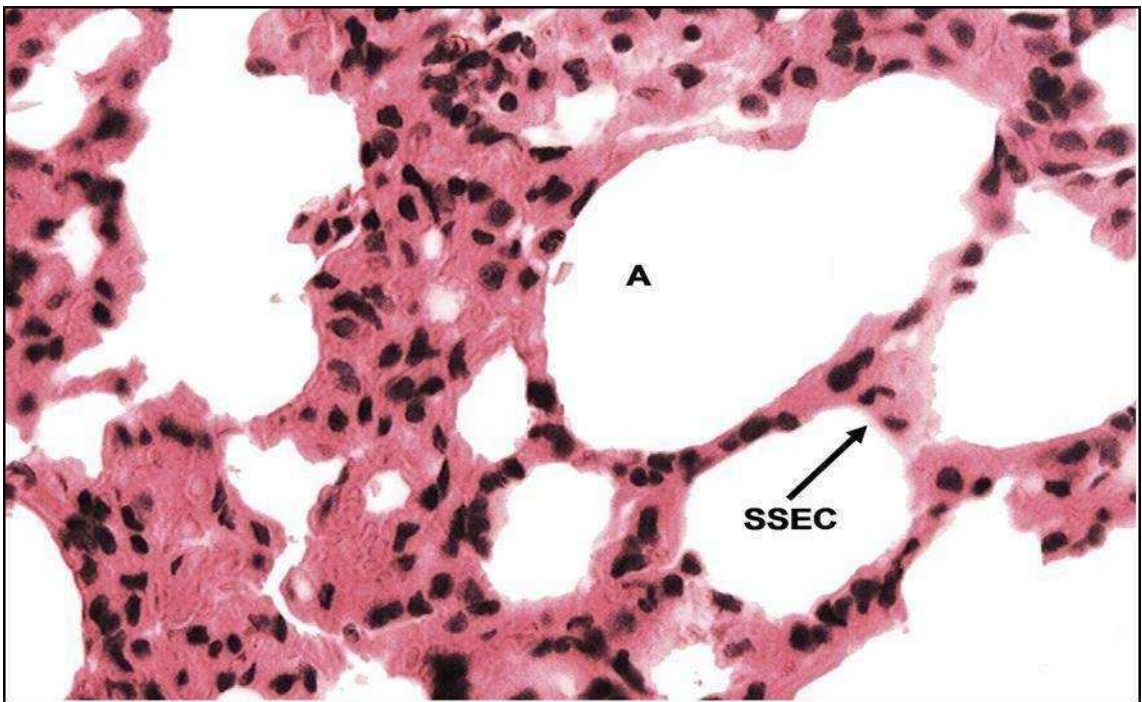


Figure 48: Lung alveoli of cigarette smoke-exposed rat after partial recovery. Showing some regions of thick alveolar walls. A: alveolus, SSEC: simple squamous epithelial cell. Magnification: 890x. H&E stain.

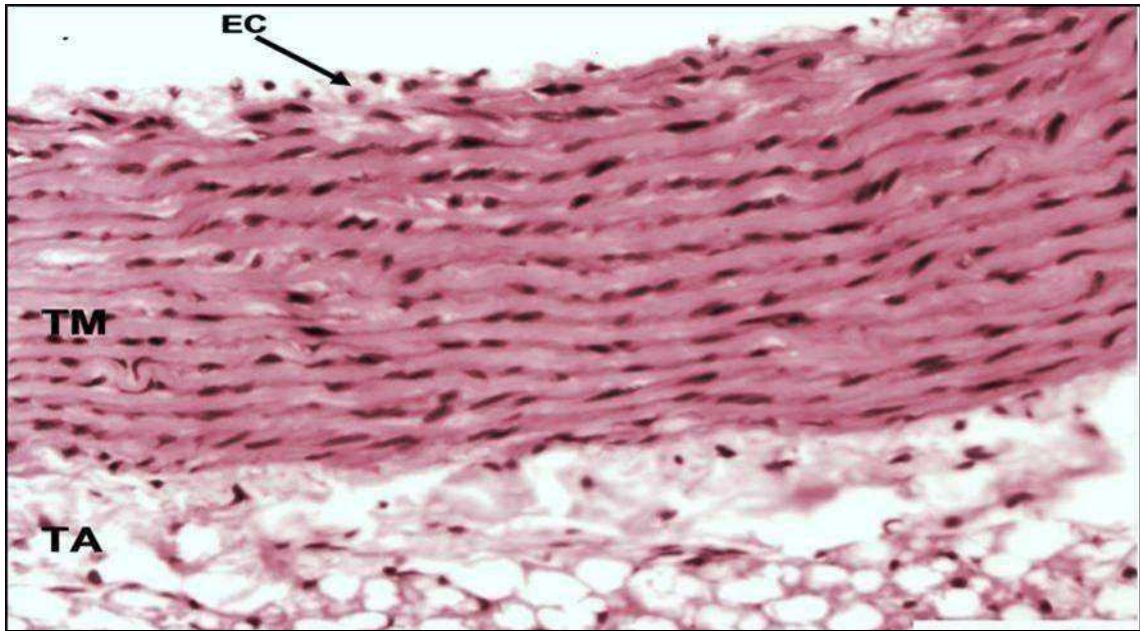


Figure 49: Normal histology of the aorta (internal elastic lamina is not evident in control). EC: endothelial cell TM: tunica media, TA: tunica adventitia. Magnification: 300x.H&E stain.

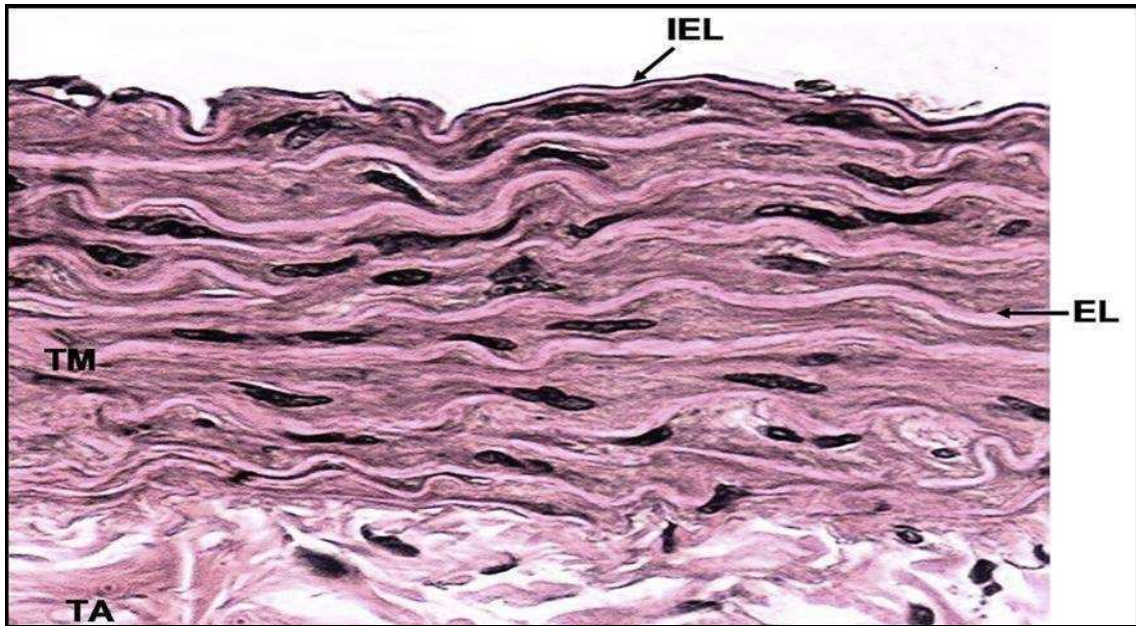


Figure 50: Aortic tissue from cigarette smoke-exposed rat, showing thickening in the internal elastic lamina and in the elastic lamellae in the media, elastic lamellae more obvious in the tunica media, elongated nuclei, slightly contracted smooth muscles are also seen. TM: Tunica media, TA: Tunica adventitia. IEL: Thick internal elastic lamina. EL: Thick elastic lamellae in tunica media. Magnification: 950x.H&E stain.

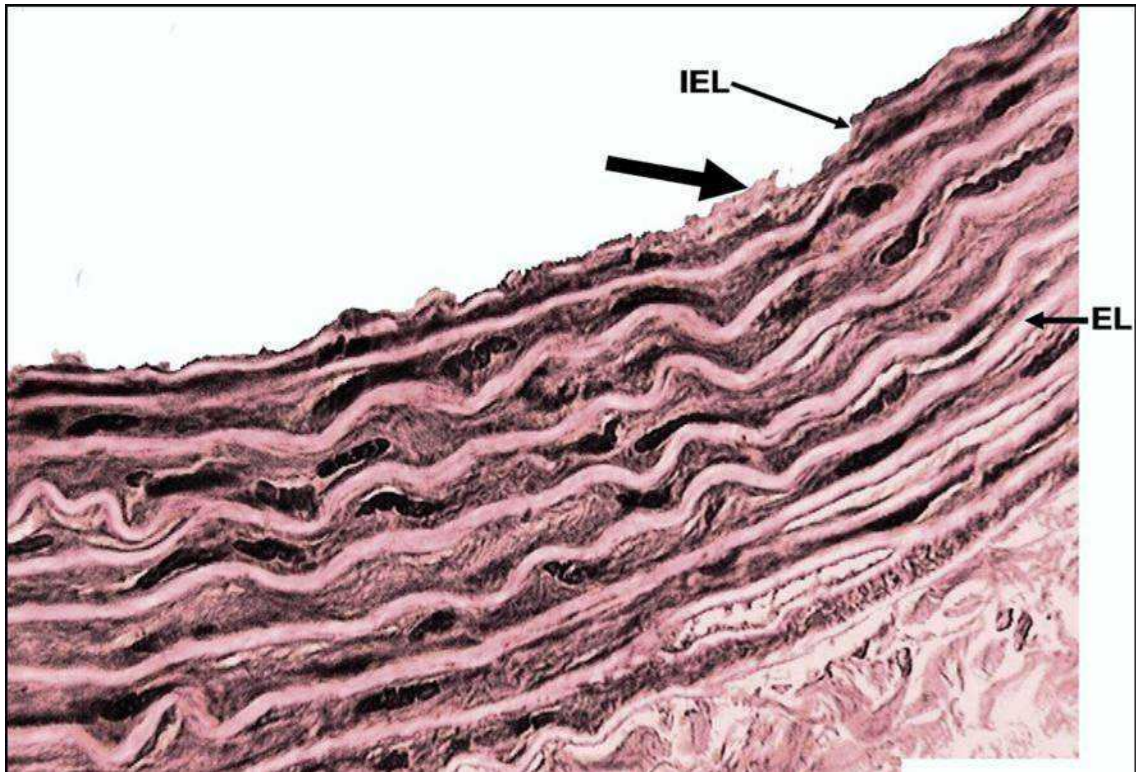


Figure 51: Aortic tissue from cigarette smoke-exposed rat. Showing thickening in the internal elastic lamina and in the elastic lamellae in the media, elastic lamellae more obvious in the tunica media. Thick arrow: endothelial cells disruption. IEL: Thick internal elastic lamina. EL: Thick elastic lamellae. Magnification: 720x . H&E stain.

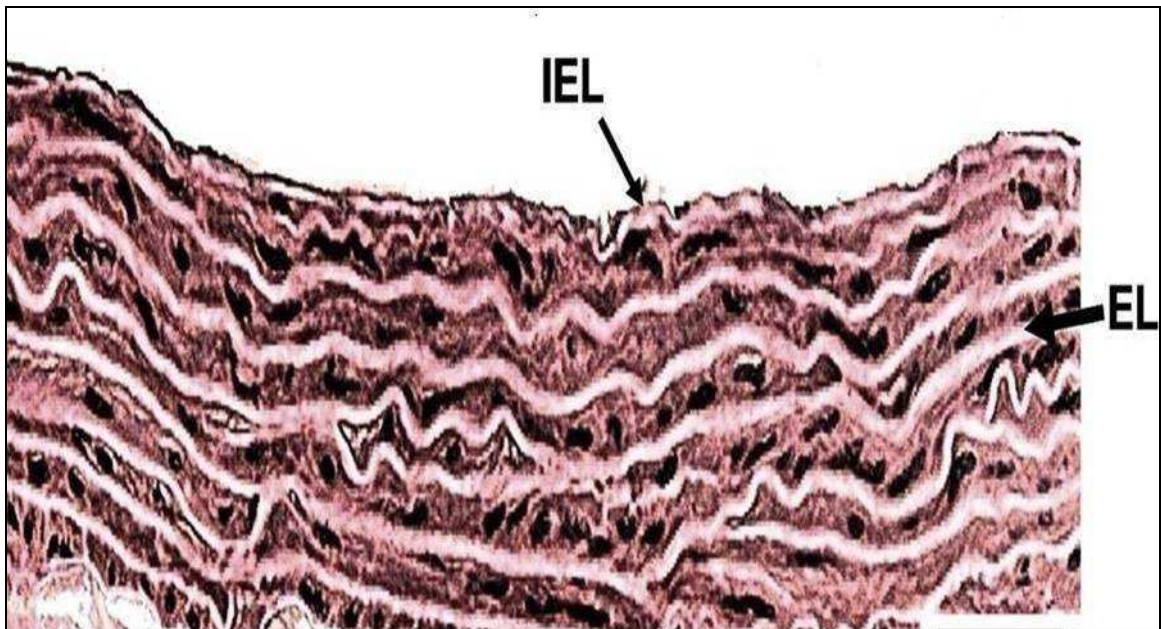


Figure 52: Aortic tissue from cigarette smoke-exposed rat, showing slight contracted smooth muscles. IEL: Thick internal elastic lamina. EL: Thick elastic lamellae in tunica media. Magnification: 385x. H&E stain.

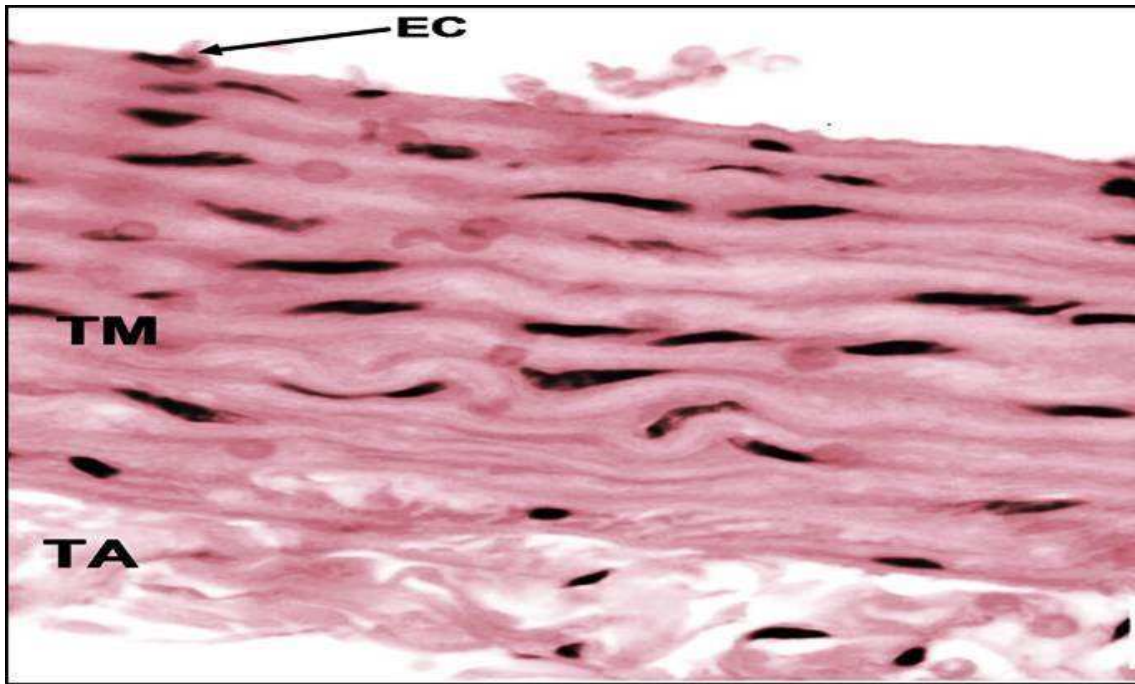


Figure 53: Aortic tissue from cigarette smoke-exposed rat after recovery period. Showing partial recovery of aortic tissue. Nuclei are still elongated. Arrow: endothelial cell. Magnification: 1500x . H&E stain.

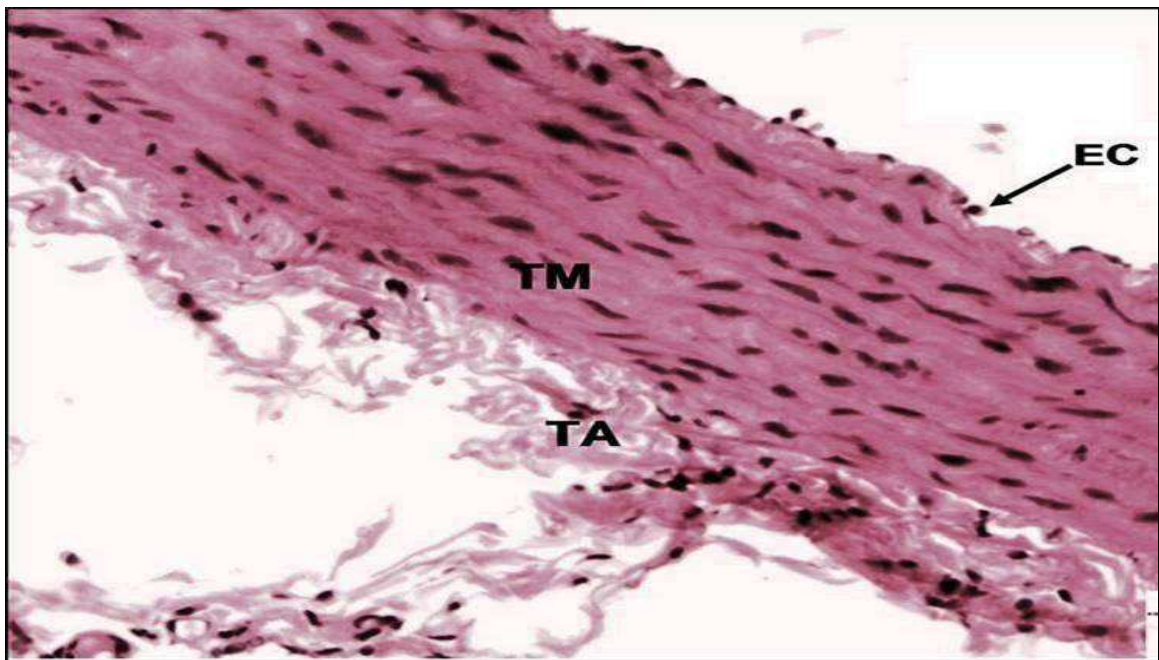


Figure 54: Aortic tissue from cigarette smoke-exposed rat after the recovery period. Showing partial recovery of aortic tissue. Nuclei are still elongated. Arrow: normal endothelial cell. Magnification: 400x.H&E stain.

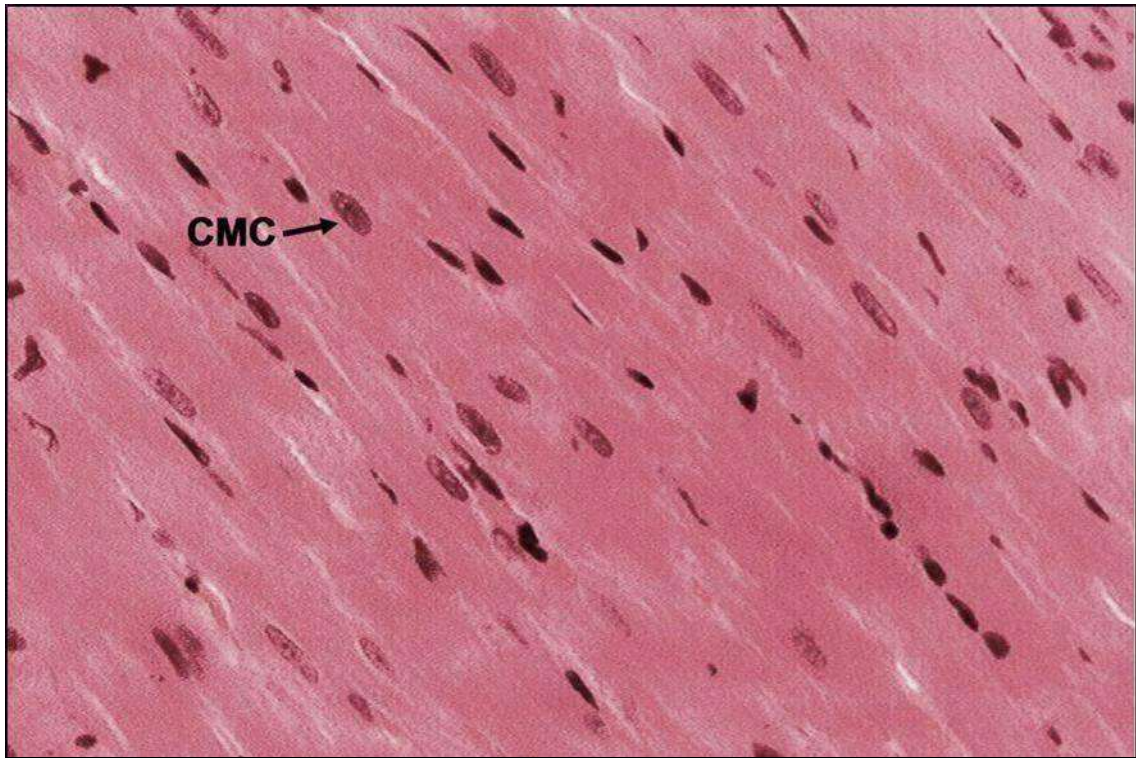


Figure 55: Normal heart ventricular tissue. CMC: nucleus cardiac muscle cell. Magnification: .830x. H&E stain

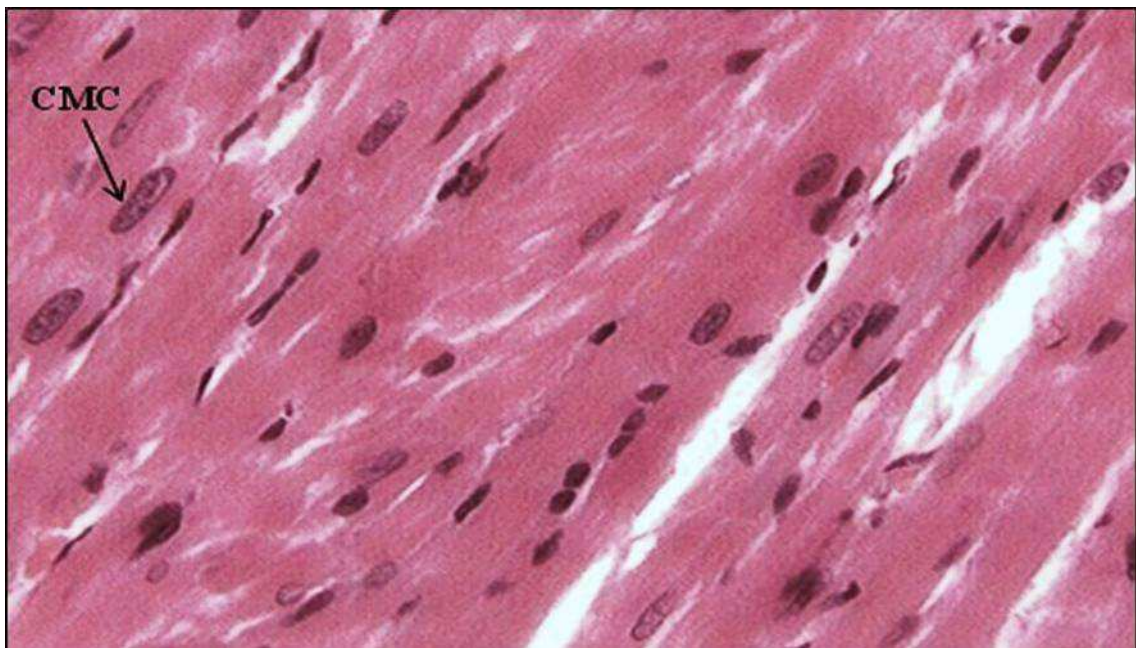


Figure 56: Magnified image of heart ventricular tissue from control rat. CMC: nucleus cardiac muscle cell. Magnification: 900x. H&E stain.

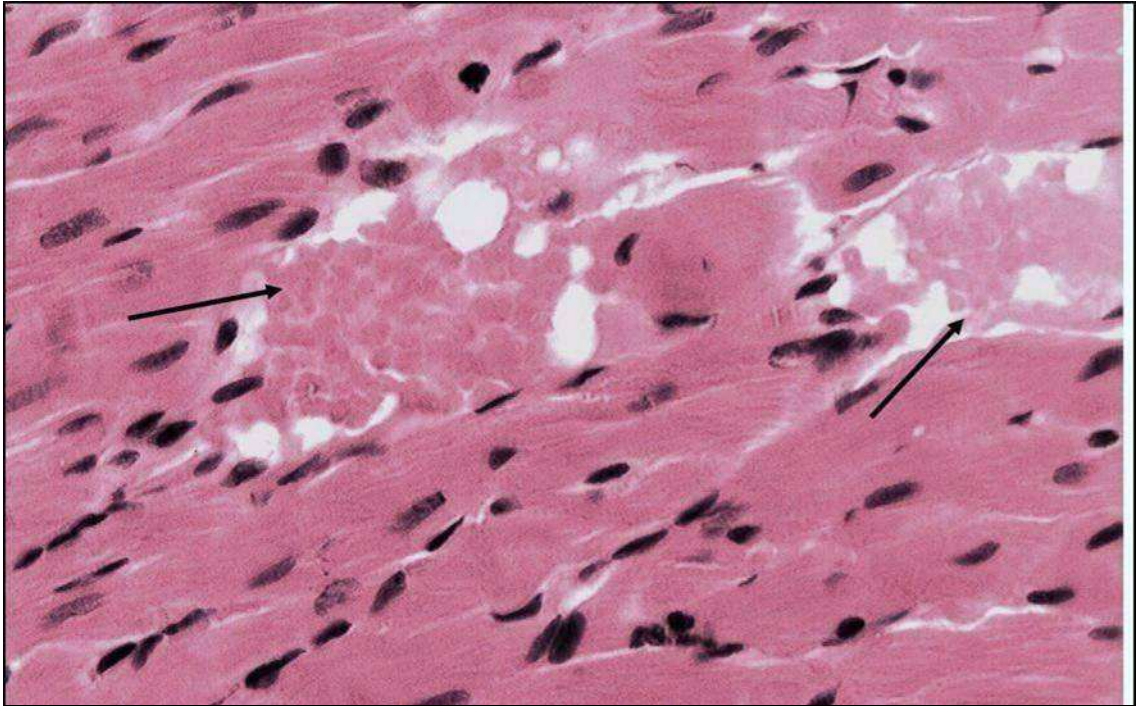


Figure 57: Heart ventricular tissue of cigarette smoke-exposed rat. Arrow: congested blood vessel. Magnification: 760x. H&E stain.

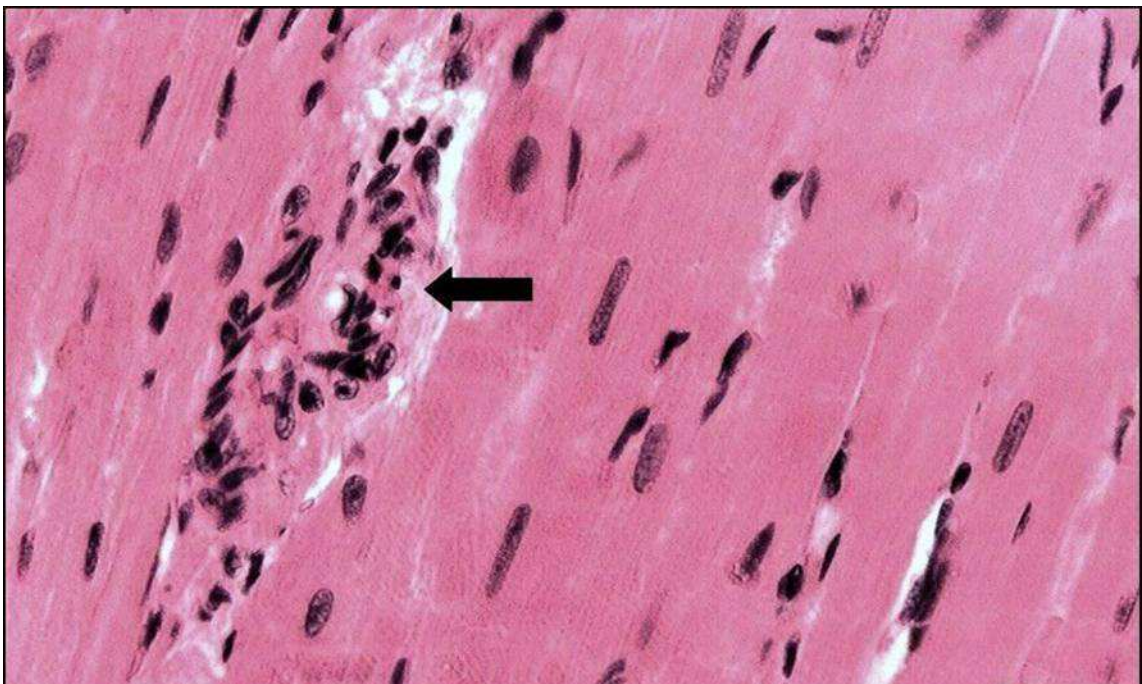


Figure 58: Heart ventricular tissue of cigarette smoke-exposed rat. Showed elongated nuclei. Arrow: inflammatory cell infiltration caused by damage of the blood vessel. Magnification: 790x .H&E stain.

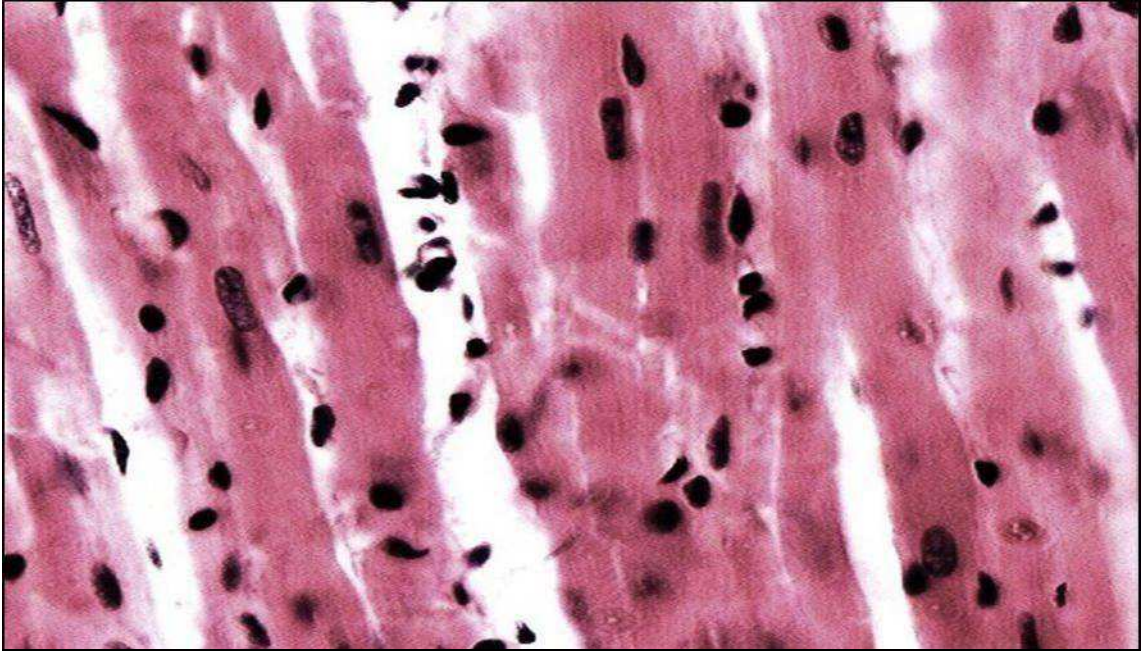


Figure 59: Heart ventricular tissue of cigarette smoke-exposed rat, showing some degree of separation between cardiac muscle fibers. Magnification: 750x.H&E stain.

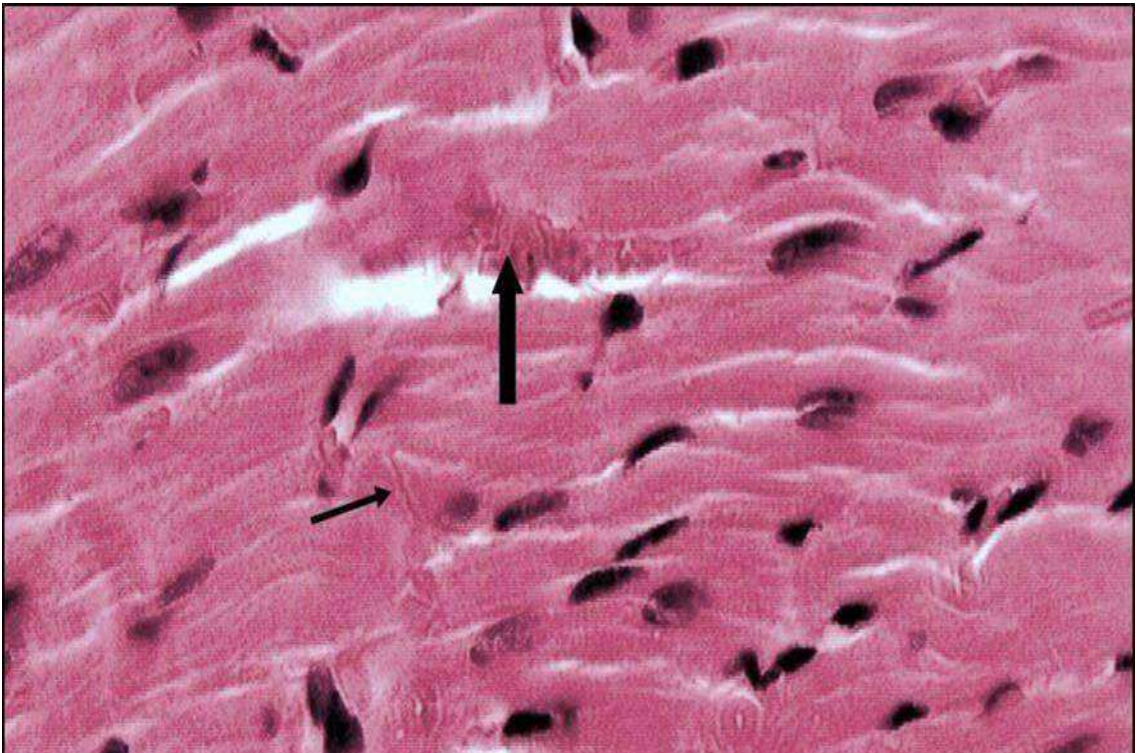


Figure 60: Heart ventricular tissue of cigarette smoke-exposed rat. Thick arrow: congested blood vessel. Thin arrow: intercalated disc. Magnification: 950x .

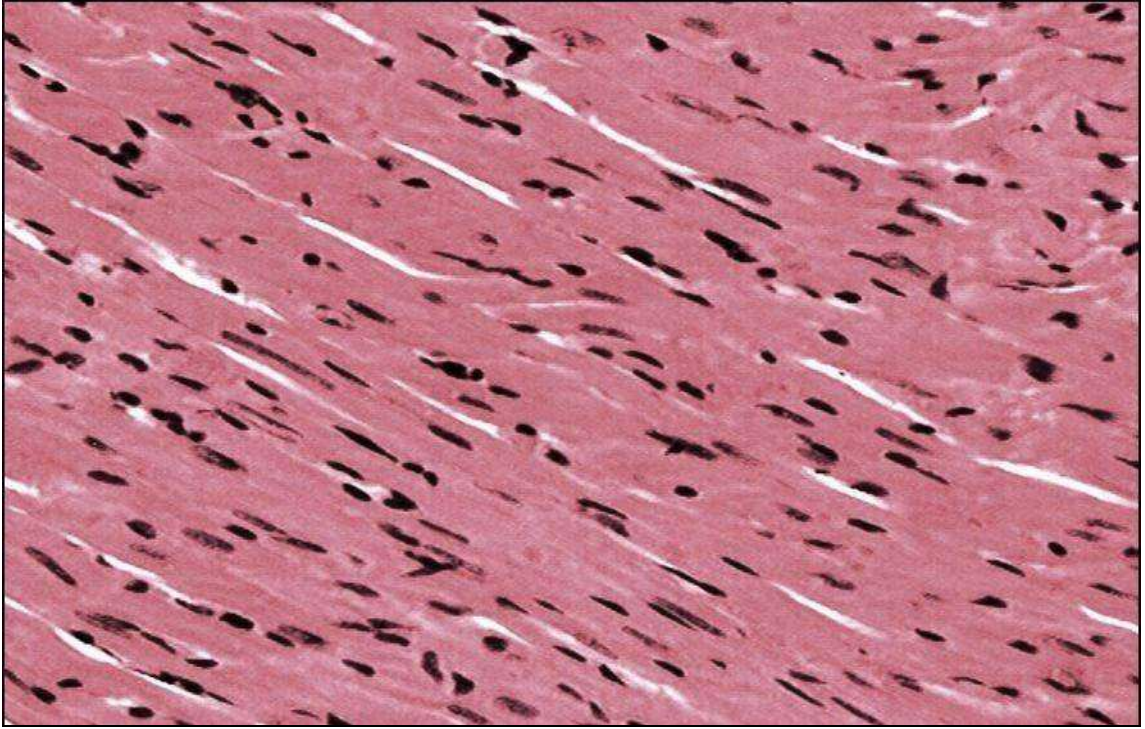


Figure 61: Heart ventricular tissue of cigarette smoke-exposed rat after the recovery period. Showing partial recovery of Heart ventricular tissue. Magnification: 640x.H&E stain.

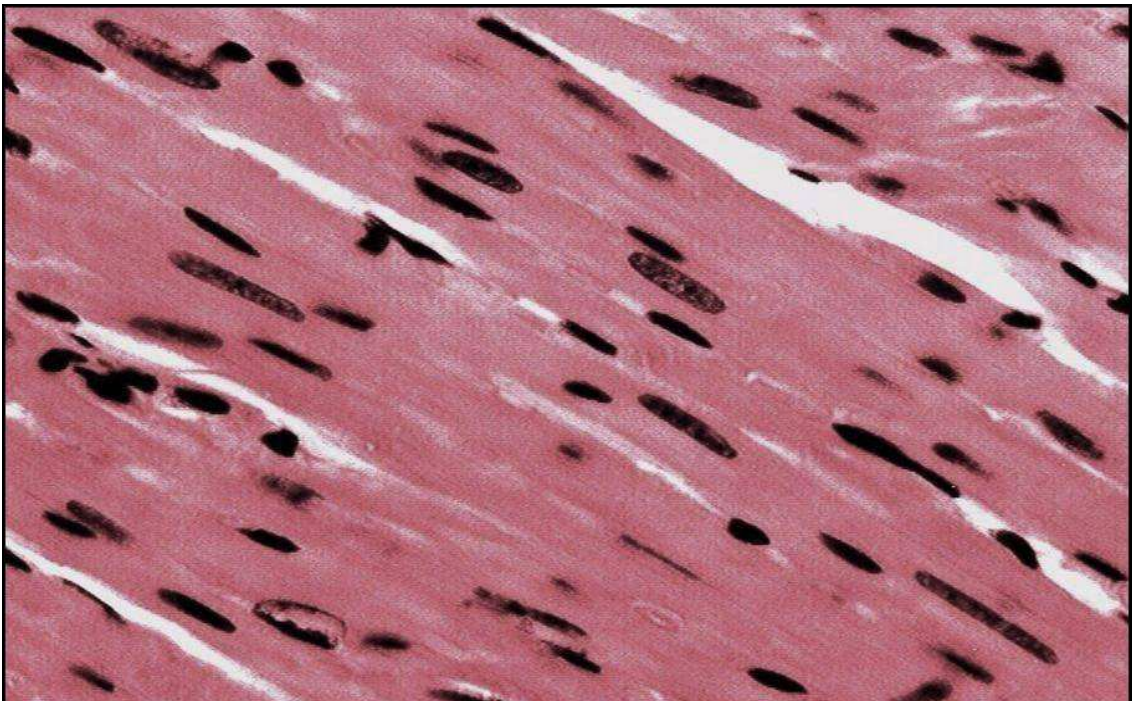


Figure 62: Heart ventricular tissue of cigarette smoke-exposed rat after the recovery period. Showing partial recovery of Heart ventricular tissue. Nuclei are still elongated. Magnification: 1130x. H&E stain.

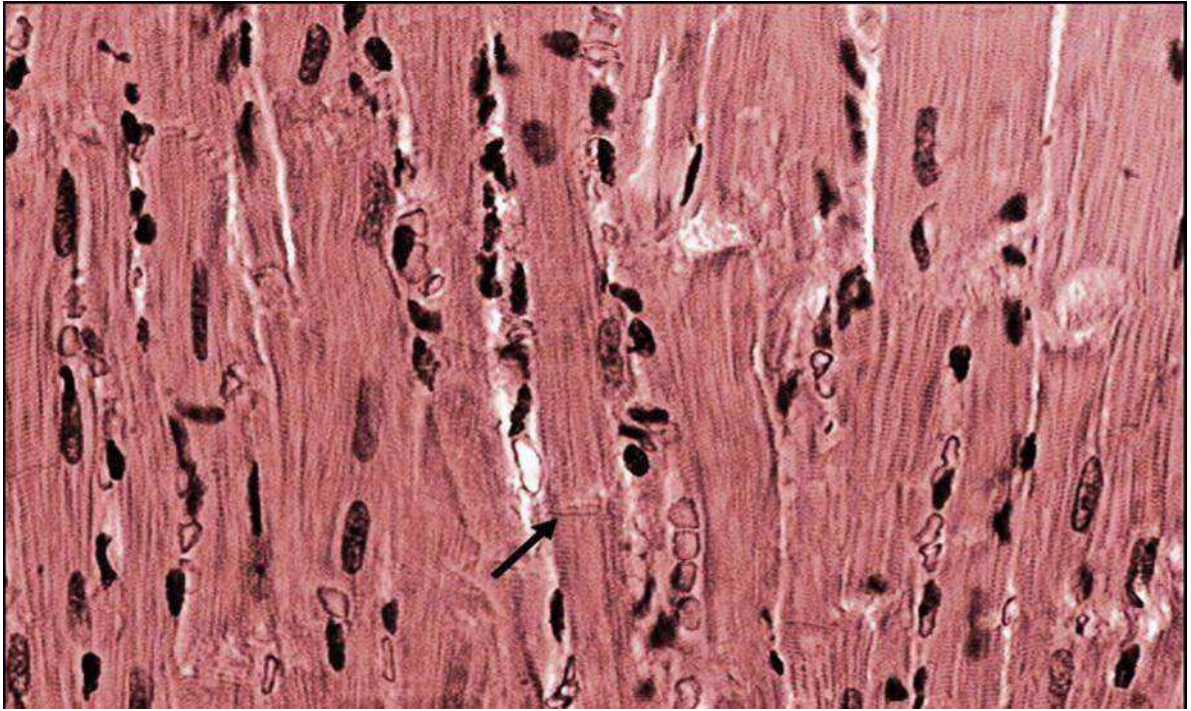


Figure 63: Heart ventricular tissue of cigarette smoke-exposed rat after the recovery period. Showing partial recovery of the Heart ventricular tissue. Nuclei are still elongated Arrow: intercalated disc. Magnification: 875x.H&E stain.

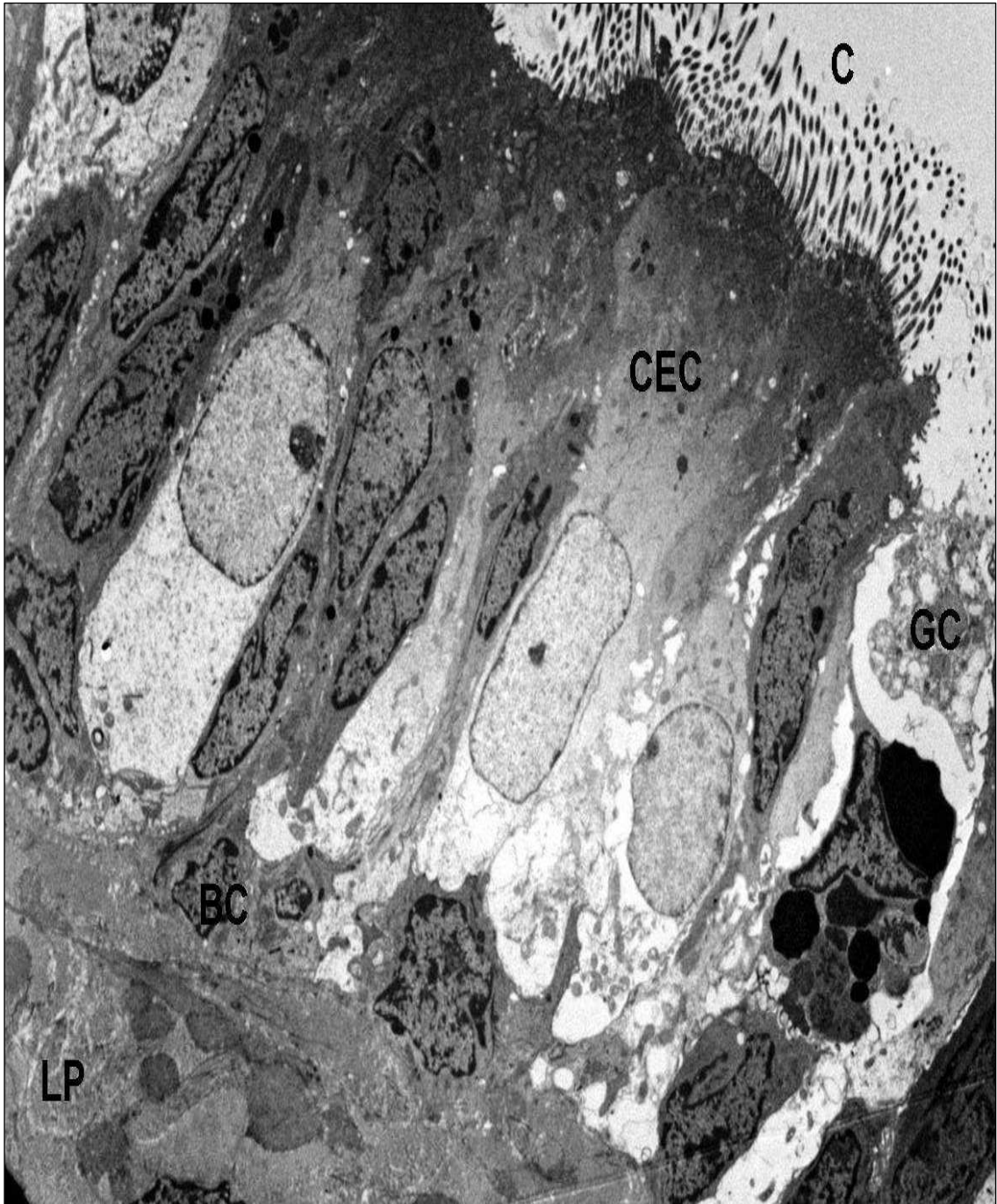


Figure 64: Thin section of control tracheal tissue. C: cilia, GC: goblet cell, CEC: columnar epithelial cell, BC: basal cell (act as stem cell), LP: lamina propria. Magnification: 3000x.

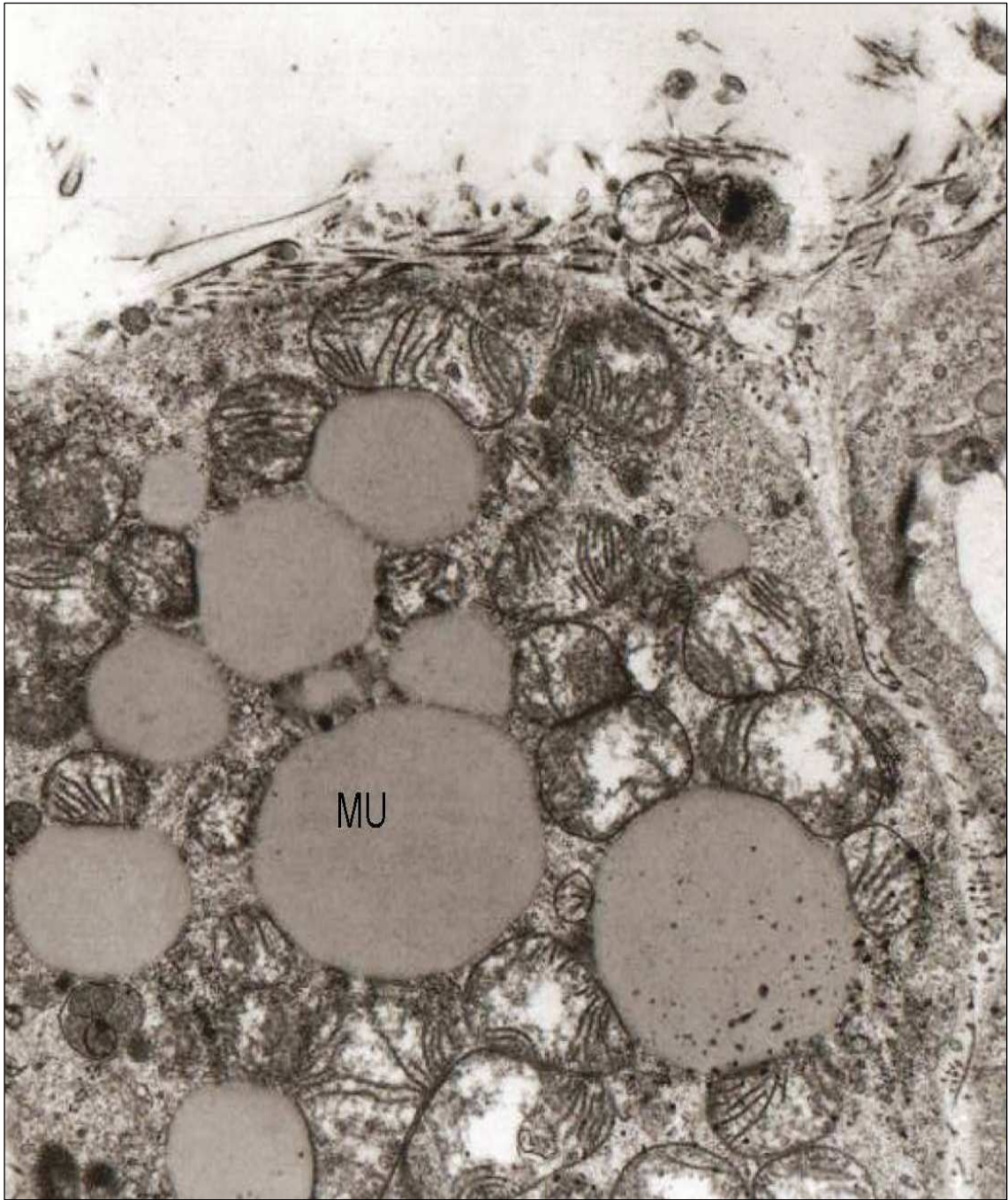


Figure 65: Closer image at a normal tracheal goblet cell, Mu: mucigen granules. Magnification: 20000 x.

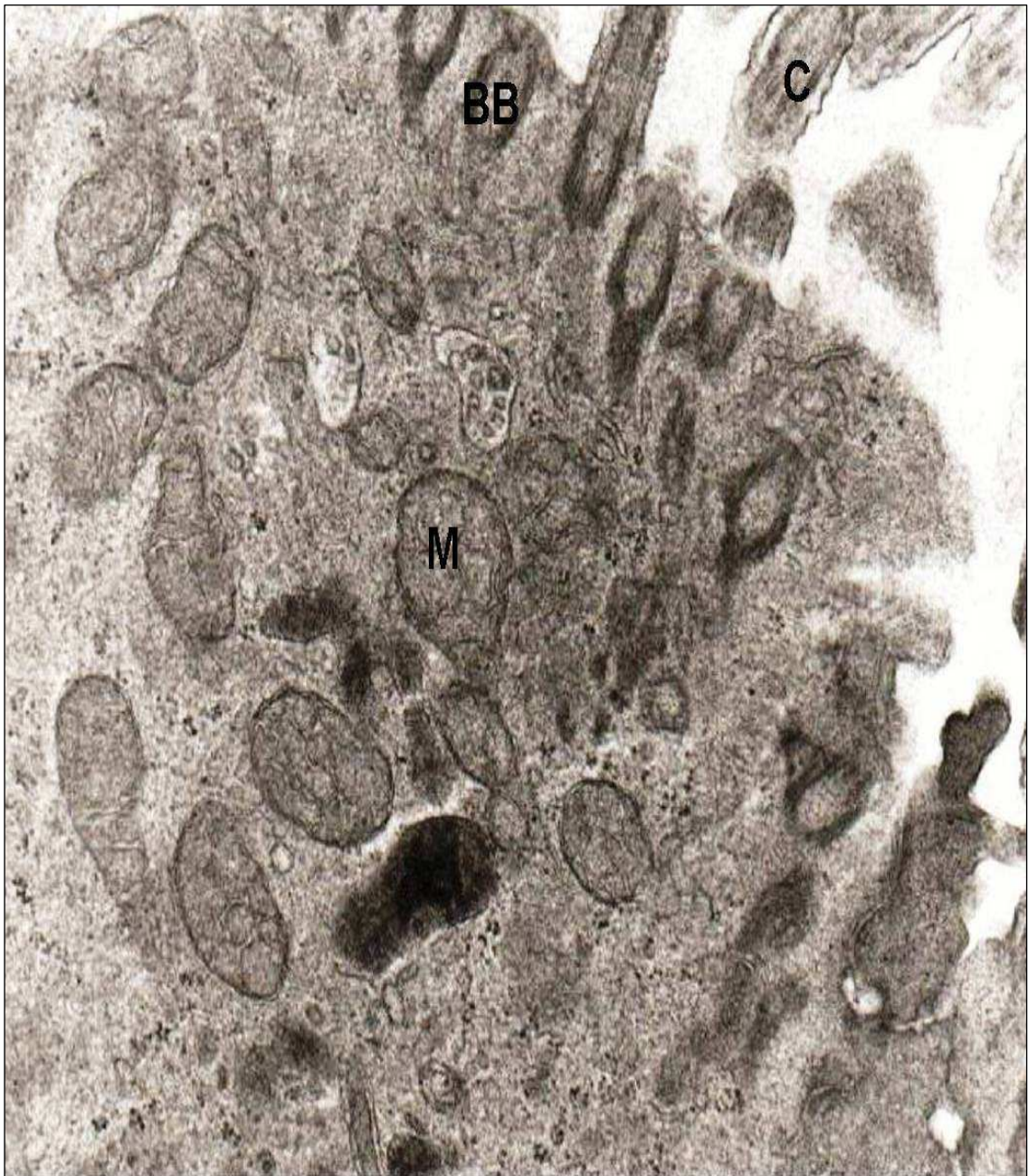


Figure 66: Thin section in the tracheal epithelium of cigarette smoke-exposed rat, where boundaries between cells can't be clearly distinguished. Mitochondria aggregate in the apical portion of epithelial cells. C: cilia, M: Mitochondria. BB: basal body. Magnification: 62500x.

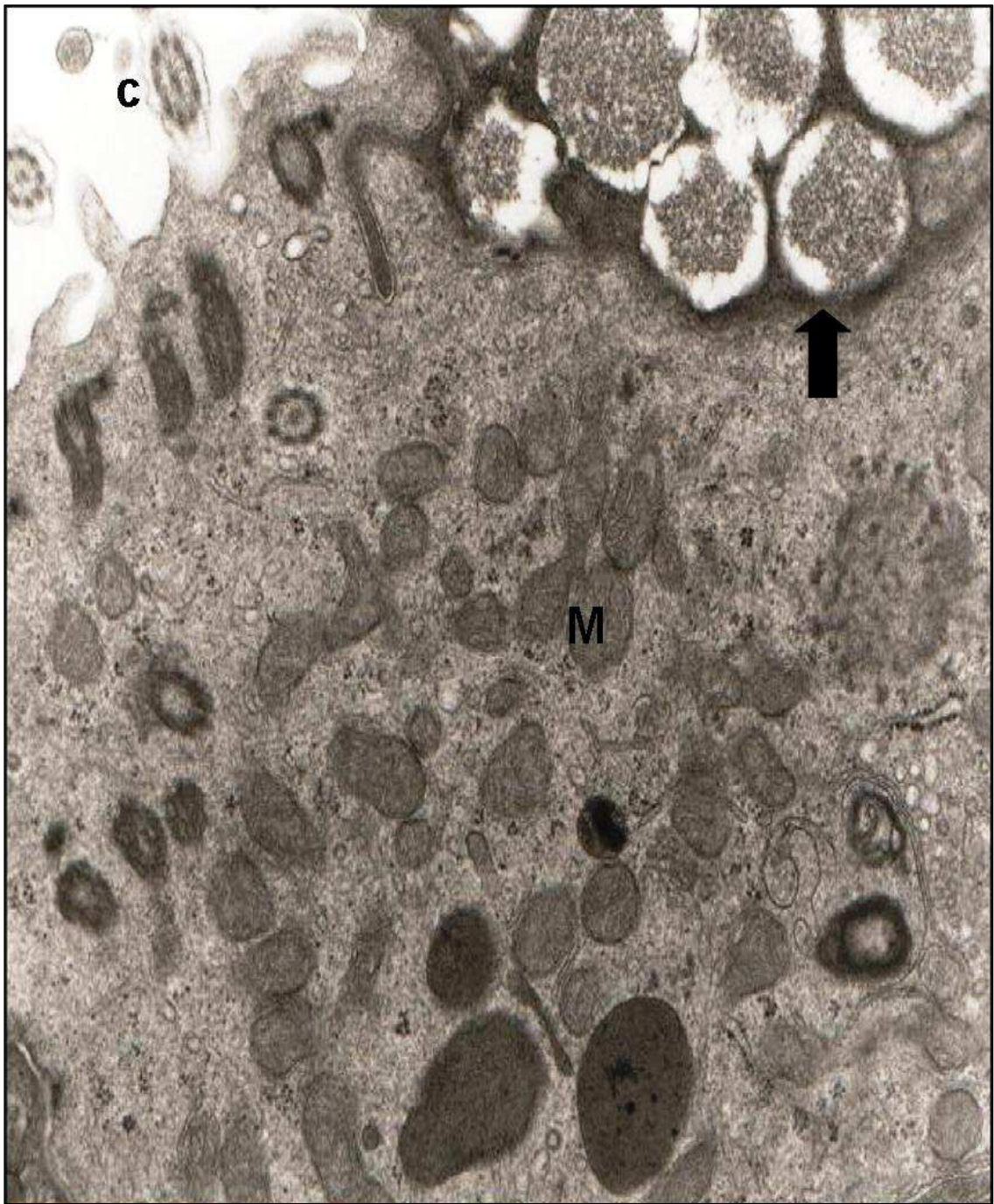


Figure 67: Thin section in a tracheal epithelium of cigarette smoke-exposed rat, showing low number of cilia. Mitochondria aggregate in the apical portion of epithelial cells. Thick arrow: inclusion body. M: Mitochondrion, C: cilia. Magnification: 40000x.

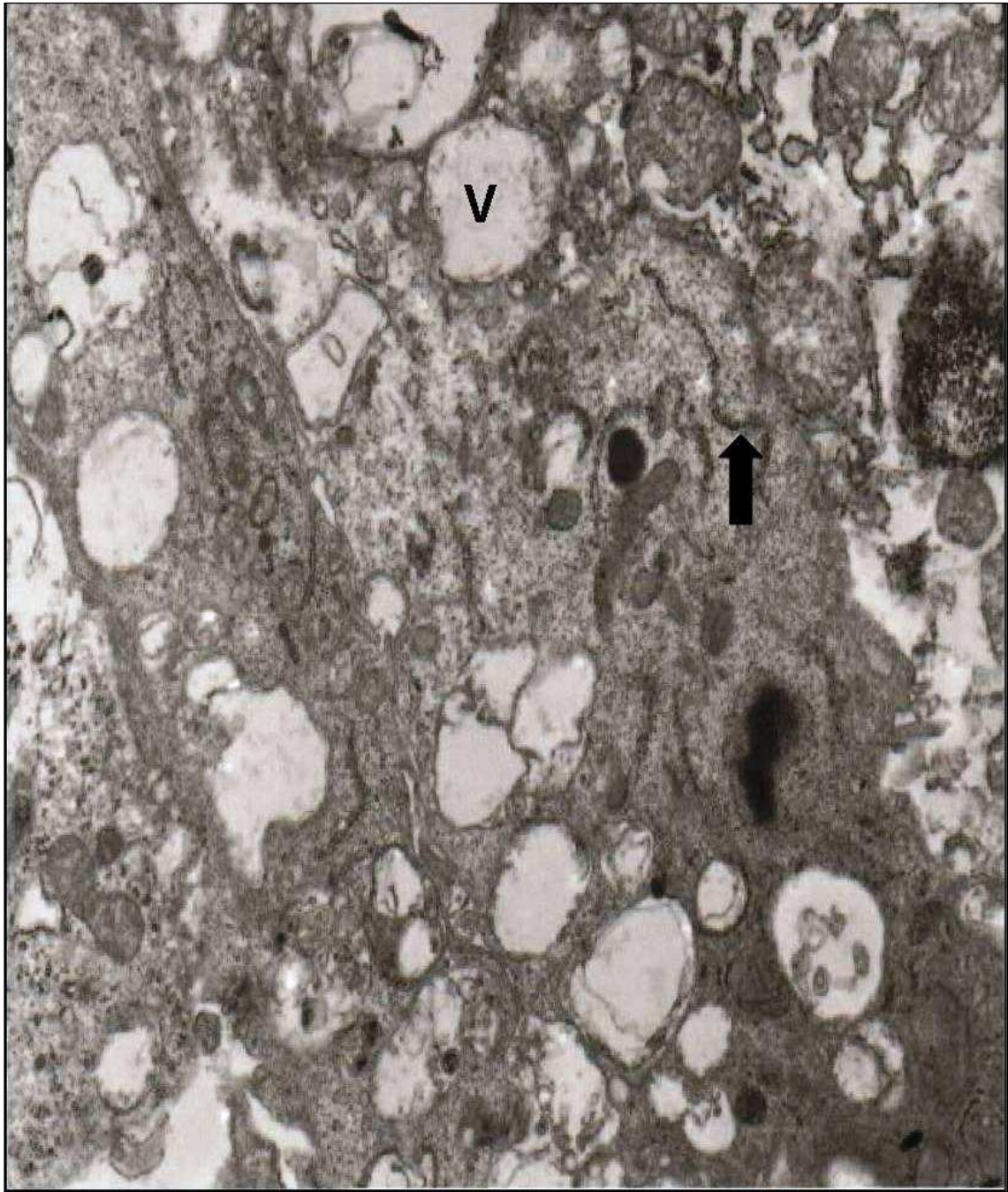


Figure 68: Thin section in a tracheal epithelium of cigarette smoke-exposed rat, showing a high degree of cytoplasmic vacuolization. Thick arrow: a disrupted endoplasmic reticulum. V: vacuole. Magnification: 20000x.



Figure 69: Thin section in the tracheal epithelium of cigarette smoke-exposed rat after the recovery period. Showing partial recovery of tracheal epithelium. Arrow: intercellular junctions. C: cilia, M: Mitochondria. BB: basal body. Magnification 50000x.



Figure 70: Thin section of control type II pneumocytes. Thick arrows indicate multilamellar bodies. Magnification: 6356x.

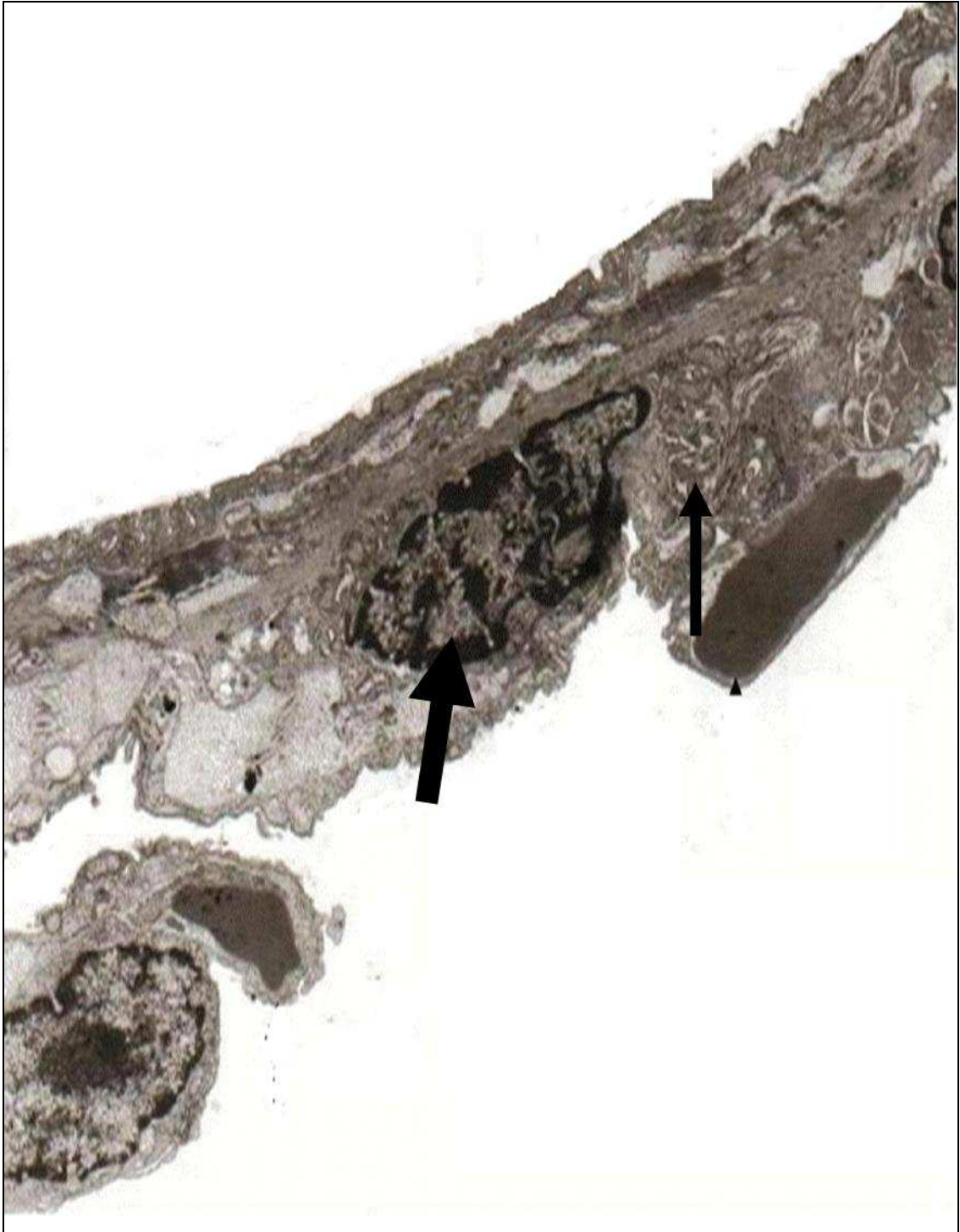


Figure 71: Thin section of control type I pneumocytes. Types I alveolar cell make up 97% of the alveolar surface. In this cell, the organelles (Thin arrow) are grouped around the nucleus (Thick arrow) to reduce the cell thickness. The thin portion contains abundant of pinocytotic vesicles. The important role of these cells is to provide very thin barrier to gas diffusion Magnification: 7874x.

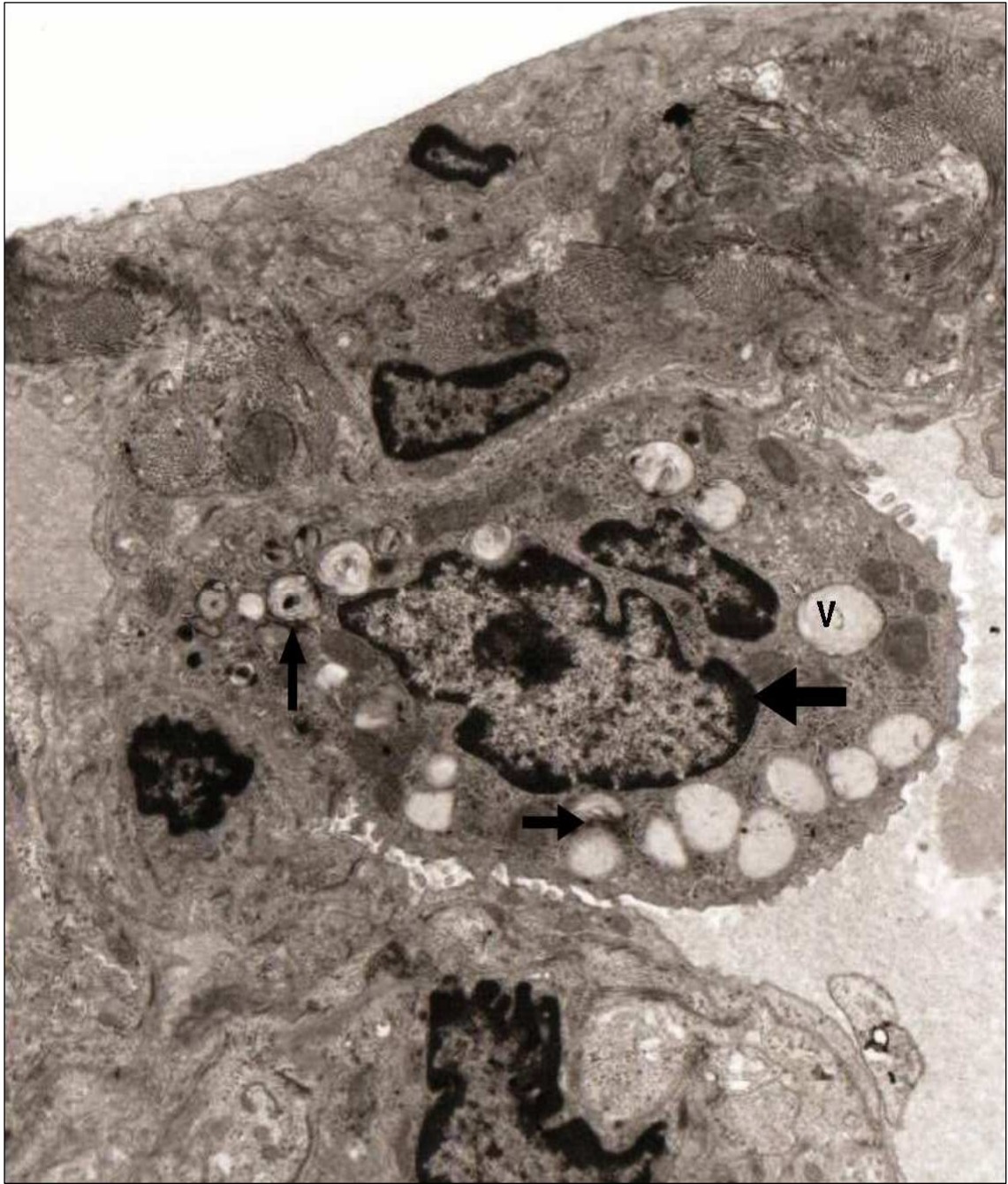


Figure 72: Photomicrograph from cigarette smoke-exposed rat. Thin arrow: damaged multilamellar bodies. V: cytoplasmic vacuolization. Thick arrow: condensed chromatin. Magnification: 10000x.



Figure 73: Photomicrograph from the lung of cigarette smoke-exposed rat, showing a programmed cell death (apoptosis) of alveolar epithelium. Apoptotic cells are characterized by certain morphological features, including membrane blebbing, cytoplasmic and nuclear shrinkage as well as chromatin condensation. Magnification: 25000x.

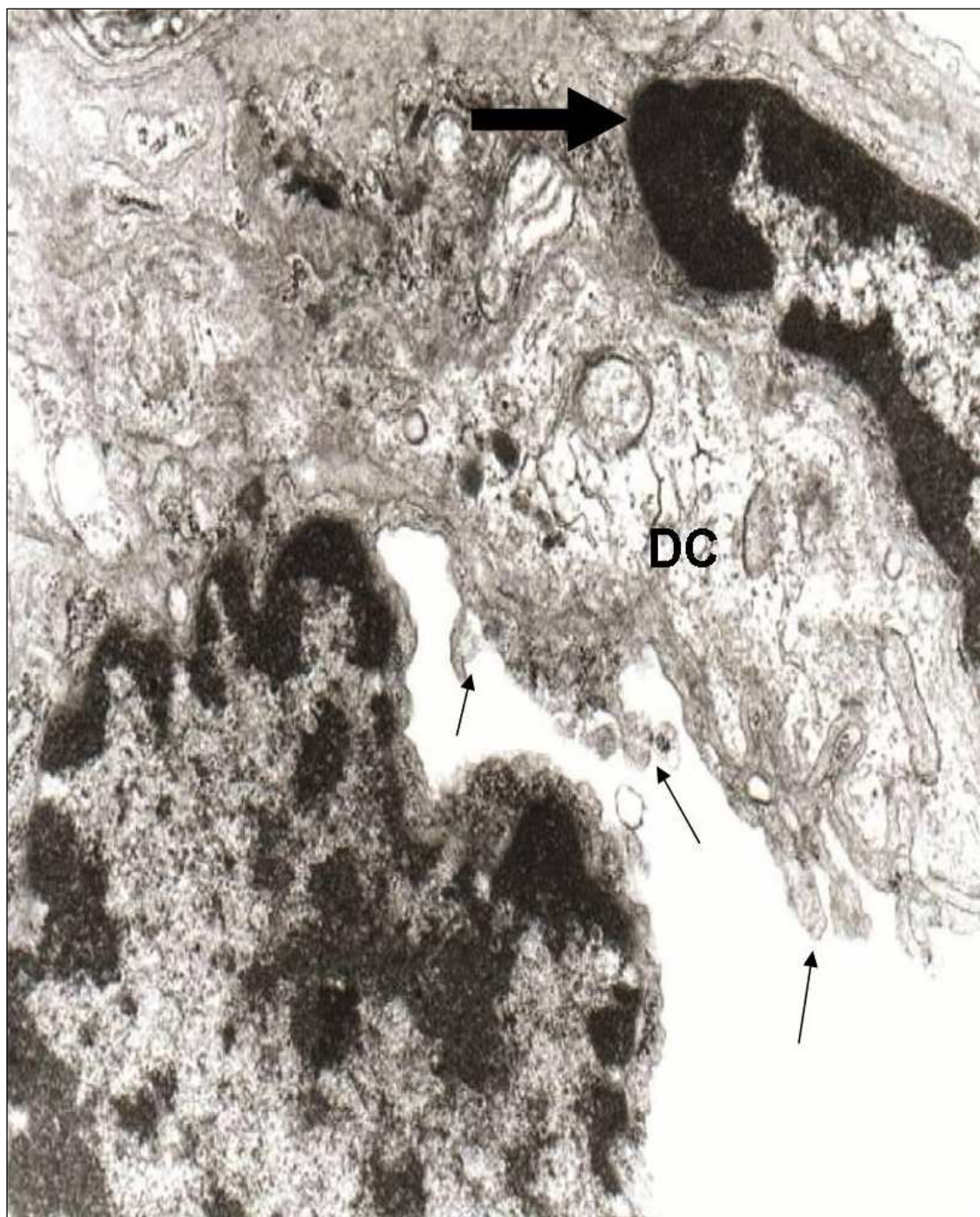


Figure 74: Thin section in the alveolar epithelium of cigarette smoke-exposed rat, showing condensed chromatin and membrane blebs projecting from the cytoplasm of type II pneumocyte as indicated by thin arrows. DC: area of disrupted cytoplasm. Thick arrow: condensed chromatin. V: vacuole. Magnification: 40000x.



Figure 75: Thin section in the alveolar epithelium of cigarette smoke-exposed rat, showing condensed chromatin. Thin arrows: inclusion bodies. V: vacuole. Magnification: 25000x.

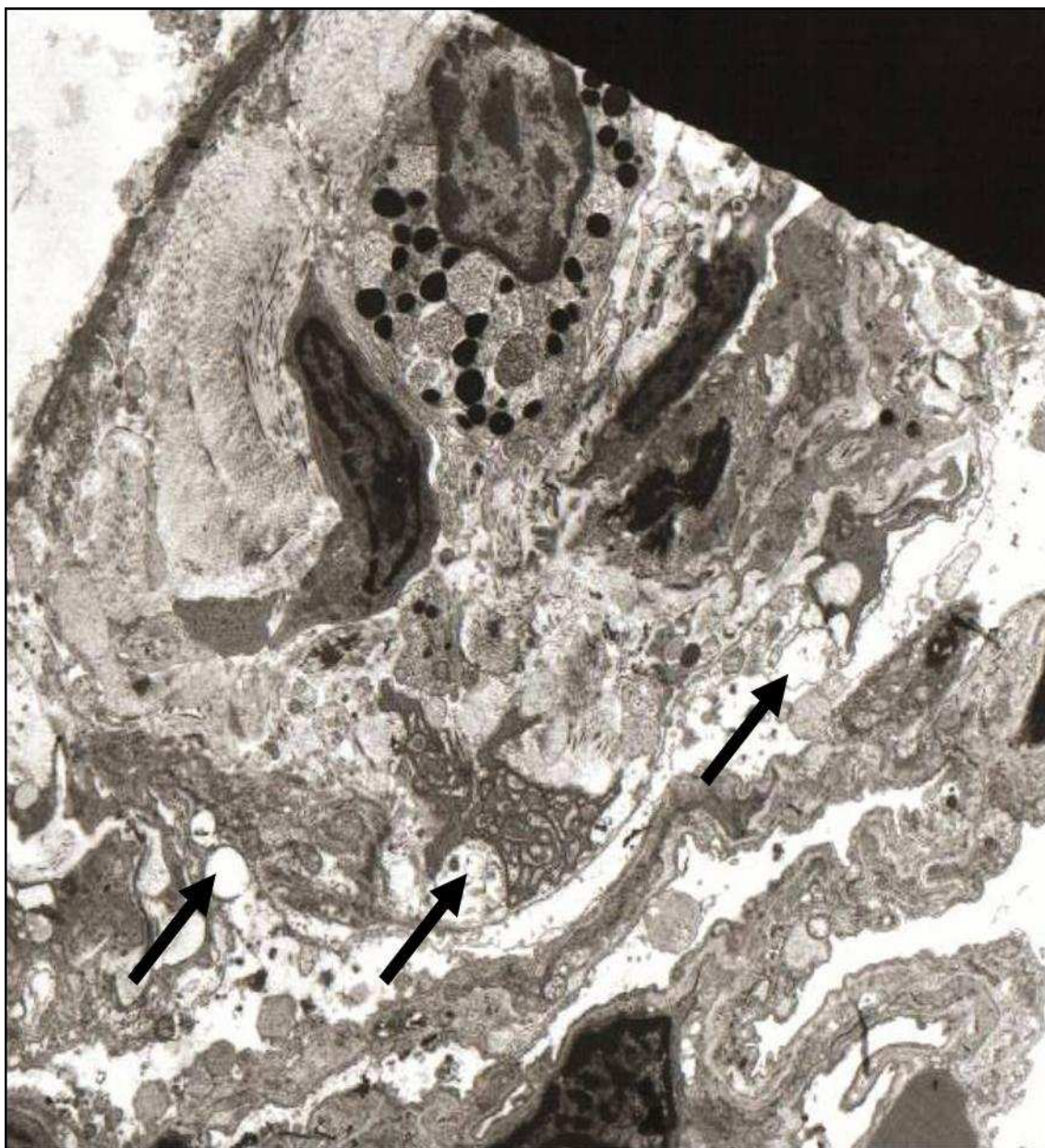


Figure 76: Thin section in the alveolar epithelium of cigarette smoke-exposed rat, showing condensed chromatin and high degree of cytoplasmic vacuolization (Thick arrows). Magnification: 6250x.

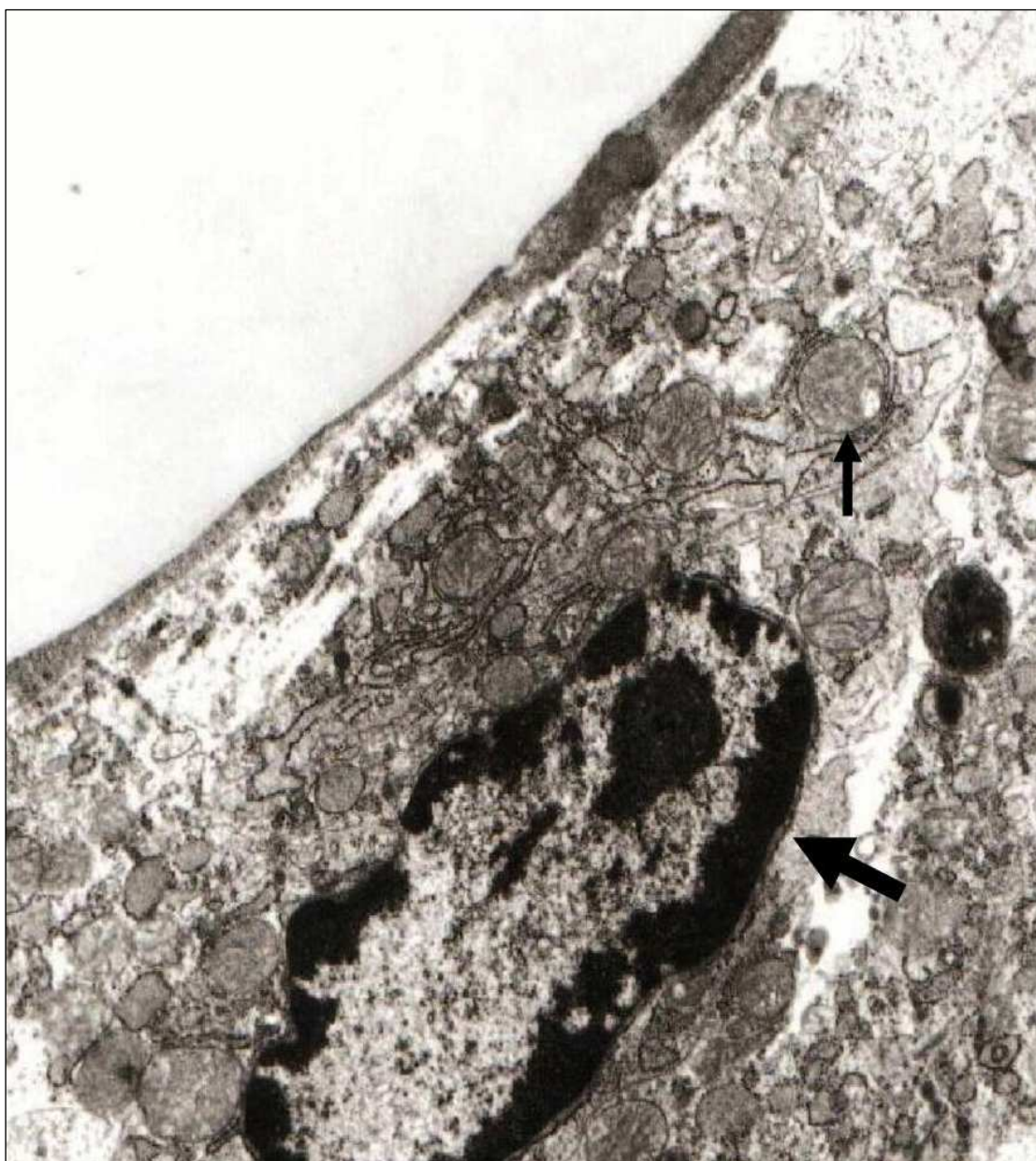


Figure 77: Thin section in the alveolar epithelium of cigarette smoke-exposed rat after the recovery period, showing condensed chromatin and increase in number of mitochondria. Thick arrow: condensed chromatin, thin arrow indicate mitochondria. Magnification: 25000x.

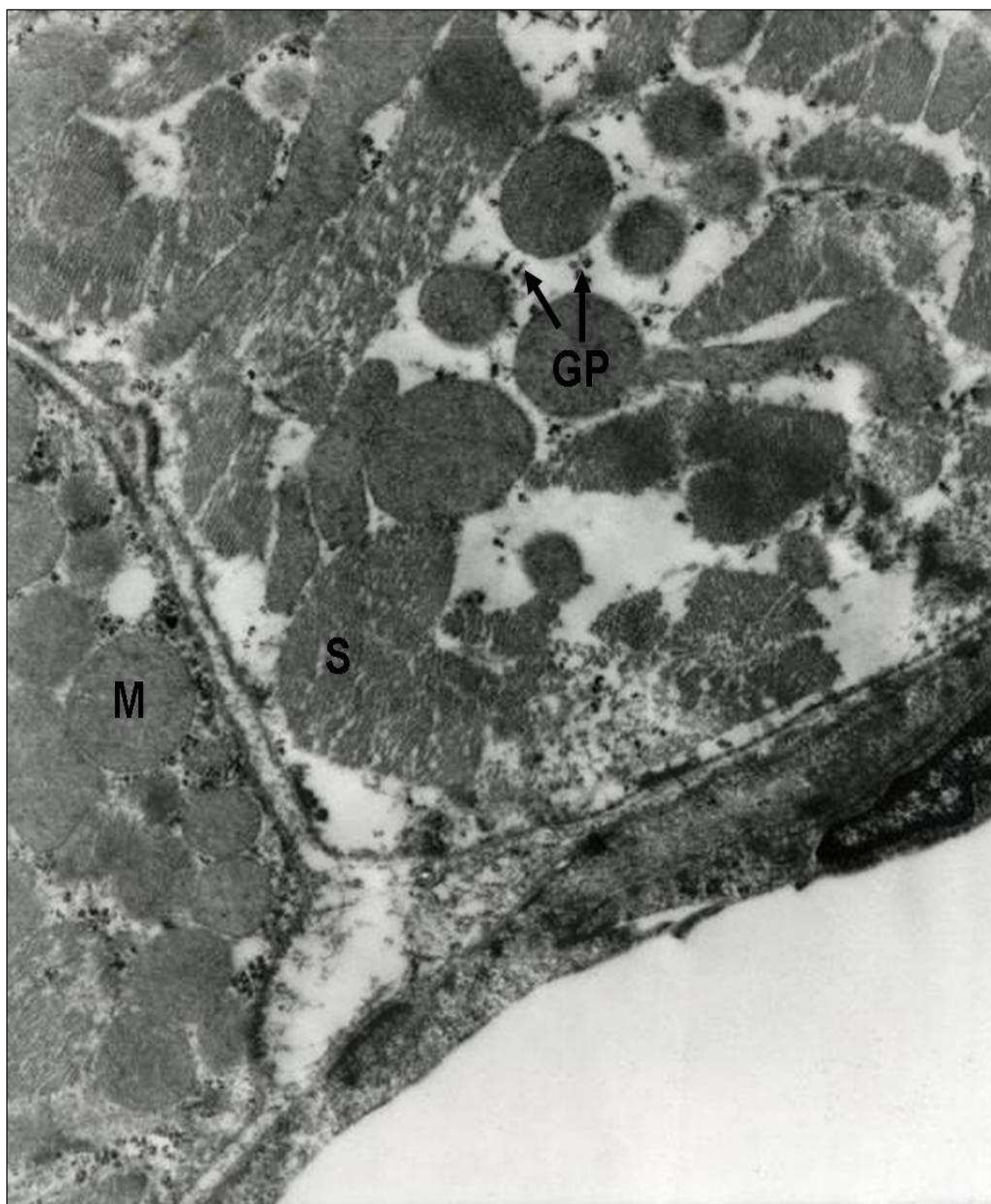


Figure 78: Closer image of control heart ventricular tissue. GP: glycogen particles, PM: plasma membrane, M: mitochondrion, S: cross-sectional view of sarcomeres. Magnification: 25000x.

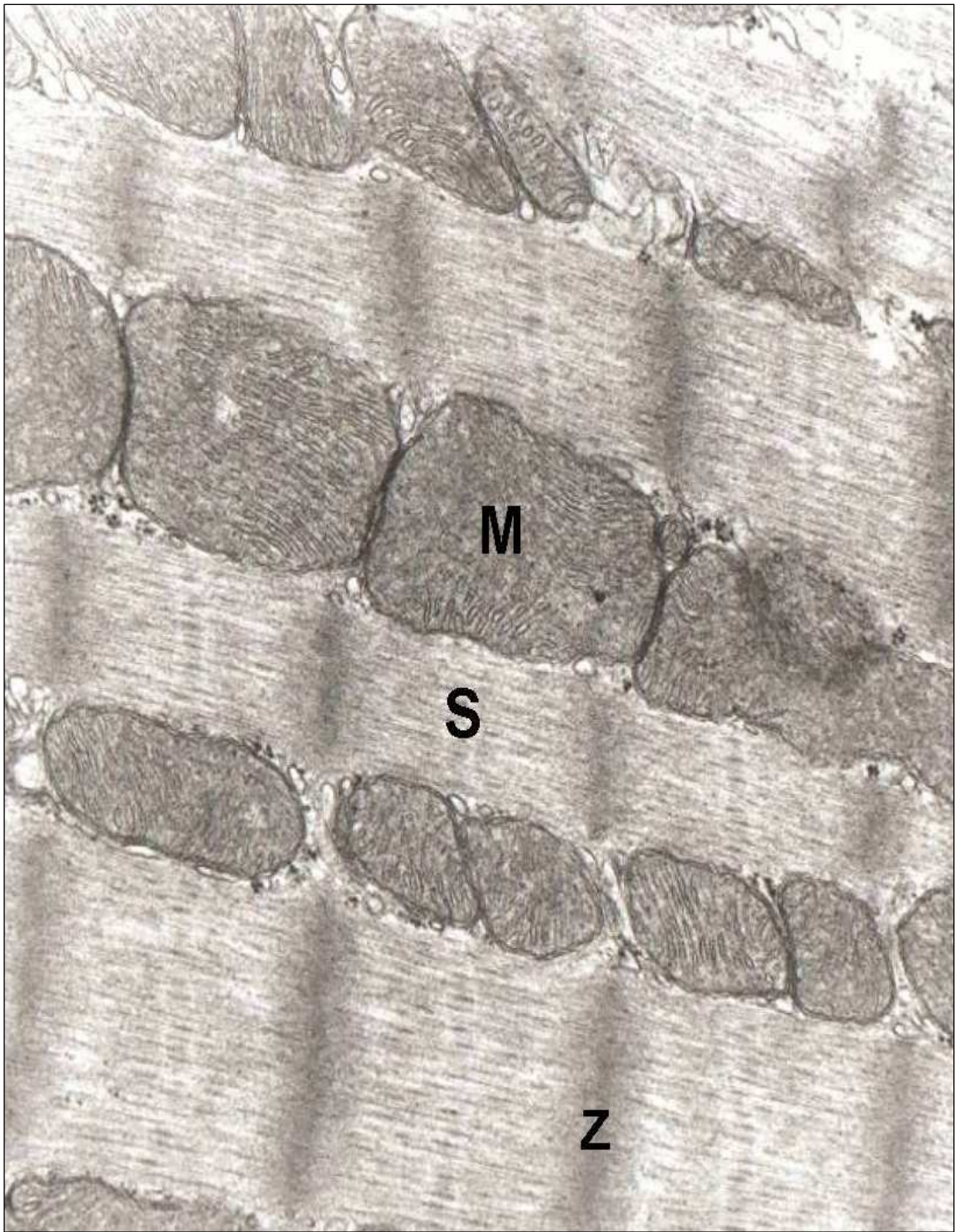


Figure 79: Thin section of control heart ventricular tissue: M: mitochondrion with normal cristae, S: sarcomeres, Z: Z-line. Magnification: 62500x.

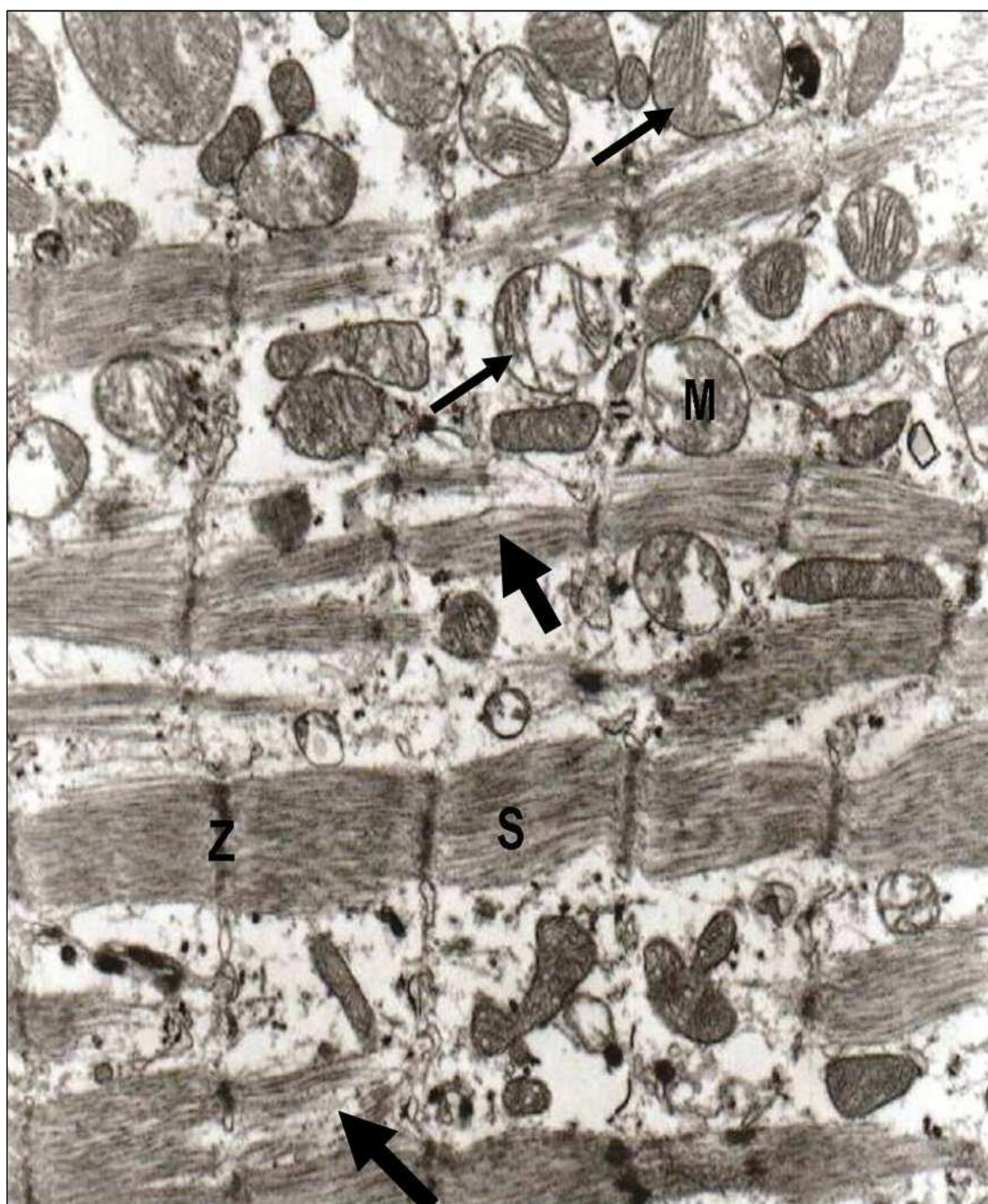


Figure 80: Thin section of heart ventricular tissue of cigarette smoke-exposed rat. The thick arrows indicate a partial disruption of the myofibrils. Thin arrows indicate pleomorphic mitochondria with partially disrupted cristae. Magnification: 5000x.



Figure 81: Thin section of heart ventricular tissue of cigarette smoke-exposed rats. Thin arrows indicate a partial disruption of the myofibrils. Thick arrows indicate enlarged mitochondria with partially disrupted cristae. The triangle indicates deposited material. Magnification: 62500x.

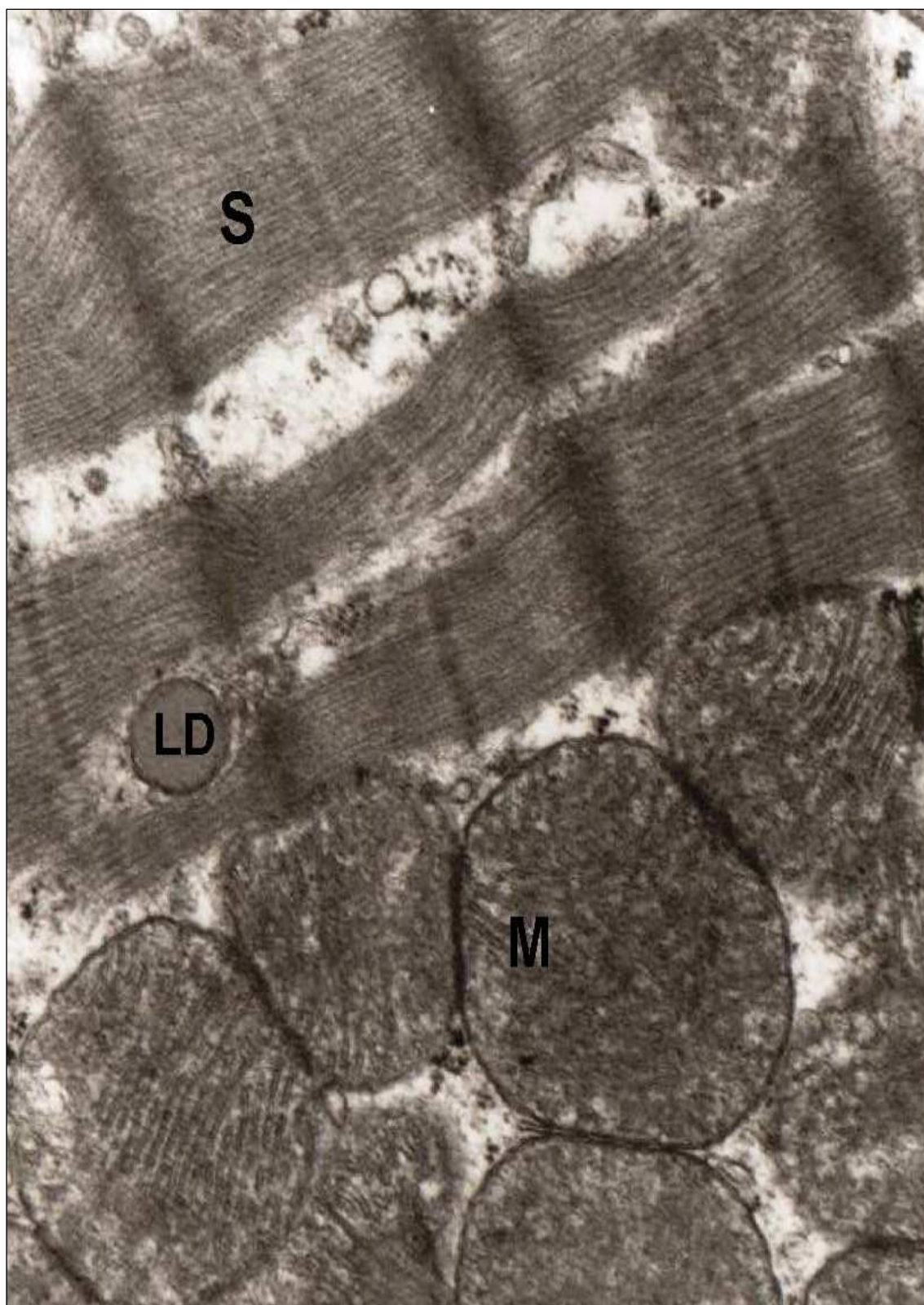


Figure 82: Thin section of cigarette smoke-exposed rat, showing enlarged mitochondria, irregularly arranged with partial disrupted cristae. M: mitochondrion, S: Sarcomeres, LD: lipid droplet. Magnification: 62500x.

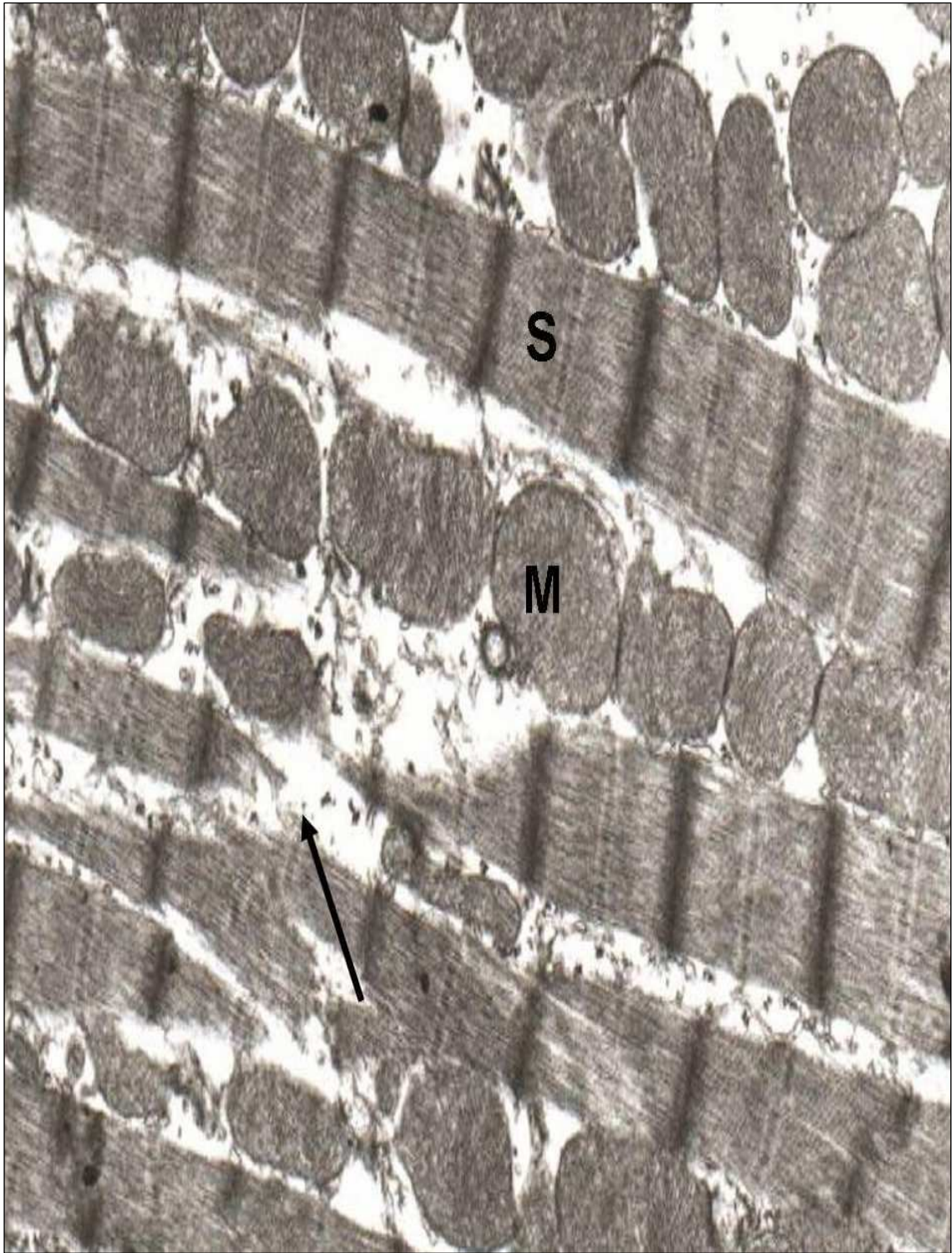


Figure 83: Thin section of heart ventricular tissue of cigarette smoke-exposed rat after the recovery period, showing partial recovery of cardiac muscle fiber. Pleomorphic mitochondria but still partially disruption cristae. Thin arrow indicates a partial disruption and separation of the myofibrils. M: mitochondrion. S: sarcomeres. Magnification: 25000x.

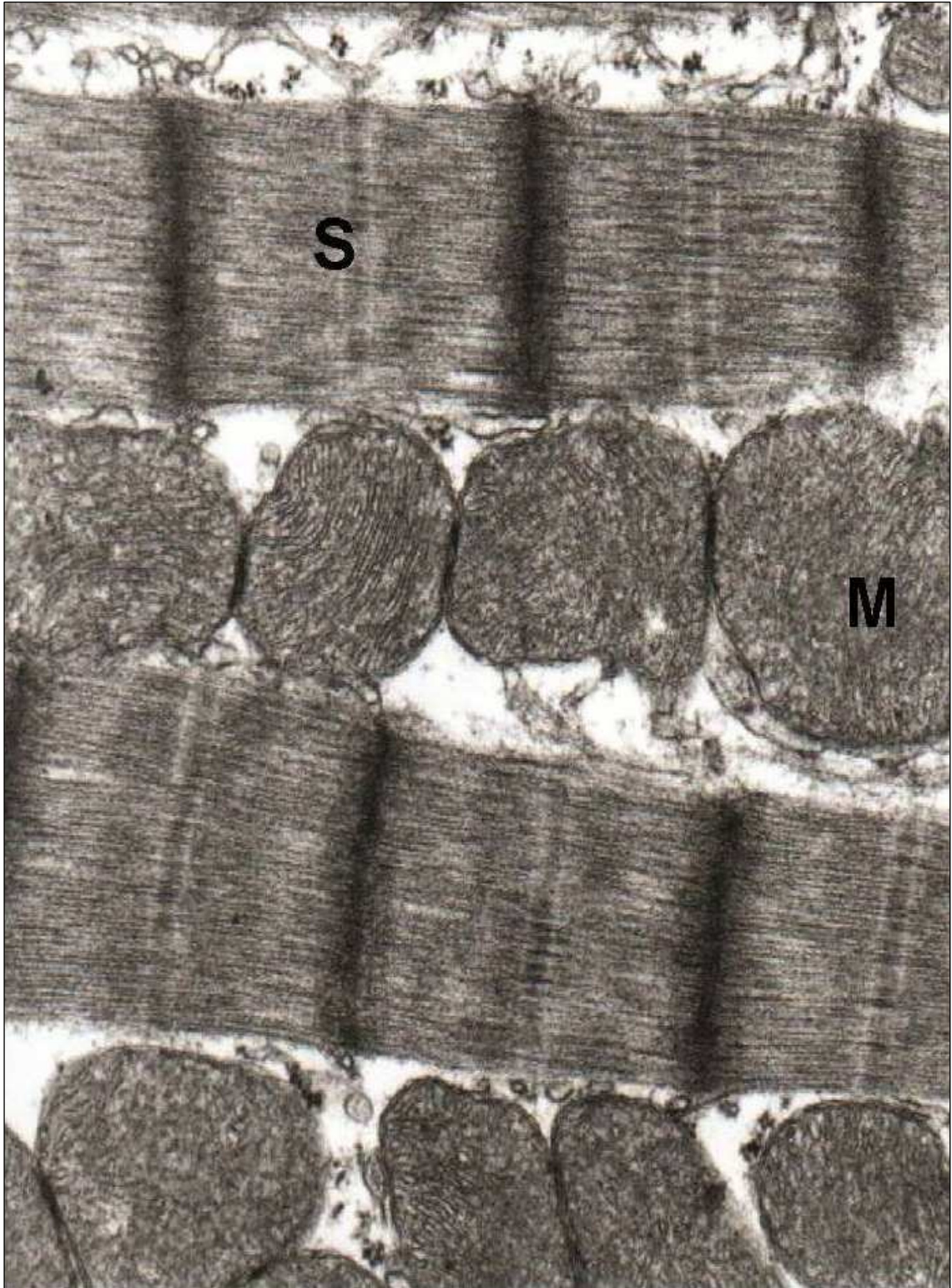


Figure 84: Thin section of heart ventricular tissue of cigarette smoke-exposed rat after the recovery period, showing partial recovery of cardiac muscle fiber. Enlarged mitochondria with partial disrupted cristae. M: mitochondrion, S: sarcomere. Magnification: 62500x.

5. DISCUSSION

5.1. Physiological studies

5.1.1. Rat isolated perfused heart experiments

5.1.1.1. Effect of CSE and L-nicotine on isolated perfused heart

In the present study, CSE induced in most concentrations a significant-concentration dependent reduction of the force and the rate of the perfused heart contraction. The treatment of isolated perfused rat heart with L-nicotine alone also produced a significant-concentration dependent decrease of the force and rate of the perfused heart contraction. From this result the reduction of the force and the rate of the perfused heart contraction at least partially depend on L-nicotine in CSE.

McGrath (1986) showed the treatment of isolated perfused rat heart by Carbon monoxide didn't affect the heart rate, while treating it with nicotine resulted in bradycardia. On the other hand treating the heart with both Carbon monoxide and nicotine decrease heart rate. Moreover, the separate effect of Carbon monoxide and nicotine was reversible, but the effect they produced in combination was irreversible. Another study is done by (Chen and McGrath, 1985), and has shown that CO caused a contractile depression, whereas unstimulated isolated rat hearts perfused with 95% CO-5% CO₂ (CO) KHs, were observed to depress the heart rate (McGrath, 1986; McGrath and Smith, 1984). In another study, long-term exposure of dogs to cigarette smoke or nicotine exhibited a significant deficit in heart contractility (Ahmed *et al.*, 1976). Furthermore, chronic exposure to nicotine in rat resulted in initial fall in heart rate, then a rise during following weeks (Lin *et al.*, 1992). However, a study by Liswi, (1998) has demonstrated a decrease in both the amplitude and the rate of contraction of an isolated perfused rat heart, caused by the cigarette smoke extract of three types of Jordanian cigarettes. The decrease in the force of heart contraction, was proposed to be due to the

presence of high amount of nitric oxide in the smoke extract, leading to an elevated level of cGMP

5.1.2. Tissue bath experiments

5.1.2.1. Effect of CSE on aorta

In the present study, the CSE induced biphasic change in tone of isolated rat aorta. Initial contraction in response to CSE may depend partially on the degradation of basally released endothelium-derived relaxing factor (nitric oxide) by superoxide anions. The contraction may result partially from L-nicotine in CSE; L-nicotine with the same concentration in CSE caused biphasic tension change on isolated precontracted aorta in the present study. The subsequent relaxation in isolated aorta also depends at least partially on L-nicotine, nitric oxide and nitrous compounds, these compounds are found in high amount in CSE.

Murohara *et al.*, (1994) showed that CSE induced biphasic tension change in isolated pig coronary arteries during stable contraction to prostaglandin F₂ alpha (PGF₂ alpha). Initial contraction to CSE was dependent on the presence of endothelium, whereas subsequent relaxation was endothelium independent. The initial contraction may be, at least in part, mediated through the degradation of basally released endothelium-derived relaxing factor (nitric oxide) by superoxide anions derived from CSE. Beside the nitrous oxide production from endothelial cell, this compound was also found in high amount in cigarette smoke (Bokhoven and Nissen, 1961; Fischer *et al.*, 1990; Chaouachi, 2009). Cigarette smoke has been reported to induce vasodilation by nitric oxide or by nitrous compounds like N-nitrosornicotine via stimulating vascular smooth muscle soluble guanylate cyclase (Gruetter *et al.*, 1980).

5.1.2.2. Effect of pure L-nicotine on aorta

In the present study, L-nicotine caused biphasic tension change of isolated rat aorta. Mayhan and Sharpe, (1998) suggest that nicotine impairs endothelium-dependent arteriolar dilatation via an increase in the synthesis or release of oxygen-derived free radicals. But, the subsequent relaxation caused by L-nicotine may be mediated by NO production (Zhang *et al.*, 1998; Hanna, 2006).

The precontraction was done by the vasoconstrictor phenylephrine, that is a selective agonist of $\alpha 1$ -adrenergic receptors, mediating its effect through G-protein that activates a phosphatidylinositol-calcium second messenger system (Macia *et al.*, 1984; Godfraind *et al.*, 1982).

5.1.2.3. Effect of CSE on trachea

In the present study, the CSE induced biphasic change in tone of isolated rat trachea. Schachter *et al.*, (2003) showed that tobacco dust extract (TDE) have contractile effect on isolated guinea pig tracheal smooth muscle. The major contractile agent in this extract is not nicotine but other low-molecular-weight substances. But, in another study, the acute exposure to CSE leads to airway relaxation in mice, which was partially mediated by nicotine (Streck *et al.*, 2010). Regarding the maximum relaxation induced by the non-selective smooth muscle relaxant papaverine, the relaxation is likely to be achieved by an intracellular accumulation of cAMP and/ or cGMP by inhibiting phosphodiesterase (Kaneda *et al.*, 2005).

5.1.2.4. Effect of pure L-nicotine on trachea

In the present study, L-nicotine with the same concentration in CSE caused biphasic change in tone of isolated rat trachea. The initial contraction may be due to activation of nicotinic acetylcholine receptors (nAChRs) in nervous tissue by nicotine, which causes contraction through acetylcholine release from cholinergic nerves. But, the subsequent relaxation caused by L-nicotine may be mediated by NO production (Cevit *et al.*, 2007).

D-nicotine and L-nicotine (that is the main isomer in cigarette smoke), have different physiological effects. For instance, L-nicotine produced a biphasic response in the guinea-pig trachea, which consists of an initial contraction followed by relaxation; however, D-nicotine produced only a concentration-dependent relaxation in the tracheal preparation (Hummel *et al.*, 1992; Funayama *et al.*, 1995). Nicotine stimulated cholinergic excitatory and adrenergic and non-adrenergic inhibitory responses in guinea-pig isolated trachea, which were blocked by tetrodotoxin; indicating that nicotinic acetylcholine receptors (nAChRs) in nervous tissue were being activated. Thus, nicotine causes contraction through acetylcholine released from cholinergic nerves (Jones *et al.*, 1980; Funayama *et al.*, 1995; Hanna, 2006). The study by Cevit *et al.*, (2007) may provide a mechanism for subsequent relaxation caused by nicotine, they found that nicotine produced a concentration-dependent relaxation on guinea-pig isolated tracheal preparations precontracted by carbachol (10^{-6} M). It was suggested that nicotine-induced relaxation is at least in part mediated by NO; since the relaxation was significantly reduced in the presence of N(w)-nitro L-arginine methyl ester (L-NAME). These results show why L-nicotine alone produced biphasic tone change of isolated tracheal preparation in the present study.

5.2. Biochemical studies

5.2.1. Correlation of antioxidant enzyme activities with tissues inflammation during smoke exposure of rats and smoke cessation

In comparison with normal tissues, present data showed that the subchronic smoke exposure caused a significant decrease in catalase specific activity by 23 %, 18 % and 50% in liver, kidney and lung tissues, respectively. However, during the recovery period the enzyme activities retained almost normal levels (97%, 99% and 95% respectively). Similarly, smoking caused a significant reduction of G6PD specific activities by 29 %, 18 % and 38% in liver, kidney and lung tissues, respectively. However, during the recovery period, the enzyme activities retained almost normal levels 98%, 97% and 96 % respectively. Also, smoke exposure caused a decrease in glutathione peroxidase (GPx) by 16 %, 13% and 35% in liver, kidney and lung tissues, respectively. In the recovery period glutathione peroxidase (GPx), the enzyme activities retained almost normal levels (97%, 99% and 96% respectively). These data suggest different effects of cigarette smoke on different organs which could be due to the differential load of metabolites of cigarette smoke in these organs (Hecht, 2002; Ebbert *et al.*, 2004; Stepanov and Hecht, 2005). That can change the antioxidant defense system leading to an oxidative stress with a variable effect on these organs.

An imbalance between cellular pro-oxidant and antioxidant levels leads to the oxidative stress resulting in tissue damage. The antioxidant enzyme interacts directly with reactive oxygen species (ROS) to convert them to non-radical products. Overproduction of these radicals has an inhibitory effect on the enzymes responsible for removal of ROS such as CAT, G6PD and GPx. It has been reported that superoxide radicals suppress CAT activity and that H₂O₂ inhibits SOD activity (Hassan and Fridovich, 1978), and the toxicity of aqueous extract of smokeless tobacco (AEST) in various organs like liver, lung, and kidney due to the formation of the radical species

(Avti et al., 2006), which might explain the inhibition of these enzymes after the subchronic administration of cigarette smoke in the present study.

In correlation with the alterations in enzymes activities, present data demonstrated an induction of inflammatory changes in tissues due to the effect of subchronic smoking exposure on rats. These changes involved an interstitial inflammation comprised of lymphocytes and plasma cells in lung, portal tract inflammation in liver and mesangial cell proliferation in kidney corpuscles. All these inflammatory changes almost diminished in tissues after the recovery period from smoking effects, indicating reversible effects of smoking on tissues and enzymes of the rat. It has been reported that subchronic smoking causes impairments in antioxidant enzyme activities of different tissues in rat (Avti et al., 2006). This impairment was due to the inhibitory effects of ROS present in tobacco constituents on these enzymes. Also, tobacco smoke containing many toxic low molecular weight compounds that are able to activate bronchoalveolar dendritic cells (DCs) directly. Activated DCs can secrete a whole range of inflammatory chemokines, inducing the recruitment and activation of more DCs and other inflammatory cells such as neutrophils (Kantengwa, 2003).

Tobacco smoking also induces dose-dependent increases in goblet cell formation and mucin secretory capacity of rat airways (Stevenson 2004). Activation of neutrophils, in turn, releases a number of mediators and proteases that spread the inflammatory response and contribute to the destruction of the lung airways and other tissues. Therefore, it is believed that the long-term administration of tobacco smoking can impair the enzymatic antioxidant defense system of the rat liver, lung, and kidney. These alterations may be one of the responsible factors for smoking-induced inflammation in these organs (Avti et al., 2006).

The findings in the present on reversible effects of smoking, support result of Pekmez *et al.*, (2010), who found that the histopathological changes of rat kidney tissue exposed to smoking were partially disappeared after treatment with the antioxidant compound caffeic acid phenethyl ester. Many studies have reported an association between chronic cigarette smoking and reduced myeloperoxidase (MAO) activity in the brain and peripheral organs, but the inhibition of MAO-B enzyme activity in the human brain returns to normal levels after smoking cessation (Lewis *et al.*, 2007; Fowler *et al.*, 2003). A recent study of platelet MAO in human smokers showing no recovery of MAO during the first week of abstinence but full recovery by 4 weeks (Rose *et al.*, 2001). In vivo studies on the interaction between cigarette smoke and oral peroxidase in smokers and nonsmokers, showed that cigarette smoke-induced inactivation of peroxidase activity was in a reversible manner (Reznick *et al.*, 2003). Cardellach *et al.*, (2003) found that chronic smoking is associated with a decrease in enzyme activities of complex IV and III of mitochondrial respiratory chain, which return to normal values after cessation of tobacco smoking.

subchronic administration of cigarette smoke impairs the enzymatic antioxidant defense system in liver, lung, and kidney. These alterations may be one of the responsible factors for cigarette smoke induced inflammation in these organs. The understanding of mechanisms for cigarette smoke induced cellular damage may offer therapeutic opportunities and ways to modify the adverse effects of cigarette smoke.

5.3. Spectrophotometric determination of nicotine concentration in cigarette smoke extract

According to a report by Public Health Laboratories (Myreland, USA, 1997), Jordanian cigarettes contain about twice the amount of nicotine and tar found in non-Jordanian cigarettes. Also, nicotine content of alcoholic water extract of most brands of Jordan market cigarettes showed higher values than the labeled amount which is usually determined by gas chromatography analysis of smoke condensate. A study by Hadidi and Mohammed, (2004), determined the average nicotine content in 13 commercial brands of hubble-bubble tobacco by gas chromatography to be 8.32 mg nicotine/g tobacco, range (1.8-41.3 mg nicotine /g tobacco). Each hubble-bubble head (20 g) of unflavored tobacco contains 35.7 mg nicotine/g tobacco, whereas the flavored type contains 3.4 mg nicotine/g tobacco. However, nicotine and its metabolite cotinine were increased significantly in the plasma, saliva and urine of habitual water-pipe smokers, following a single run of hubble-bubble smoking, as has been observed by (Shafagoj *et al.*, 2002). In the present study, the spectrophotometric determination of nicotine showed that One gram of cigarette tobacco produces an equivalent 57 mg L-nicotine in CSE.

5.4. The smoking machine

We describe a modified smoking machine to be used for monitoring the effects of cigarette tobacco smoke on experimental animals; a vacuum pump, a time controller, and an electronic valve that control the sequence of puff- and fresh air-inlet and exit into and out of the inhalation chamber. The design allows intake of enough tobacco smoke and prevents oxygen deprivation in the inhalation chamber.

5.5. The ability of cigarette smoke to induce apoptosis in tissue sections

In the present study, only lung tissues of smoke-exposed rats showed apoptotic cells. It is important to indicate the study by (Das *et al.*, 2009) who tried to investigate the effect of the aqueous extract of cigarette smoke on microtubules in a tissue culture. Vital cellular processes mediated by microtubules such as cell proliferation and maintenance of the cellular morphology, have been adversely affected in a dose and time-dependent manner in the extract-treated human lung epithelial cells (A549), and noncarcinoma human lung alveolar epithelial cells (L132). There was an observed disruption in the microtubule network. The damage of microtubules by the smoke extract may be correlated with the pathogenesis of cigarette smoke induced disorders, which result in cellular apoptosis and tissue damage. In another study, Kuo *et al.*, (2005) demonstrated that the effect of CS-induced lung injury including apoptosis may be via reactive oxygen species and nitrogen oxides generation. The formation of these oxidizing agents leads either to the phosphorylation of p38/JNK MAPK pathway and then activation of Fas cascades, or to stimulate the stabilization of p53 and increase in the ratio of Bax/Bcl-2. This effect may induce apoptosis and may be an important pathway in the lung pathogenesis of CS.

5.6. Histological studies:

5.6.1. Effect of cigarette smoke on the trachea

In the present study, mucosa disruption that was frequently observed within the tracheal epithelium is due to cell degeneration. Also, ciliary amalgamation that can be viewed as part of epithelial disruption, may result from the hyperplasia of mucus-secreting submucosal glands, and may affect the airway clearance mechanisms. Inclusion bodies (any small amorphous blackish aggregate of smoke toxicants, primarily tar components) were observed.

The observed loss of cilia may be related to the high concentration of nicotine that may have destructive effects on microtubules and alteration of their polymerization/depolymerization. Acetaldehyde and acrolein are suspected to play a role in the damage of cilia. Acetaldehyde was able to impair the ciliary function and beat frequency, by inhibiting ciliary dynein ATPase activity, and binding to ciliary proteins critical in the functioning of dynein and tubulin. Acrolein was found to adversely perturb the cilia by reducing its beat frequency, in cultured bovine bronchial epithelial cells (Dye and Adler, 1994). Cigarette smoke produced alteration in the morphology of epithelial cells, including mitochondrial swelling and their aggregation in the apical portion of the cells, membrane blebbing, swollen RER and cytoplasmic vacuolation, which are indicators of epithelial injury (Lewis and Jakins, 1981).

The effect of cigarette smoke on trachea tissue of wistar rat showed several morphological changes in the epithelium, including desquamation, loss of cilia and an increase of goblet cells. Activation of serous glands in the submucosa, and cell infiltration were also noted. These morphological changes were correlated with the amount of toxic substances in the cigarette smoke (Kurus *et al*, 2009). The infiltrating inflammatory cells during chronic inflammation, amplifies the tissue damage by releasing

more oxygen free radical or through secretion of lytic enzymes (Masubuchi *et al.*, 1998). It was found that exposure of rat tracheal explants to varying amounts of cigarette smoke for 10 min, can induce a dose-related blebbing of the apical membrane, and loss of cilia (Dye and Adler, 1994).

5.6.2 Effect of cigarette smoke on the alveoli of the lung

In the present study, lung alveoli of cigarette smoke-exposed rats showed clear thickening in the alveolar wall tissue, collapsed alveoli, inflammatory cell infiltration, blood extravasations, damaged multilamellar bodies of type II pneumocyte, together with cytoplasmic vacuolization and chromatin condensation, membrane blebs projecting from the cytoplasm, and degeneration of alveolar epithelium.

Fransca *et al.*, (1974) investigated the effect of cigarette smoke on the lung of dogs. A proliferation of alveolar type II cells was found in the alveolar epithelium, almost completely lining some alveoli. In some alveolar type II cells an unusual RER component was observed. Many of the cells showed characteristic lamellar bodies, free ribosomes were more abundant, and the Golgi complex was rarely seen. Occasionally 2-3 vacuoles and what appear to be lipid droplets were seen. Multiple microinvasions of the underlying basal lamina by cytoplasmic processes of these cells frequently occurred. This unusual RER system even persists in cells which appear to be degenerating. In another study, Alarifi, *et al.*, (2004) studied the ultrastructural changes of pneumocytes of rat exposed to arabian incense (bakhour), Alveolar pneumocytes of exposed animals revealed significant ultrastructural changes which involved the cell organelles and surfactant material of type II cells. Hyperplasia of alveolar cells was a feature in the affected lung tissue also observed in the present study. Deposition of collagen fibrils in the alveolar walls was also observed. Hyperplasia of the alveolar epithelium has been

described in a variety of experimental and clinical disorders such as pulmonary edema (Ortega, 1970) and exposure to chemical irritants (Steffee and Baetjer, 1967) carcinogens (Kaufman, 1972) and radioactive material (Sanders *et al.*, 1971).

The importance of surfactant alterations comes from the important role of surfactant in the prevention of alveolar collapse were observed in the present study, and its act as an active component of the lung host -defense mechanism (Ochs *et al.*, 1999; Janqueira and Carneiro, 2005). Decreased rate of surfactant secretion can lead to increased density of the surfactant material. (Fehrenbach *et al.*, 1998) It is supposed that some active particulates in the smoke have bound to the cell membrane of type II pneumocytes and affect its capability of surfactant secretion.

The pneumocytes hyperplasia is considered as an early response of the alveolar wall to injury (Adamson *et al.*, 1980). It is suggested that cellular hyperplasia occur through a regenerative process to replace the damaged alveolar cells. Type II pneumocytes are known to be the progenitors of Alveolar type I cells. As in the present study, cigarette smoke caused an accumulation of inflammatory cells in the lung tissue. These inflammatory cells may contribute in damaging of the alveolar and interstitial pulmonary structures through secretion of lytic enzymes and oxygen free radical (Masubuchi *et al.*, 1998).

5.6.3. Effect of cigarette smoke on the aorta

In the present study, aortic tissue sections of cigarette smoke-exposed rats showed thickening in internal elastic lamina and elastic lamellae in the tunica media, elastic lamellae more obvious in the tunica media, slightly contraction of smooth muscle, and endothelial cells disruption. Lin *et al.*, (1992) study the effect of long-term nicotine exposure on the rat, as experienced with cigarette smoking; they found an increase in the frequency of endothelial cell death, resulting in an enhanced transendothelial leakage to macromolecules, such as low density lipoproteins, leading to the acceleration of atherogenesis. In the present study, cigarette smoke also caused an increase in the frequency endothelial cell death.

The aortic tunica media disarrangement may represent a destructive remodeling, involving a probable alteration in the turnover of elastin and other connective tissue components. Accordingly, the aortic wall stiffness will be reduced, especially when considering the importance of elastic lamellae in giving the needed resilience to the aorta, and also in distributing stresses throughout the vessel wall (Berry *et al.*, 1972; Long and tranquillo, 2003). A study by Stefanadis *et al.*, (1997) reported that cigarette smoking caused an acute decrease in aortic elastic properties. In the present study, CS induce thickening in both internal elastic lamina and elastic lamellae and became more appearance, which indicate decrease aortic elastic properties.

Light and electron microscopic studies of pulmonary arteries from rats exposed to cigarette smoking showed a pronounced muscularization of the small pulmonary arteries. Also, there was an intimal and medial thickening that was associated with the cellular elements and extracellular matrix (He, 1991; 1992). Polycyclic aromatic hydrocarbons in cigarette smoke, often implicated in the development of atherogenesis, have also been shown to increase smooth muscle cell proliferation and viability

(Rasmussen *et al.*, 1991). The slight contraction of smooth muscle was observed in the present study was suggested by impaired endothelium-derived relaxation from endothelium-derived relaxing factor/s in cigarette smokers (Higman *et al.*, 1993)

5.6.4 Effect of cigarette smoke on the heart ventricles

In the present study, exposure of rats to the cigarette smoke lead to an extensive changes in the heart ventricle, characterized by swelling and polymorphism of mitochondria and deterioration of myofibrils, elongated nuclei and congested blood vessels. However, Lough, (1978) demonstrated both filtered and unfiltered cigarette smoking to show mitochondria irregular in size and shape with frequent separation of the outer mitochondrial membrane, increased lipid droplet and enhanced autophagosomal activity. Though, there was not changes detected in the myofibers, Lough, (1978) suggested these changes to be caused by carbon monoxide and that resemble the changes of chronic intermittent hypoxia. Moreover, in the present study a mild separation between muscle fibers was observed, this separation will have a negative impact on the capacity of the cardiac muscle of pumping blood efficiently into body organs. The toxic compounds in cigarette smoke may affect muscle fiber through deterioration of both actin-myosine fibers and intercalated disc.

5.6.5. Recovery period

In the present study, tissues of trachea, lung alveoli, aorta and heart ventricles showed a partial recovery after cigarette smoke cessation. However, Pekmez *et al.*, 2010 found that the histopathological changes of rat kidney tissue exposed to smoking were partially disappeared after treatment with the antioxidant compound caffeic acid phenethyl ester.

6. CONCLUSION AND RECOMMENDATIONS

- 1- A modified smoking machine has been constructed and used for monitoring the effects of cigarette smoke on albino rats.
2. One gram tobacco of LM brand (Jordan Cigarettes Company) contains an equivalent 21.5 mg L-nicotine in CSE.
3. subchronic administration of cigarette smoke lowers the activity of antioxidant enzymes in liver, lung, and kidney. These alterations may be one of the factors for induced inflammation in these organs. The effect was nearly reversible.
4. Cigarette smoke causes severe histological effects especially in trachea and lung alveoli. It induces also apoptosis only in lung alveoli. Smoking has more severe inhibitory and damaging effects on lung due to the differential load of metabolites of cigarette smoke in this organ
5. L-nicotine is expected to be CSE component that causes biphasic tone changes of isolated rat aorta and trachea
6. L-nicotine is expected to be CSE component that causes a significant concentration-dependent decrease in the force and rate of the contractions of perfused heart
7. Inflammatory cell infiltration was present in all examined tissues, amplifying the tissue damage by releasing more oxygen free radical or through secretion of lytic enzyme.

5. REFERENCES

- Abboud, A., Al-Awaida, W. (2010). Synchrony of G6PD activity and RBC fragility under oxidative stress exerted at normal and G6PD deficiency. **Clinical Biochemistry**, 43, 455–460.
- Abdalla, S., Bilito, Y., Disi, A.(1992) .Effects of sand viper (*Cerastes cerastes*) venom on isolated smooth muscle and heart and on haematological and cardiovascular parameters in the guinea-pig. *Toxicon*, 30,1247-1255.
- Adamson, R., Bowden, D. H. (1980).Role of monocytes and interstitial cells in the generation of alveolar macrophages.**Laboratory investigation**, 42, 518-524.
- Adesina, A. M., Vallyathan, V., McQuillen, E. N., Weaver, S. O. and Craighead, J. E. (1991). Bronchiolar inflammation and fibrosis associated with smoking. **American Review of Respiratory Disease**, 143, 144 149.
- Agostini, F., Balansky, R. M., Izzotti, A., Lubet, R. A., Kelloff, G. J., and Flora, S. D. (2001) . Modulation of apoptosis by cigarette smoke and cancer chemopreventive agents in the respiratory tract of rats. **Carcinogenesis**, 22,375-380.
- Ahmed , S. S., Moschos, C. B., Lyons, M. M., Oldewurtel, H. A., Coumbis, R. J., and Regan T. J. (1976). Cardiovascular effects of long-term cigarette smoking and nicotine administration. **The American journal of cardiology**,7, 33-40.
- Alarifi, S., Mubarak, M., and Alokail, M. (2004). Ultrastructural changes of pneumocytes of rat exposed to Arabian incense (Bakhour). **Saudi Medical Journal**, 25, 1689-1693
- Al-Kurd R., Takruri H. and Shraideh, Z. (2002). Effects of cigarette smoke on anemia, the iron and ascorbic acid status, body weight and energy intake in guinea pigs. **Arab Journal of Food and Nutrition**, 6, 276-285.
- Al-Tamrah, S. A. (1999). Spectrophotometric determination of nicotine. **Analytica Chimica Acta**, 379, 75-80.
- Ambrose, J., and Barua, R. (2004). The pathophysiology of cigarette smoking and cardiovascular disease, An update. **Journal of the American College of Cardiology**. 43, 1731-1737.

Anderson, R. N, and Smith, B. L. (2003). Deaths, leading causes for 2001. **National Vital Statistics Reports**. 52, 7–11.

Andrea, J. E., and Walsh, M. P. (1992). Protein kinase C of smooth muscle. **Hypertension**, 20, 585-595.

Aoshiba, A., Tamaoki, J., Nagai, A. (2001). Acute cigarette smoke exposure induces apoptosis of alveolar macrophages. American journal of physiology. **Lung cellular and molecular physiology**, 281,L1392-L1401.

Aoshiba, K., and Nagai, A. (2003). Oxidative stress, cell death, and other damage to alveolar epithelial cells induced by cigarette smoke. **Tobacco induced diseases**. 15, 219–226.

Arends, M. J., Morris, R. G., Wyllie, A. H. (1990). Apoptosis. The role of the endonuclease. **The American journal of pathology**, 136,593-608

Arthur, J. (2000). The glutathione peroxidases. **Cellular and Molecular Life Sciences**, 57, 1825–1835.

Avti, A., Kumar, S., Pathak, C., Vaiphei, K., and Khanduja, K. (2006). Smokeless Tobacco Impairs the Antioxidant Defense in Liver, Lung, and Kidney of Rats . **Toxicological Sciences**. 89, 547–553.

Baeza-Squiban, A., Bonvallot, V., Boland, S., and Marano, F. (1999). Airborne particles evoke an inflammatory response in human airway epithelium. Activation of transcription factors. **Cell biology and toxicology**. 15, 375-380.

Bai, Y., and Sanderson, M. (2006). Airway smooth muscle relaxation results from a reduction in the frequency of Ca^{+2} oscillations induced by a cAMP-mediated inhibition of the IP3 receptor. **Respiratory Research**, 7, 1-20.

Baker, R., Pereira, d., and Smith, G. (2004). The effect of tobacco ingredients on smoke chemistry. Part I, Flavourings and additives. **Food and chemical toxicology**, 42, 3-37.

Banerjee, S., Maity, P., Mukherjee, S., Sil, A. K., Panda, K., Chattopadhyay, D., and Chatterjee, I. B. (2007). Black tea prevents cigarette smoke-induced apoptosis and lung damage. **Journal of inflammation**, 4,1-12.

Barnoya, J., Glantz, S. A.(2005). Cardiovascular effects of secondhand smoke, nearly as large as smoking. **Circulation**, 111, 2684-98.

Barua, R. S., Ambrose, J. A., Eales-Reynolds, L. J., DeVoe, M. C., Zervas, J. G., and Saha, D. C. (2001). Dysfunctional endothelial nitric oxide biosynthesis in healthy smokers with impaired endothelium-dependent vasodilatation. **Circulation**, 104,1905-10.

Barua, R. S., Ambrose, J. A., Srivastava, S., DeVoe, M. C., and Reynolds, L. J. (2003). Reactive oxygen species are involved in smoking-induced dysfunction of nitric oxide biosynthesis and upregulation of endothelial nitric oxide synthase, an in vitro demonstration in human coronary artery endothelial cells. **Circulation**, 107, 2342-2347.

Benowitz, N. L., and Jacob, P. (2000). Effects of cigarette smoking and carbon monoxide on nicotine and cotinine metabolism. **Clinical pharmacology and therapeutics** ,67,653-659.

Berry, C., Looker, T., and Germain, J. (1972). The growth and development of the rat aorta. I. Morphological aspects. **Journal of Anatomy**, 113, 1-16.

Bnait, K. S., and Seller, M. J. (1995). Ultrastructural changes in 9-day old mouse embryos following maternal tobacco smoke inhalation. **Experimental and toxicologic pathology**,47, 453-461.

Bokhoven, C., Nilssen, H. J.(1961). Amounts of oxides of nitrogen and carbon monoxide in cigarette smoke, with and without inhalation. **La Nature**, 192,458-9.

Bosken, C. H., Hards, J., Gatter, K. and Hogg, J. C. (1992). Characterization of the inflammatory reaction in the peripheral airways of cigarette smokers using immunocytochemistry. **American Review of Respiratory Disease**, 145, 911-917.

Brette, F., and Orchard, C. (2003). T-Tubule function in mammalian cardiac myocytes. **Circulation Research**, 92, 1182-1192.

Cardellach, F., Alonso, J. R., Lopez, S., Casademont, and J., Miro, O.(2003). Effect of smoking cessation on mitochondrial respiratory chain function. **Journal of toxicology. Clinical toxicology**, 41,223-8

Carnevali, S., Petruzzelli, S., Longoni, B., Vanacore, R., Barale, R., Cipollini, M., Scatena, F., Paggiaro, P., Celi, A., and Giuntini, C. (2003). Cigarette smoke extract induces oxidative stress and apoptosis in human lung fibroblasts. **American journal of physiology-lung cellular and molecular physiology**. 284, L955–L963.

Cevit, O., Bagecivan, I., Sarac, B., Parlak, A., Durmus, N., and Kaya, T. (2007). Mechanism of relaxation induced by nicotine in normal and ovalbumin-sensitized guinea-pig trachea. **European Journal of Pharmacology**, 567, 149-154.

Chaouachi, K. (2009). Hookah (Shisha, Narghile) smoking and environmental tobacco smoke (ETS), a critical review of the relevant literature and the public health consequences. **International Journal of Environmental Research and Public Health**, 6,798-843.

Chelikani, P., Fita, I., Loewen, P. C.(2004). Diversity of structures and properties among catalases. **Cellular and molecular life sciences**. 61 , 192–208

Chen, J., Higby, R., Tian, D., Tan, D., Johnson, M. D., Xiao, Y., Kellar, K. J., Feng, S., and Shields, P. G. (2008). Toxicological analysis of low-nicotine and nicotine-free cigarettes. **Toxicology**. 249(2-3), 194-203

Chen, K. C., and McGrath, J. J. (1985). Response of the isolated heart to carbon monoxide and nitrogen anoxia, **Toxicology and applied pharmacolog**. 81,363-70.

Christ, G., and Brink., P. (2000). Gap junctions in isolated rat aorta, evidence for contractile responses that exhibit a differential dependence on intercellular communication. **Brazilian Journal of Medical and Biological Research**, 33, 423-429.

Cobine, C. A., Callaghan, B. P., Keef, K. D. (2007). Role of L-type calcium channels and PKC in active tone development in rabbit coronary artery. **American journal of physiology. Heart and circulatory physiology**, 292,H3079-3088

Counts, M., Morton, M., Laffoon, S., Cox, R., and Lipowicz, P. (2005). Smoke composition and predicting relationships for international commercial cigarettes smoked with three machine-smoking conditions. **Regulatory toxicology and pharmacology**, 41, 185-227.

Das, A., Bhattacharya, A., and Chakrabarti, G. (2009). Cigarette smoke extract induces disruption of structure and function of tubulin-microtubule in lung epithelium cells and *in vitro*. **Chemical Research in Toxicology**, 22, 446-459.

De Rosa, S., Pacileo, M., Sasso, L., Di Palma, V., Maietta, P., Paglia A., Brevetti, L., Cirillo, P., and Chiariello, M. (2008). Insights into pathophysiology of smoke-related cardiovascular disease. **Monaldi archives for chest disease**, 70,59-67.

Deisseroth, A., and Dounce, A. (1970). Catalase, Physical and chemical properties, mechanism of catalysis, and physiological role. **Physiological reviews**, 50,319-375.

Desai, N., Mega, J., Jiang, S., Cannon, C., and Sabatine, M. (2009). Interaction between cigarette Smoking and clinical benefit of clopidogrel. **Journal of the american college of cardiology**.53, 1273-1278.

Ding, Y., Zhang, L., Jain, R., Jain, N., Wang, R., Ashley, D., and Watson, C. (2008). Levels of Tobacco-Specific Nitrosamines and Polycyclic Aromatic Hydrocarbons in Mainstream Smoke from Different Tobacco Varieties. **Cancer Epidemiology, Biomarkers and Prevention**. 17, 3366–71.

Donald, H., and Davida, N. (1997). Differentiation of muscarinic receptors mediating negative chronotropic and vasoconstrictor responses to acetylcholine in isolated rat hearts. **Journal of Pharmacology and Experimental Therapeutics**. 282,1337–1344.

Dye, J., and Adler, K. (1994). Effects of cigarette smoke on epithelial cells of the respiratory tract. **Thorax**, 49,825-834.

Ebbert, J. O., Dale, L. C., Nirelli, L. M., Schroeder, D. R., Moyer, T. P., and Hurt, R. D. (2004). Cotinine as a biomarker of systemic nicotine exposure in spit tobacco users. **Addictive behaviors**, 29, 349–355.

Fehrenbach, H., Brasch, F., Uhlig, S., Weisser, M., Stamme, C. (1998). Wendel et al. Early alterations in intracellular and alveolar surfactant of the rat lung in response to endotoxin. **American journal of respiratory and critical care medicine**.157, 1630-1639.

Ferrer, E., Víctor, P., Marta, D., Josep, L., Melina, M., Anna, M., Robert, R., and Joan, A. (2009). Effects of cigarette smoke on endothelial function of pulmonary arteries in the guinea pig. **Respiratory Research**. 10,76.

Fischer, S., Spiegelhalder, B., Eisenbarth, J., Preussmann, R. (1990). Investigations on the origin of tobacco-specific nitrosamines in mainstream smoke of cigarettes. **Carcinogenesis**, 11,723-30.

Fitzgerald, A. G. (1997). Cigarettes and the Wages of Sn-2,oxidized species of PAF in smoking Hamsters. **The Journal of Clinical Investigation**. 99, 2300-2301.

Fowler, J. S., Logan, J., Wang, G. J., and Volkow, N. D. (2003). Monoamine oxidase and cigarette smoking. *NeuroToxicology*, 24,75–82.

Frasca, J. M., Auerbach, O., Parks, V. R., and Jamieson, J. D. (1974). Alveolar cell hyperplasia in the lungs of smoking dogs. **Experimental and molecular pathology**, 21,300-12.

Fukuda, N., Sasaki, D., Ishiwata, S., and Kurihara, S. (2001). Length dependence of tension generation in rat skinned cardiac muscle, role of titin in the frank-starling mechanism of the heart. **Circulation**, 104,1639-1645.

Funayama, N., Shinkai, M., and Takayanagi, I. (1995). Inhibitory effects of d-nicotine on the responses evoked by l-isomer in trachea and bronchus isolated from guinea-pig and rabbit. **General Pharmacology**, 26, 977-981.

Galazyn-Sidorczuk, M., Brzoska, M., and Moniuszko-Jakoniuk, J. (2008). Estimation of Polish cigarettes contamination with cadmium and lead, and exposure to these metals via smoking. **Environmental monitoring and assessment**. 13, 481-49.

Glantz, S. A., and Parmley, W. W. (1991). passive smoking and heart disease, eidemiology, physiology, and biochemistry. **Circulation**. 83, 1-13.

Glasser, S., Selwyn, A., and Ganz, P. (1996). Atherosclerosis, Risk factors and the vascular endothelium. **American Heart Journal**. 131, 379-384.

Godfraind, T., Miller, R., and Lima, J. (1982). Selective $\alpha 1$ -and $\alpha 2$ -adrenoceptor agonist-induced contractions and ^{45}Ca fluxes in the rat isolated aorta. **British Journal of Pharmacology**, 77, 597-604.

Godoy, MAF., Rattan, N., and Rattan, S. (2009). COX-1 vs. COX-2 as a determinant of basal tone in the internal anal sphincter. **American Journal of Physiology-Gastrointestinal and Liver Physiology**, 296, 219-225.

Goich, J. (1995). cardiovascular Disease secondary to active and passive smoking. **Revista medica de chile journal**. 122,556-562.

Gottlieb, S. O.(1992). Cardiovascular benefits of smoking cessation. **Heart disease and stroke**, 4,173-175.

Greenlee, R. T., Hill-Harmon, M. B., Murray, T. and Thun, M. (2001). Cancer statistics. **A cancer journal for clinicians**. 51, 15–36.

Gruetter, C. A., Barry, B. K., McNamara, D. B., Kadowitz, P. J., and Ignarro, L. J. (1980). Coronary arterial relaxation and guanylate cyclase activation by cigarette smoke, N'-nitrosonornicotine and nitric oxide. **The Journal of pharmacology and experimental therapeutics**, 214,9-15.

Hadidi, KA., and Mohammed, FI. (2004). Nicotine content in tobacco used in hubble-bubble smoking. **Saudi Medical Journal**, 25, 912-917.

Halmi, R., Szijjarto, I., Brasnyo, P., Fesiis, G., Toth, P., Pusch, G., Koller, A., and Wittmann, I. (2009). Water extracts of cigarette smoke elicit smooth muscle dependent relaxation of rat renal arteries. **The Federation of American Societies for Experimental Biology**, 804(23).

Hanna, S .T. (2006). Nicotine effect on cardiovascular system and ion channels. **Journal of cardiovascular pharmacology**, 47,348-58.

Hassan, H. M., and Fridovich, I. (1978). Superoxide radical and the oxygen enhancement of the toxicity of paraquat in *E. coli*. **The Journal of biological chemistry**, 253, 8143–8148.

He, J. F. (1991). Morphologic and morphometric studies of pulmonary artery endothelial abnormalities in rats induced by smoking. **Zhonghua bing li xue za zhi Chinese journal of pathology**, 20,165-8.

He, J. F.(1992). Qualitative and quantitative observations of smoking-induced morphologic changes in muscular pulmonary arteries. **Chinese journal of tuberculosis and respiratory diseases**,15,92-94.

Hecht, S. S. (2002). Human urinary carcinogen metabolites, Biomarkers for investigating tobacco and cancer. **Carcinogenesis**, 23, 907–922.

Hecht, S. S. (2003). Tobacco carcinogens, their biomarkers and tobacco-induced cancer. **Nature Reviews Cancer**. 3, 733–744.

Heitzer, T., Yla-Herttuala, S., Luoma, J., Kurz, S., Münzel, T., Just, H., Olschewski, M., and Drexler, H. (1996). Cigarette smoking potentiates endothelial dysfunction of forearm resistance vessels in patients with hypercholesterolemia. Role of oxidized LDL. **Circulation**, 93, 1346-1353.

Hemmati, A. A., and Jayhoon, A. (2011). Pharmacologic Effects Of Nicotine On Isolated Aorta, Trachea And Lung Function Of Rat. **WebmedCentral Pharmacology**, 2(2), WMC001602.

Higman, D. J., and Powell, J. T. (1994). Smoking and Vascular Reactivity. **Journal of Smoking-related disorders**, 5, 157-162.

Higman, D. J., Greenhalgh, R. M., and Powell, J. T. (1993). Smoking impairs endothelium-dependent relaxation of saphenous vein. **European journal of surgery**, 80, 1242-5.

Hinken, A. C., and Solaro, R. J. (2006). A dominant role of cardiac molecular motors in the intrinsic regulation of ventricular ejection and relaxation. **Physiology**, 22, 73-80.

Hoffmann, D. and Wynder, E. (1986). Chemical constituents and bioactivity of tobacco smoke. **International Agency for Research on Cancer**, 74, 145-65.

Hua, Y., Ying-jun, Y., and SHeng-ming, Z. (2007). A study on the initial ultrastructure and expression of surfactant protein A in the lung of passive smoking mice. **Practical Journal of Medicine and Pharmacy**, 10.

Hummel, T., Hummel, C., Pauli, E., and Kobal, G. (1992). Olfactory discrimination of nicotine-enantiomers by smokers and non-smokers. **Chemical Senses**, 17, 13-21.

Ignaz, W., Torsten, R., Gernot, B., Gary, A., Jennifer, M., and Kurt, R. (1994). β -Adrenoceptors mediate inhibition of [3H]-acetylcholine release from the isolated rat and guinea-pig trachea, role of the airway mucosa and prostaglandins. **British Journal of Pharmacology**, 113, 1221-1230.

Igoillo-Esteve, M., and Cazzulo, J. J. (2006). The glucose-6-phosphate dehydrogenase from *Trypanosoma cruzi*, its role in the defense of the parasite against oxidative stress. **Molecular and biochemical parasitology**, 149, 170-81.

International Agency for Research on Cancer (IARC). (1986). Tobacco smoking, monograph on the evaluation of carcinogenic risk of chemicals to man. **Lyon (France), International agency for research on cancer.** 38, 1-5

Ji, S., Tosaka, T., Whitfield, B., Katchman, A., Kandil, A., Knollmann, B., and Ebert, S. (2002). Differential rate responses to nicotine in rat heart, evidence for two classes of nicotinic receptors. **The Journal of Pharmacology and Experimental Therapeutics**, 301, 893-899.

Jones T. R., Hamilton J. T. and Lefcoe N. M. (1980). Pharmacological modulation of cholinergic neurotransmission in guinea pig trachea. **Canadian Journal of Physiology and Pharmacology**, 58, 810-822.

Jorge, P. A., Ozaki, M. R., and Almeida, E. A. (1995). Endothelial dysfunction in coronary vessels and thoracic aorta of rats exposed to cigarette smoke. **Clinical and experimental pharmacology & physiology**, 22, 410-413.

Joshi, M., Kodavanti, P., and Mehendale, H. (1988). Glutathione metabolism and utilization of external thiols by cigarette smoke-challenged, isolated rat and rabbit lungs. **Toxicology and Applied Pharmacology**, 96, 324-335.

Junqueira, C L., Carneiro, J. and Kelly. O.R. (1992). Basic histology. 11th edition. **McGraw-Hill Companies**, USA, 182-360.

Kaiserman, M. J. and Rickert, W. (1992). Carcinogens in Tobacco Smoke, Benzo {a} Pyrene from Canadian Cigarette and Cigarette Tobacco. **American Journal of Public Health**. 82, 1023-1026.

Kaneda, T., Takeuchi, Y., Matsui, H., Shimizu, K., Urakawa, N., and Nakajyo, S. (2005). Inhibitory mechanism of papaverine on carbachol-induced contraction in bovine trachea. **Journal of Pharmacological Sciences**, 98, 275-282.

Kantengwa, S., Jornot, L., Devenoges, C., Nicod, L. P. (2003). Superoxide anions induce the maturation of human dendritic cells. **American journal of respiratory and critical care medicine**, 167, 431-437.

Karnovsky, M .J., (1965). A formaldehyde-glutaraldehyde fixative of high osmolality for use in electron microscopy. **The Journal of cell biology**, 27, 137-138.

- Kaufman, S. L. (1972). Alterations in cell proliferation in mouse lung following urethane exposure. **The American journal of pathology**, 68, 317-324.
- Keech, M.K. (1960). Electron microscope study of the normal rat aorta. **The Journal of Biophysical and Biochemical Cytology**. 7, 533-538.
- Kessler, A. (1995). Nicotine addiction in young people. **The New England Journal of Medicine**, 333, 186-189.
- Khader, Y. and Alsadi, A. (2008). Smoking habits among university students in Jordan, prevalence and associated factors. **Eastern Mediterranean Health Journal**. 14, 897-904.
- Kobrinisky, L., Klug, G., Hokanson, J., Sjolander, E., Burd, L. (2003). Impact of smoking on cancer stage at diagnosis. **Journal of Clinical Oncology**. 21, 907-913.
- Korzick, D. H. (2003). Regulation of cardiac excitation-contraction coupling, a cellular update. **Advances in Physiology Education**, 27, 192-200.
- Kuo, W. H., Chen, J. H., Lin, H. H., Chen, B. C., Hsu, J. D., and Wang, C. J. (2005). Induction of apoptosis in the lung tissue from rats exposed to cigarette smoke involves p38/JNK MAPK pathway. **Chemico-biological interactions**, 155,31-42.
- Kurus, M., Firat, Y., Cetin, A., Kelles, M., Otlü, A. (2009). The effect of resveratrol in tracheal tissue of rats exposed to cigarette smoke. **Inhalation toxicology**, 21,979-984.
- Laporte, R., Hui, A., and Laher, I. (2004). Pharmacological modulation of sarcoplasmic reticulum function in smooth muscle. **Pharmacological Reviews**, 56 ,4 439-513.
- Leguillette, R., Zitouni, N. B., Govindaraju, K., Fong, L. M., and Lauzon, A. M. (2008). Affinity for MgADP and force of unbinding from actin of myosin purified from tonic and phasic smooth muscle. **American Journal of Physiology-Cell Physiology**, 295, 653-660.
- Leon, A. (1993). Cardiovascular damage from smoking, A Fact or belief?. **International Journal of Cardiology**. 38, 113-117.
- Leon, A. (1994). Cigarette smoking and cardiovascular damage, Analytic Review of the subject. **Singapore Medical Journal**. 35, 442-444.

- Leon, A. (1995). Cigarette smoking and and health of the heart. **The journal of the royal society for the promotion of health**, 115, 354-5.
- Lewis, A., Miller, J. H., and Lea R. A. (2007). Monoamine oxidase and tobacco dependence. **Neurotoxicology**, 28,182-95.
- Lewis, D., and Jakins, P. (1981). Effect of tobacco smoke exposure on rat tracheal submucosal glands, an ultrastructural study. **Thorax**, 36, 622-624.
- Lin, S., Hong, C., Chang, M., Chiang, B., and Chien, S. (1992). Long-term nicotine exposure increases aortic endothelial cell death and enhances transendothelial macromolecular transport in rats. **Arteriosclerosis, Thrombosis, and Vascular Biology**, 12,1305-1312.
- Liswi, W. (1998). Effects of smokes of three types of Jordanian cigarettes on the physiology and ultrastructure of selected tissues from the cardiovascular system of the rat, **Master's Thesis**, The University of Jordan, Amman.
- Loirand, G., Guerin, P., and Pacaud, P. (2006). Rho kinases in cardiovascular physiology and pathophysiology. **Circulation Research**, 98, 322-334.
- Long, J., and Tranquillo, R. (2003). Elastic fiber production in cardiovascular tissue-equivalents. **Matrix Biology**, 22, 339-350.
- Lotriet, C., Oliver, D., and Venter, D. (2007). The pharmacological effects of ozone on isolated guinea pig tracheal preparations. **Archives of Toxicology**, 81, 433-440.
- Lough, J. (1978). Cardiomyopathy produced by cigarette smoke. Ultrastructural observations in guinea pigs. **Archives of pathology & laboratory medicin**, 102, 377-380
- Lowry, O. H., Rosebrough, N. J., Farr, A. L., Randall, R. J. (1951). Protein measurement with the Folin phenol reagent. **The Journal of biological chemistry**, 193,265-75.
- Luck, H. (1963). Catalase. **In Methods of Enzymatic Analysis**, 3, 885–894.
- Lukas, M. (2004). A signal transduction pathway model prototype I, From agonist to cellular endpoint. **Biophysical Journal**, 87, 1406-1416.
- Luzzatto, L., Battistuzzi, G. (1985). Glucose-6-phosphate dehydrogenase. **Advanced Human Genetics**, 14, 217–329.

Macia, R., Matthews, W., Lafferty, J., and DeMarinis, R. (1984). Assessment of alpha-adrenergic receptor subtypes in isolated rat aortic segments. **Naunyn-Schmiedeberg's Archives of Pharmacology**, 325, 306-309.

Malson, J., Sims, K., Murty, R., and Pickworth, B. (2001). Comparison of the nicotine content of tobacco used in bidis and conventional cigarettes. **Tobacco Control**.10, 181-183.

Martin, M., Carlene, H., Daryl, R., John, R., and Anna, D. (1997). Sex differences in the abundance of endothelial nitric oxide in a model of genetic hypertension. **Hypertension**, 30,1517-1524.

Masubuchi, T., Koyama, S., Sato, E., Takamizawa, A., Kubo, K., and Sekiguchi, M.(1998). Smoke extract stimulates lung epithelial cells to release neutrophil and monocyte chemotactic activity. **The American journal of pathology**,153, 1903-1912.

Matthew, A., Shmygol, A., and Wray, S. (2004). Ca^{+2} entry, efflux and release in smooth muscle. **Biological Research**, 37, 617-624.

Mayhan, W. G., and Sharpe, G. M. (1998). Superoxide dismutase restores endothelium-dependent arteriolar dilatation during acute infusion of nicotine. **Journal of Applied Physiology**, 85,1292–1298.

Maziak, M., Ward, K., Soweid, R and Eissenberg, T. (2004).Tobacco smoking using a waterpipe, a re-emerging strain in a global epidemic. **Tobacco Control**.13,327-333

McGrath, J. J. (1986). Nicotine and carbon monoxide, effects on the isolated rat heart. **Alcohol**, 3,157-60.

McGrath, J. J., and Smith, D. (1984). Nicotine-depressed function in isolated rat heart. **Drug and chemical toxicology**, 7,1-10.

Metsios, G., Flouris A., Jamurtas, A., Carrillo, A., Kouretas, D., Germenis, A., Gourgoulisanis, K., Kiropoulos, T., Tzatzarakis, M., Tsatsakis, A., and Koutedakis, Y. (2007). A brief exposure to moderate passive smoke increases metabolism and thyroid hormone secretion. **The Journal of Clinical Endocrinology and Metabolism**. 92, 208-211

Michael, R. (2000). Cigarette smoking, endothelial injury and cardiovascular disease. **International journal of experimental pathology**, 81, 219-30.

Mizuno, Y., Isotani, E., Huang, J., Ding, H., Stull, J. T., and Kamm, K. E. (2008). Myosin light chain kinase activation and calcium sensitization in smooth muscle in vivo. **American Journal of Physiology-Cell Physiology**, 295, 358-364.

Mohrman, D. and Heller, L. (2006). Cardiovascular Physiology. McGraw-Hill companies.

Motoyama, T., Kawano, H., and Kugiyama, K. (1997). Endothelium dependent vasodilatation in the brachial artery is impaired in smokers, effect of vitamin C. **American journal of physiology**, 273, H1644–H1650.

Mukherjee, S., Woods, L., Weston, Z., Williams, A., Das, S. (1993). The effect of mainstream and sidestream cigarette smoke exposure on oxygen defense mechanisms of guinea pig erythrocytes. **Journal of Biochemical Toxicology**, 8, 111–166.

Murohara, T., Kugiyama K., Ohgushi, M., Sugiyama, S., and Yasue, H. (1994). Cigarette smoke extract contracts isolated porcine coronary arteries by superoxide anion-mediated degradation of EDRF, **American journal of physiology**. 266,874-80.

Nakamura, K., Barzi, F., Lam, L., Huxley, R., Feigin, V., Ueshima, H., Woo, J., Gu, D., Ohkubo, T., Lawes, C., Suh, I. and Woodward, M. (2008). Cigarette Smoking, Systolic Blood Pressure, and Cardiovascular Diseases in the Asia-Pacific Region. **Stroke**. 39,1694-1702.

Ochs, M., Nenadic, I., Fehrenbach, A., Albes, J. M., Wahlers, T., and Richter, J. (1999). Ultrastructural alterations in intraalveolar surfactant subtypes after experimental ischemia and reperfusion. **American journal of respiratory and critical care medicine**, 160, 718-724.

Ogut, O., Yuen, S., and Brozovich, F. (2007). Regulation of the smooth muscle contractile phenotype by nonmuscle myosin. **Journal of Muscle Research and Cell Motility**, 28, 409-414.

Orchard, C., and Brette, F. (2008). T-tubules and sarcoplasmic reticulum function in cardiac ventricular myocytes. **Cardiovascular Research**, 77, 237-244.

Ortega, P., Uhley, H. N., Leeds, S. E., Ffidman, N. M., and Sampson, J. J. (1970). Serial electron and light microscopic studies on the dog lung in chronic experimental pulmonary edema. **The American journal of pathology**, 60,57-72

Ota, Y., Kugiyama, K., Sugiyama, S., Ohgushi, M., Matsumura, T., Doi, H., Ogata, N., Oka, H., and Yasue, H. (1997). Impairment of endothelium-dependent relaxation of rabbit aortas by cigarette smoke extract--role of free radicals and attenuation by captopril. **Atherosclerosis**, 131,195-202.

Ozbay, B., Yener, Z., Acar, S., and Kanter, M. (2009). Histopathological changes in the lung of rat following long -term exposure to biomass smoke. **Turkiye Klinikleri Journal of Medical Sciences**, 29,877-883.

Paglia, E., and Valentine. N. (1967). Studies on the quantitative and qualitative characterization of erythrocyte glutathione peroxidase. **Journal of Laboratory and Clinical Medicine**, 70, 158–169.

Pandolfi, P., Sonati, F., Rivi, R.,Mason, P., Grosveld, F., and Luzzatto, L. (1995) .Targeted disruption of the housekeeping gene encoding glucose 6-phosphate dehydrogenase (G6PD), G6PD is dispensable for pentose synthesis but essential for defense against oxidative stress. **European Molecular Biology Organization Journal**, 14, 5209–5215.

Patel, C. A., and Rattan, S. (2007). Cellular regulation of basal tone in internal anal sphincter smooth muscle by RhoA/ROCK. **American Journal of Physiology-Gastrointestinal and Liver Physiology**, 292, 1747-1756.

Pekmez, H., Ogeturk, M., Ozyurt, H., Sonmez, M. F., Colakoglu, N., and Kus, I. (2010). Ameliorative effect of caffeic acid phenethyl ester on histopathological and biochemical changes induced by cigarette smoke in rat kidney. **Toxicology and industrial health**, 26,175-82.

Peters, S., and Michel, M. (2003). cAMP-independent relaxation of smooth muscle cells via Gs-coupled receptors. **Naunyn-Schmiedeberg's Archives of Pharmacology**, 368, 329-330.

Pfitzer, G. (2001). Signal transduction in smooth muscle invited review, regulation of myosin phosphorylation in smooth muscle. **Journal of Applied Physiology**, 91, 497-503.

Pittilo, R. M., Mackie, I. J., Rowles, P. M., Machin, S. J., and Woolf, N. (1982). Effects of cigarette smoking on the ultrastructure of rat thoracic aorta and its ability to produce prostacyclin. **International Society on Thrombosis and Haemostasis**, 48, 173-6.

Plowman, P. N. (1982). The pulmonary macrophage population of human smokers. **American Review of Respiratory Disease**, 25, 393-405.

Proctor, R. N. (2001). Tobacco and the global lung cancer epidemic. **Nature Reviews Cancer**, 1, 82–86.

Public health laboratories report. Myreland N.j.-USA. (1997). **Report on smoking and health**.

Rahman, I., Li, Y., Donaldson, K., Harrison, D., and MacNee, W. (1995). Glutathione homeostasis in alveolar epithelial cells in vitro and lung in vivo under oxidative stress. **The American journal of physiology**, 269, L285–L292.

Rasmussen, H., Stavenow, L., Xu, C. B., Berglund, A. (1991). Increased smooth muscle cell proliferation by dimethylbenzanthracene is correlated to variations in activity of ornithine decarboxylase but not arylhydrocarbonhydroxylase. **Artery**, 18, 240-55.

Reynolds, E. S. (1963). The use of lead citrate at high pH as an electron-opaque stain in electron microscopy. **The Journal of cell biology**, 12, 208-212.

Reznick, A. Z., Klein, I., Eiserich, J. P., Cross, C. E., and Nagler, R. M. 2003. Inhibition of oral peroxidase activity by cigarette smoke, in vivo and in vitro studies. **Free radical biology and medicine**, 34, 377-384.

Rose, J. E., Behm, F. M., Ramsey, C., and Ritchie, J. (2001). Platelet monoamine oxidase, smoking cessation, and tobacco withdrawal symptoms. **Nicotine and tobacco research** **Nicotine and tobacco research**, 3, 383–90.

Ross, M., Gordon, K., and Wojciech, P. (2003). Histology, A text and atlas. 4th edition. Philadelphia, Lippincott Williams & Wilkins. 246-600.

Rubins, J. (2003). Alveolar macrophages wielding the double-edged sword of inflammation. **American Journal of Respiratory and Clinical Care Medicine**. 167, 103-104.

Ruobao, L., Hongxian¹, L., Qifu, B., Yan, H., and Jinping, W. (2008). Effect of long-term environmental tobacco smoke on the ultrastructure and expression of TGF- β 1 in rat alveolar epithelium. **Chinese Journal of Anatomy**, 0.01.

Salvemini, F., Franzé, A., Iervolino, A., Filosa, S., Salzano, S., and Ursini, M. (1999). Enhanced glutathione levels and oxidoresistance mediated by increased glucose-6-phosphate dehydrogenase expression. **The Journal of Biological Chemistry**, 274, 2750–7.

Sanders, C. L., Adee, R. R., and Jackson, T. A. (1971). Fine structure of alveolar areas in the lung following inhalation of 2sgPuOZ particles. **Archives of environmental health**, 22, 525-533.

Sanders, K. (2001). Signal transduction in smooth muscle invited review, Mechanisms of calcium handling in smooth muscles. **Journal of Applied Physiology**, 91, 1438-1449.

Schachter, E. N., Zuskin, E., Goswami, S., Castranova, V., Siegel, P., Whitmer, M., and Gadgil, A. (2003). Pharmacologic effects of tobacco dust extract on isolated Guinea pig trachea. **Chest**, 123,862-8.

Scharte, J., Schön, H., Tjaden, Z., Weis, E., and von Schaewen, A. (2009). Isoenzyme replacement of glucose-6-phosphate dehydrogenase in the cytosol improves stress tolerance in plants. **Proceedings of the National Academy of Sciences of the United States of America**, 106,8061-6.

Schramm, C. (2000). β -Adrenergic Relaxation of rabbit tracheal smooth muscle, A receptor deficit that improves with corticosteroid administration. **The Journal of Pharmacology and Experimental Therapeutics**, 292, 280-287.

Scriven, D.R.L., Dian, P., and Moore, D. W. (2000). Distribution of proteins implicated in excitation-contraction coupling in rat ventricular myocytes. **Biophysical Journal**, 79, 2682-2691.

Shafagoj, Y. A., Mohammad, F. I., and Hadidi, K. M. (2002). Hubble-bubble (water pipe) smoking, levels of nicotine and cotinine in plasma, saliva and urine. **International Journal of Clinical Pharmacology and Therapeutics**, 40, 249-255.

Shraideh, Z., Awaidah, W., Najar, H., and Musleh, M. (2011). A modified smoking machine for monitoring the effect of tobacco smoke on albino rats. **The Jordan Journal of Biological Sciences**, 4, 109-112.

Simet, S. M., Sisson, J. H., Pavlik, J. A., Devasure, J. M., Boyer, C., Liu, X., Kawasaki, S., Sharp, J. G., Rennard, S. I., and Wyatt, T. A. (2010). Long-term cigarette smoke exposure in a mouse model of ciliated epithelial cell function. **American journal of respiratory cell and molecular biology**, 43,635-40.

Soeller, C., and Cannell, M. B (1999). Examination of the transverse tubular system in living cardiac rat myocytes by 2-photon microscopy and digital image-processing techniques. **Circulation Research**, 84, 266-275.

Solaro, R. J. (2008). Multiplex kinase signaling modifies cardiac function at the level of sarcomeric proteins. **The Journal of Biological Chemistry**, 283, 26829-26833.

Stampfli, M., and Anderson, G. (2009). How cigarette smoke skews immune responses to promote infection, lung disease and cancer. **Nature Reviews Immunology**, 9, 377-384.

Stefanadis, C., Tsiamis, E., Vlachopoulos, C., Stratos, C., Toutouzas, K., Pitsavos, C., Marakas, S., Boudoulas, H., Toutouzas, P. (1997). Unfavorable effect of smoking on the elastic properties of the human aorta. **Circulation**, 95, 31-38.

Steffee, C. H., and Baetjer, A. M. (1965). Histopathologic effects of chromate chemicals. **Archives of Environmental Health**, 11, 66-75.

Stepanov, I., and Hecht, S. S. (2005). Tobacco-specific nitrosamines and their pyridine-N-glucuronides in the urine of smokers and smokeless tobacco users. **Cancer epidemiology, biomarkers and prevention**, 14, 885-888.

Stephen, M. (2010). The toxicological effect of cigarette smoke and environmental tobacco smoke. **Report Assignment-Biochemical Toxicology**. BC4927.

Stevenson, C. S., Coote, K., Webster, R., Johnston, H., Atherton, H. C., Nicholls, A., Giddings, J., Sugar, R., Jackson, A., Press, N. J., Brown, Z., Butler, K., Danahay, H. (2005). Characterization of cigarette smoke-induced inflammatory and mucus hypersecretory changes in rat lung and the role of CXCR2 ligands in mediating this effect. **American journal of physiology. Lung cellular and molecular physiology**, 288, L514-522.

Streck, E., Jorres, RA., Huber, RM., and Bergner, A. (2010). Effects of cigarette smoke extract and nicotine on bronchial tone and acetylcholine-induced airway contraction in mouse lung slices. **Journal of Investigational Allergology and Clinical Immunology**, 20, 324-330.

Sugiyama, S., Kugiyama, K., Ohgushi, M., Matsumura, T., Ota, Y., Doi, H., Ogata, N., Oka, H., and Yasue, H. (1989). Supersensitivity of atherosclerotic artery to constrictor effect of cigarette smoke extract. **Cardiovascular research**, 38, 508-15.

Taggart, M. J. (2001). Smooth muscle excitation-contraction coupling, a role for caveolae and caveolins. **News of Physiological Science**, 16, 61-65.

Taggart, MJ., and Wray, S. (1998). Hypoxia and smooth muscle function, key regulatory events during metabolic stress. **Journal of Physiology**, 509, 315-325.

Terry, D., Miller, B., Jones, G., and Rohan, E.(2003). Cigarette smoking and the risk of invasive epithelial ovarian cancer in a prospective cohort study. **European journal of cancer**. 39, 1157-1164.

Thomas, D. (1993). Tobacco smoking and cardiovascular disease. **La Revue du praticien** . 43(10), 1218-1222.

Tian, W. N., Pignatere, J. N., Stanton, R. C. (1994). Signal transduction proteins that associate with the platelet-derived growth factor (PDGF) receptor mediate the PDGF- induced release of glucose-6-phosphate dehydrogenase from permeabilized cells. **The Journal of Biological Chemistry**. 269,14798–805.

Torok, J., Gvozdjakova, A., Kucharska, J., Balazovjech, I., Kysela, S., Simko, F., and Gvozdjak, J. (2000). Passive smoking impairs endothelium-dependent relaxation of isolated rabbit arteries. **Physiological research**, 49,135–141.

U. S. Public Health Service. (2005). Smoking and Health. A Report of the Surgeon General. U. S. Department of Health Education, and Welfare, **Public Health Service**, 79, 2-47.

Varlamova, O., Spektor, A., Bresnick, R. (2001). Protein kinase C mediates phosphorylation of the regulatory light chain of myosin-II during mitosis. **Journal of muscle research and cell motility**, 22,243-50.

Wannamethee, S. G., Lowe, G. D., Shaper, A.G., Rumley, A., Lennon, L., AND Whincup, P. H.(2005). Associations between cigarette smoking, pipe/cigar smoking, and smoking cessation, and haemostatic and inflammatory markers for cardiovascular disease. **European heart journal**. 26,1765-73.

Webb, R. (2003). Smooth muscle contraction and relaxation. **Advances in Physiology Education**, 27, 201-206.

Widlansky, M. E., Gokce, N., Keaney, J., and Vita, J. A. (2003). The clinical implications of endothelial dysfunction. **Journal of the American College of Cardiology**, 42, 1149-1160.

Winkelmann, B., Holt, K., and Unverdorben, M. (2009). Smoking and atherosclerotic cardiovascular disease, Part I, Atherosclerotic disease process. **Biomarkers in Medicine**, 4, 411-428.

Yanbaeva, D. G., Dentener, M. A., Creutzberg, E. C., Wesseling, G., and Wouters, E. F. (2007). Systemic effects of smoking. **Chest**, 131, 1557-66.

Yang, Z., Harrison, C. M., Chuang, G. C., Ballinger, S. W. (2007). The role of tobacco smoke induced mitochondrial damage in vascular dysfunction and atherosclerosis. **Mutation research**, 621, 61-74.

Yarnell, G. J. (1996). Smoking and Cardiovascular Disease. **Quarterly Journal of Medicine**. 89, 493-498.

York, G. K., Peirce, T. H., Schwartz, L. W., and Cross, C. E. (1976). Stimulation by cigarette smoke of glutathione peroxidase system enzyme activities in rat lung. **Archives of environmental health**, 31, 286-290.

Young, B., Lowe, J., Stevens, A., and Heath, J. (2006). Functional Histology. 5th edition. **Elsevier, Philadelphia, USA**.

Zeiber, A. M., Schächinger, V., Minners, J. (1995). Long-term cigarette smoking impairs endothelium-dependent coronary arterial vasodilator function. **Circulation**, 92, 1094-1100.

Zhang, W., Edvinsson, L., and Lee, T. (1998). Mechanism of nicotine-induced relaxation in the porcine basilar artery. **The Journal of Pharmacology and Experimental Therapeutics**, 284, 790-797.

Zimmermann, K. C., Green, D. R. (2001). How cells die, apoptosis pathways. **The Journal of allergy and clinical immunology**, 108, S99-103.

APPENDICES

Appendix A

Preparation of solutions:

1. 10% Salined formalin

It Consists of: 9 g NaCl, 100 ml distilled water, 100 ml of 37% formalin, and the volume was completed to 1 L with distilled water.

2. Alcoholic eosin Y

One gram eosin Y (Riedel-de Haën, Seelze, Germany) was dissolved in 100 ml distilled water. 10 ml from stock phloxine B (the stock was already prepared by dissolving 1 g in 10 ml distilled water) was then added, together with 4 ml glacial acetic acid and 780 ml ethanol 95%.

3. Lithium carbonate

Ten grams lithium carbonate (Sigma, USA) was dissolved in 100 ml distilled water.

4. Egg albumin

Five grams of egg albumin grade (II) (Sigma, USA), together with 0.5 g NaCl, were dissolved in 100 ml distilled water. The solution was then filtered, and an equal volume of glycerol was added to the filtrate.

5. rTdT reaction mix

Components of this buffer were: an equilibration buffer, biotinylated nucleotide mix, and rTdT enzyme, being added in the ratio 98:1:1, respectively.

6. Stock sodium cacodylate buffer

Sodium cacodylate (42.8 g) was dissolved in 500 ml distilled water. Then 8.6 ml of 0.2 M HCl was added to the solution.

7. Working buffer

Only 25 ml of the stock sodium cacodylate buffer was used. After that, 4 ml of 0.2 M HCl was added to reach a pH of 7.2. Then, 10 drops of 1% CaCl_2 was added to the mixture. Finally, distilled water was added up to 100 ml.

8. Washing buffer

It was made by adding 3 g of sucrose to each 100 ml of the above.

9. 8% Paraformaldehyde

Paraformaldehyde powder (8 g) was dissolved in 100 ml distilled water. Then, 12 drops of 1 M NaOH was added to the solution, and the mixture was heated to 55 °C. Finally, the solution was filtered to get rid of undissolved particles.

10. Karnovsky's fixative

A mixture of 25 ml 8% paraformaldehyde, and 5 ml of 50% glutaraldehyde was made, working buffer was added up to 50 ml. Then, 1.5 g of sucrose was dissolved in the mixture.

11. The embedding medium (Spurr's medium)

This medium was prepared by mixing the following ingredients in order:

10 g Vinyl cyclohexane dioxide (ERL-2406). (Fluka AG, Switzerland).

4 g Diglycidyl ether of polypropylene glycol (DER-736). (Fluka AG, Switzerland).

26 g Neonyl succinic anhydride. (Ted Pella, Redding).

0.4 g Dimethyl aminoethanol (D.M.A.E). (Fluka AG, Switzerland).

The medium was gently mixed for 30 min using a magnetic stirrer.

12. Aqueous uranyl acetate

One half a gram of uranyl acetate was dissolved in 10 ml distilled water. The stain was stored in a brown glass bottle at 5 C°.

13. Lead citrate

One tenth gram of lead citrate was dissolved in 10 ml of boiled distilled water. Then, 0.1 ml of 10 M NaOH was added to the mixture.

14. Physiological saline solution(PSS)

It is composed of the following chemicals, provided the molecular formula and the final concentration of each given in mM: NaCl 118, KCl 4.7, CaCl₂.2H₂O 2.5, MgCl₂.6H₂O 0.5, NaH₂PO₄ 1.0, NaHCO₃ 25, C₆H₁₂O₆ 11.1.

15. Papaverine hydrochloride (Sigma, India)

The final concentration was (1 mM). Papaverine was dissolved in distilled water.

16. Carbamoylcholine chloride (Carbachol) (Aldrich, Germany)

The final concentration was (0.02 mM). Carbachol was dissolved in distilled water.

17. Phenylephrine hydrochloride (Sigma-Aldrich, Germany)

The final concentration was (0.01 mM). Phenylephrine was dissolved in 0.9% NaCl.

18. L-Nicotine

A solution with a concentration of (1010 $\mu\text{g}/\text{ml}$) was prepared by taking 100 μl from pure L-nicotine (Merck, Stuttgart, Germany), and completing the volume to 100 ml with PSS.

19. Sodium hydroxide

A solution with a concentration of 6.25 M was prepared by dissolving 12.5 g from NaOH in 50 ml distilled water.

20. Potassium permanganate

A stock solution of 0.125 M was prepared by dissolving 1.97 g KMnO_4 (Riedel-de Haën, Seelze, Germany) in 100 ml distilled water.

21. Protein content determination**21.1. Analytical reagents:**

A- 50 ml of 2% sodium carbonate mixed with 50 ml of 0.1 N NaOH solution

B- 10 ml of 1.56% copper sulphate solution mixed with 10 ml of 2.37% sodium potassium tartarate solution.

C- Prepare analytical reagents by mixing 2 ml of (B) with 100 ml of (A).

D- Folin - Ciocalteu reagent solution (1N) Dilute commercial reagent (2N) with an equal volume of distilled water on the day of use.

21.2. Protocol

1. Set up eleven sets of three 16 x 150 mm test tubes in rack.
2. Add 10 μ l of sample to these tubes.
3. Add 2 mL of solution C to each test tube.
4. Incubate for 10 minutes at room temperature.
5. Add 0.2 mL of dilute Folin-phenol solution to each tube.
6. Vortex each tube immediately.
9. Incubate at room temperature for 30 minutes.
10. Determine absorbance of each sample at 600 nm.
11. Determine protein content from standard curve.

Appendix B

1. Spectrophotometric determination of L-nicotine

1.1. Calibration curve

Table 1 and Figure 1 showed a linear relationship between L-nicotine and absorbance over the entire concentration range (0-8 $\mu\text{g/ml}$), with a correlation coefficient ($R^2 = 0.99$).

Table 1: Absorbance values for the different L-nicotine concentrations

L-nicotine concentration ($\mu\text{g /ml}$)	Absorbance
0	0
0.5	0.037
1	0.102
1.5	0.162
2	0.212
3	0.337
4	0.426
5	0.54
6	0.642
7	0.876
8	0.956

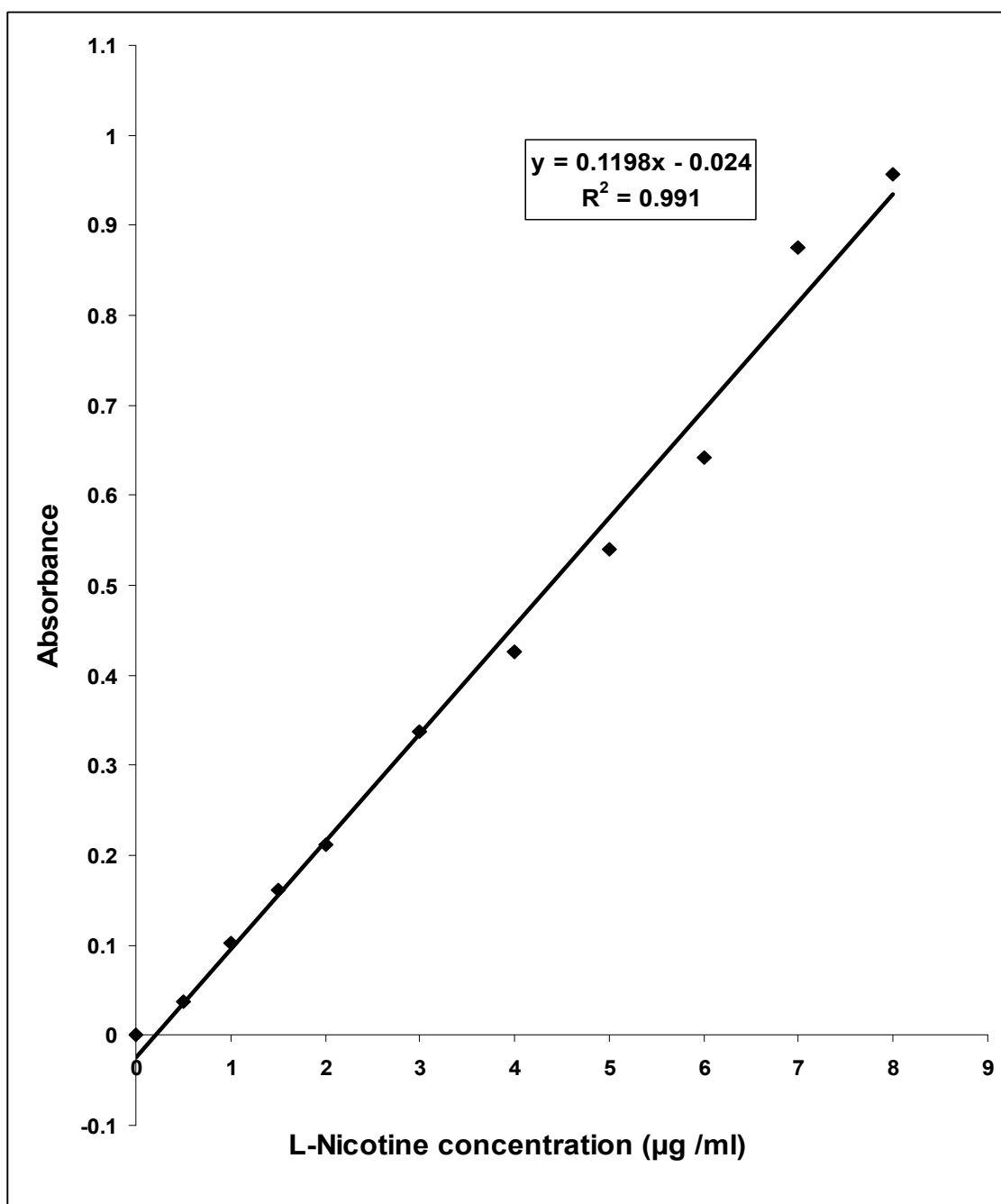


Figure1: Calibration curve for peak absorbance versus L-nicotine concentration

Appendix C

1. Protein determinations:

Table 1: Absorbance values for the different Protein concentrations

Protein concentrations (µg/ml)	Absorbance at 600 nm
0	0
5	0.074
15	0.114
30	0.201
45	0.279
60	0.369
75	0.483
90	0.536
100	0.593

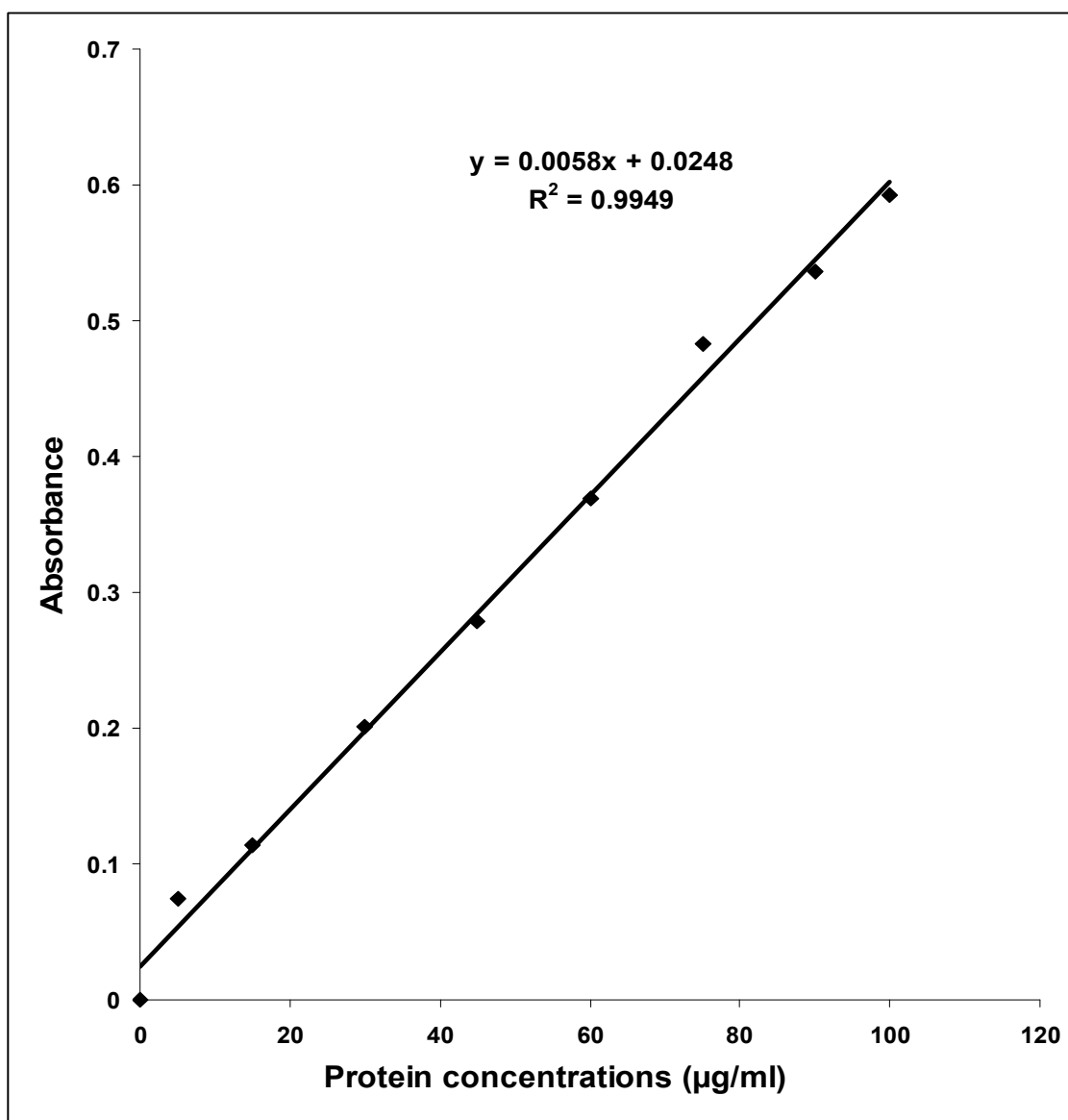


Figure 1: Calibration graph for peak absorbance versus different bovine serum albumin (BSA) concentrations.

تأثير دخان السجائر على الجهازين التنفسي و الدوري الدموي للجرذ الأمهق: دراسات نسيجية و فسيولوجية و بيوكيميائية.

إعداد

وجدي جمعة محمد العوايدة

المشرف

الاستاذ الدكتور زياد عاهد الشريدة

المشرف المشارك (الاول)

الاستاذ الدكتور غالب موسى أبو الريش

المشرف المشارك (الثاني)

الدكتور درويش حسن بدران

يسعى هذا البحث لكشف مخاطر تدخين السجائر على أنسجة مختارة من الجرذ الأمهق على المستوى الخلوي، عن طريق تعريض مجموعة من الجرذان المخبرية لدخان السجائر لثلاثة أشهر يوميا بواسطة جهاز أعد خصيصا لهذا الغرض. وقد تضمن الجزء الأول من البحث دراسة فسيولوجية لتحديد تأثير مادة النيكوتين النقية، و المستخلص الملحي الفسيولوجي لدخان السجائر على بعض الجوانب الوظيفية للعضلات الملساء للقصبه الهوائية و الشريان الأبهر.

و درس أيضا تأثير مادة النيكوتين النقية و المستخلص الملحي الفسيولوجي لدخان السجائر على عضلة القلب، بإجراء تجربة القلب المنضوح المعزول. كذلك حسب تركيز مادة النيكوتين في مستخلص دخان السجائر، بطريقة تعتمد على (القياس الطيفي).

وركز الجزء الثاني من البحث على تأثير دخان السجائر على نشاطية بعض الأنزيمات المضادة للأكسدة، ومقارنتها بالقيم الطبيعية، وقد تم تقييم الأثر الذي يحدثه انقطاع تعريض الجرذان لدخان السجائر لمدة مماثلة لمدة التعريض على نشاطية تلك الأنزيمات.

وتضمن الجزء الثالث من البحث إجراء تحضيرات نسيجية لتقييم ما حدث من تغيرات شكلية بنوية للأنسجة التي درست، وهي: القصبه الهوائية و الحويصلات الهوائية و الشريان الأبهر و الجزء البطيني من القلب، بواسطة المجهر الضوئي و المجهر الإلكتروني النفاذ، وتبين في هذا الفصل قدرة دخان السجائر على إحداث (موت الخلية المبرمج)، و ذلك باستخدام معايرة dUTP الموسوم المضاف للنهاية المكسورة بوساطة الناقل الطرفي للنيكليوتيدات منقوصة الأكسجين (Tunnel assay).

أما الجزء الأخير من الدراسة النسيجية فقد سعى إلى تقييم الأثر الذي يحدثه انقطاع تعريض الجرذان لدخان السجائر لمدة مماثلة لمدة التعريض في الأنسجة المذكورة بواسطة المجهر الضوئي والإلكتروني.

وقد أظهرت التجارب أن مستخلص الدخان له تأثير مزدوج (انقباض تلاح انبساط) ضمن التراكيز التي درست على نسيجي القصبه و الشريان الأبهر، إذ كان تأثيره مشابها لتأثير مادة النيكوتين النقية بتركيز يكافئ تركيزها في مستخلص الدخان. وفي تجارب القلب المنضوح فقد أحدث مستخلص الدخان تباطؤا في سرعة دقات القلب و قوة خفقه، فكان تأثيره مشابها لتأثير مادة النيكوتين النقية. و أظهر حساب تركيز مادة النيكوتين بطريقة تعتمد على الحساب الطيفي، احتواء الغرام الواحد من التبغ ما يعادل 57 ملغم نيكوتين في المحلول الملحي.

أما الدراسة البيوكيميائية فقد أظهرت ان دخان السجائر أحدث نقصانا ملحوظا في نشاط كل من الأنزيمات التالية: كاتاليز بنسبة 23%، 18%، 50% في كل من أنسجة الكبد و الكلية و الرئة على الترتيب، غلوكوز 6 فسفوديهيدروجينيز بنسبة 29%، 18%، 38% في الكبد و الكلية و الرئة على الترتيب. و أخيرا إنزيم غلوتاثيون بيروكسيداز بنسبة 16%، 13%، 35% في الكبد و الكلية و الرئة على الترتيب. و تجدر الإشارة إلى تسجيل مستويات طبيعية للأنزيمات الثلاث بعد إيقاف التدخين.

واتضح أن أبرز التغيرات النسيجية في القصبة الهوائية ما لوحظ من تدمير في الأهداب، وتكاثر غير طبيعي في الخلايا المكونة للطبقة الطلائية، بالإضافة إلى درجة عالية من تركيز الحويصلات والعصيات المنتجة للطاقة (الميتوكوندريا) في الجزء الأقمي للخلايا الطلائية. أما الحويصلات الهوائية فقد أدى دخان السجائر إلى تغلظ في جدارها، وانهايار في الحويصلات الهوائية، وحدث تسرب للدم من الأوعية الدموية إلى الأنسجة المحيطة به، ونقصان في أحد أهم إفرازات خلايا الحويصلات الهوائية (النوع الثاني)، الذي يسمى (السيرفاكتنت)، و تشكل الفجوات السيتوبلازمية، وزيادة في كثافة المادة الوراثية.

وفيما يختص بالأبهر بالشریان الأبهر لوحظ تدمير في الخلايا البطانية التي تبطن جداره من الداخل، أما في نسيج (البطين) فقد لوحظ انفصال بسيط بين الألياف العضلية وتواجد الأوعية الدموية المحتقنة. العضيات المنتجة للطاقة (الميتوكوندريا) في نسيج البطين وقد كانت الجسيمات الأشد تأثراً بدخان السجائر. و تجدر الإشارة إلى ملاحظة انقباض بسيط في العضلات الملساء في جدار الأبهر، وكذلك زيادة في سمك الألياف المرنة والتي أصبحت أكثر وضوحا. كما لوحظ في معظم الأنسجة وجود كريات دم بيضاء إشارة إلى حدوث الالتهاب المزمن.

كشفت معايرة dUTP الموسوم المضاف للنهاية المكسورة بواسطة الناقل الطرفي للنيكليوتيدات منقوصة الأكسجين (Tunnel assay) عن قدرة دخان السجائر على حث خلايا الحويصلات الهوائية على القيام بموت مبرمج للخلايا، وقد كشف عنها عن طريق اللون ها البني الداكن لانويتها. كما كشف الجزء الأخير من الدراسة النسيجية، ان الانسجة عادت الى الوضع الطبيعي بعد انقطاع التدخين لمدة ثلاثة اشهر، وهذا التحسن في الأنسجة يلغي احتمالية نشوء خلايا خبيثة.